



JÖNKÖPING UNIVERSITY
School of Engineering

Licentiate Thesis

Deformation of human soft tissues

Experimental and numerical aspects

Sara Kallin

Licentiate thesis in Machine Design

Deformation of human soft tissues
– Experimental and numerical aspects
Dissertation Series No. 049

© 2019 Sara Kallin

Published by
School of Engineering, Jönköping University
P.O. Box 1026
SE-551 11 Jönköping
Tel. +46 36 10 10 00
www.ju.se

Printed by BrandFactory AB 2019

ISBN 978-91-87289-52-1

Acknowledgements

I would like to express my sincere gratitude to all who have supported me and made this work possible.

To my supervisors, Professor Peter Hansbo, Docent Kent Salomonsson and Professor Maria Faresjö for all their support and fruitful discussions during this work.

To Dr Asim Rashid for his engagement and collaboration in study I.

To all members of the PEOPLE project at Hotswap Norden AB, Ottobock Scandinavia AB and Ossur Nordic HF for their collaboration and support.

I would like to express my appreciation to persons involved during tests of the questionnaire, the clinical assessment protocol and the development of equipment.

I gratefully thank the volunteering participant in study II, and Hans Eklund, Aleris Röntgen, Jönköping together with Anna Engdahl, Wetterhälsan, Jönköping, for collaboration in data collection.

For their financial support, the Jönköping Regional Research Programme, Sweden, the project PEOPLE, the School of Engineering and School of Health and Welfare at Jönköping University are greatly acknowledged.

To colleagues and friends at the School of Engineering, School of Health and Welfare and the community of Prosthetics & Orthotics for your support and encouragement, and for making my work more joyful.

Finally, I would like to thank my friends and family, especially my husband Jonas and daughters Sofia and Kristina, for your patience, support and love.

To my father who always encourages me, Thank you.

Sara Kallin

Jönköping, Sweden

July 2019

Abstract

Understanding human soft tissue deformation is important for preventing and decreasing the tissue damage due to mechanical load by external products. Experimental data for material properties of living human tissue are limited. Moreover, tissue tolerance to loads seems depend on the individual-specific conditions including health. Predictions of mechanical behaviour with finite element (FE) models exist, however FE simulations of human soft tissue apply simplified material representation of which impacts on outcomes are yet unclear. Strategies to investigate human tissue load response need to be improved for better understanding of tissue deformation.

This thesis aims to investigate aspects of deformation in human soft tissue of the leg when exposed to external loading. The focus is on soft tissue representation in FE simulation models and individual-specific live tissue deformation under established health conditions.

To investigate the influence of tissue material representation in FE simulation a strategy with a 2D generic multilayer model of the lower leg was introduced. Two material sets were applied, each representing skin, fat, vessels and bones separately while fascia and muscle tissues had either separate or combined material properties. External loads were applied by three different shapes of prosthetic sockets. The relative change between the two used material sets were considerable regarding the distribution and magnitudes of tissue's stresses and strains as well as the contact pressures. Thus, the FE model was sensitive to how muscle and fascia were modelled.

An experimental strategy for obtaining deformation in the leg tissues of a person with specified health condition was then developed and demonstrated in a case study. A tissue-indentation instrument (TIM) was designed so that the induced mechanical deformation could be captured by magnetic resonance imaging (MRI). A questionnaire and a clinical assessment protocol addressed health conditions related to pressure injury development. The investigated deformations were the displacement and stretch ratio λ per layer, the volume change by volume ratio J on cross-section slice and by the deformation gradient \mathbf{F} and Jacobian determinant J^{FEM} in a defined element within a specific muscle tissue region. Individual-specific results for one healthy male subject demonstrated that the layers of skin, fat, muscles and deep vessels were

compressed and underwent large strains, while the connective tissues behaved incompressible and with small strains.

The combined results suggest that the deformation of the human lower leg soft tissue should be investigated by tissue types and layers, and represented by separate material behaviour instead of combined types and layers.

This work is relevant to the increase of the human tissue material property reference data set with subjects of diverse health conditions, and to verification and validation of related simulation models.

Key words: Human soft tissue, Deformation, Material property, Simulation, Finite element, Biomechanics, Pressure injury, Multidisciplinary

Nomenclature

aetiology the cause or origin of a disease

anterior in front

anoxia lack of oxygen in body tissue

connective tissue tissue which forms the main part of bones and cartilage, ligaments and tendons, in which a large proportion of fibrous material surrounds the tissue cells

distal further away from the centre of the body (is opposite to proximal)

epidermium outer nonvascular, non-sensitive cell layer of skin

ex vivo experimentation or measurements which takes place outside an organism, done in or on tissue from an organism in an external environment

fascia band or sheet of connective tissue, primarily collagen, that attaches, encapsulates, stabilize and separate muscles and other internal organs

gluteal, gluteus muscles muscles in the buttocks

hematoma collection of blood outside blood vessels, e.g. in muscle tissues, mass of blood under the skin

hypoxia inadequate supply of oxygen to tissue or an organ

immobilize hinder movements, stop from moving

immunological disease disease related to the immune system

inferior lower down than another part

inserts insoles (in current context)

in vitro experiment which takes place in the laboratory

in vivo in living tissue

ischemia deficient blood supply to part of the body

lateral further away from the midline of the body

limb extremity, leg or arm

liner a removable protective limb cover item/layer worn between the skin and

inner surface of the prosthesis/orthosis (current context)

lymphatic referring to lymph

medial nearer to the central midline of the body or to the centre of an organ

metabolism chemical transformations within living cells for sustaining life, e.g. processing food/fuel to energy or to building blocks for proteins, breaking down organic matter

morphology study of the structure and shape of living organisms, objects

necrosis death of a part of the body such as a bone, tissue or an organ

occlusion blockage

orthosis, orthotic device externally applied device used to modify the structural and functional characteristics of the neuro-muscular and skeletal systems

oxygenation becoming filled with oxygen

pathology study of diseases and the changes in structure and function which diseases causes in the body

pathologies diseases, malfunctions, abnormalities

periosteum dense layer of connective tissue around a bone

peripheral arterial disease (PAD) arterial vessel disease in peripheral body parts, such as feet and leg, and peripheral vessels, such as capillaries

physiology, human study of the human body and its normal functions

posterior at the back

prominence part of the body which stands out, e.g. bone knuckle.

prosthesis, prosthetic device externally applied device used to replace wholly, or in part, an absent or deficient limb segment

prosthetic socket the individual specific structural component encapsulating the residual limb/stump for axial and transverse stabilization of forces

proximal near the midline or the central part of the body (the opposite is distal)

reactive hyperaemia congestion (excessive fluid) of blood vessels after an occlusion has been removed

reperfusion return of blood supply after a period of ischemia or hypoxia

residual limb the portion of a limb remaining after an amputation

spinal referring to the spine, the backbones, a series of bones linked together to form a flexible column

subcutaneous under the skin

subcutis, hypodermis subcutaneous fat

superior higher up than another part

trans-tibial through the tibia, shinbone, crus

type 1 diabetes (T1D) the pancreas does not produce insulin

type 2 diabetes (T2D) insulin resistance, the body can't use insulin properly (most common form of diabetes)

ulcer (open) sore in the skin

vascular disease disease affecting the blood vessels

Symbols

σ	sigma, mechanical stress
ε	epsilon, strain, engineering strain
λ	lambda, stretch ratio
E	Green StVenant strain Young's modulus of elasticity
L	length, at deformed, current condition
L_0	length, at undeformed, reference condition
Δ	delta, denotes the difference on a variable
e	Almansi finite strain
TPE	Total potential energy
U	Strain energy
W	External work
F	force
u	displacement
μ	mu, shear modulus
μ_s	coefficient of friction skin/indenter
∇	nabla, gradient
I	matrix of unit entity, identity matrix
ν	nu, Poisson's ratio
F	deformation gradient, matrix
dX, dx	a line element in undeformed and deformed state respectively
$C = F^T F$	the right Cauchy-Green deformation tensor
$b = FF^T$	the left Cauchy-Green deformation tensor
A	a squared matrix named A
$\det A$	determinant of A
$\det F$	determinant of the deformation gradient F
J	Jacobian determinant
J	Jacobian matrix
V_0	volume, at undeformed, reference condition
V	volume, at deformed, current condition

Abbreviations

ABPI	Ankle Brachial Pressure Index
ABS	Acrylonitrile Butadiene Styrene
AMP	Absolute Maximum Principal Strain
BMI	Body Mass Index
CAE	Computer Aided Engineering
CPO	Certified Prosthetist-Orthotist
CT	Computed Tomography
DIC	Digital Image Correlation
DICOM	Digital Imaging and Communications in Medicine
DRV	Damage Risk Volume
DTI	Deep Tissue Injury
EPUAP	European Pressure Ulcer Advisory Panel
FE	Finite Element
FEA	Finite Element Analysis
FEM	Finite Element Method
FOV	Field of View
kPa	kilo Pascal
LVDT	Linear Variable Differential Transformer
MRI, MR	Magnetic Resonance Imaging
NPUAP	National Pressure Ulcer Advisory Panel
PETG	Glycol-modified Polyethylene Terephthalate
PI	Pressure Injury
PU	Pressure Ulcer
RQ	Research Question
TIM	Tissue Indenter Measurement

Contents

1.	Introduction	1
1.1.	Problem statement.....	1
1.2.	Purpose and aim.....	2
1.3.	Outline	3
2.	Background	5
2.1.	Human leg tissues	5
2.2.	Soft tissue damage	8
2.2.1.	Definition Pressure Injuries.....	8
2.2.2.	Suggested mechanisms and factors	9
2.2.3.	Prevalence of soft tissue damage related to PI	12
2.2.4.	Evaluation of soft tissue status and PI.....	12
2.3.	Deformation.....	13
2.4.	Material models and parameters for large deformation.....	16
2.5.	Experimental investigation of deformation	22
2.6.	Computer simulations of soft tissue by Finite Element Method...	24
2.6.1.	Finite element method – a brief introduction	24
2.6.2.	FEM in tissue biomechanics.....	26
2.7.	Position in the Industrial Product Realisation context.....	29
2.8.	Rationale	31
3.	Research approach.....	33
3.1.	Scope and delimitations	33
3.2.	Research perspective and strategy	35
3.3.	Study I.....	36
3.3.1.	Research design.....	36
3.3.2.	The Finite Element Model.....	36
3.3.3.	Material properties	39

3.3.4.	Boundary conditions.....	42
3.3.5.	Procedures for analyses	43
3.4.	Study II	44
3.4.1.	Research design.....	44
3.4.2.	Equipment for deformation by indentation in MR	46
3.4.3.	Clinical assessment.....	49
3.4.4.	Questionnaire.....	50
3.4.5.	Human subject.....	52
3.4.6.	Data collection procedure.....	52
3.4.7.	Data processing	54
3.5.	Ethical considerations	59
4.	Results	61
4.1.	Study I.....	61
4.1.1.	Comparisons of stresses and strains	61
4.1.2.	Comparisons of contact pressures	66
4.2.	Study II	68
4.2.1.	Subject specific health conditions	68
4.2.2.	Deformation measures from image analyses.....	70
4.2.3.	Force-displacement by TIM	75
4.3.	Geometry model from MR data in Study II.....	76
5.	Discussion	77
5.1.	Influence of differentiated tissue representation in FEA	77
5.1.1.	Influence on stresses, strains and contact pressures	77
5.1.2.	Discussion of the simulation model	79
5.2.	Process for measuring individual-specific soft tissue deformation in separate tissue layers <i>in vivo</i> under established health conditions	82
5.2.1.	Data collection techniques.....	83
5.2.2.	Analyses of data	87

5.3. Individual-specific soft tissue deformation measured in separate tissue layers <i>in vivo</i> under established health conditions	90
5.3.1. Deformations.....	90
5.3.2. Health measures and clinical findings.....	92
5.4. Contribution.....	93
5.5. Implications	95
5.5.1. Tissue configurations in FE simulations	95
5.5.2. Individual specific tissue deformation in vivo	95
5.5.3. Product realization process.....	96
6. Concluding remarks	99
7. Future work	101
Sammanfattning	103
References	105
List of Figures	120
Appendices	123
I. Material parameters from indentation studies on human leg.....	125
II. Study II Clinical assessment protocol.....	130
III. Study II Questionnaire	137
IV. Study II Data collection sequence.....	145
V. Study I Additional data	146

1.Introduction

1.1. Problem statement

In my profession as orthotist-prosthetist I meet individuals with diseases or physical disabilities who need external biomechanical supportive devices to facilitate their daily living activities. These external supportive devices, such as prostheses, orthoses, seating devices etc expose soft tissues to external loads and many users experience soft tissue problems. Different skin wounds and soft tissue problems may occur due to the interaction between the body tissues and the external supporting surfaces, manifesting as, for example, numbness, redness in skin, blisters, open wounds and sometimes deep tissue death (necrosis) [1]. Load-related wounds such as bedsores and pressure ulcers are also common in healthcare [2]. Problems in the loaded soft tissues may impact the person's participation in activities. Severe ulcers may lead to amputation or even death. Tolerance of soft tissues to externally applied load is individual and varies with health status, age, morphology, skin conditions and mechanical properties of tissues [3]. It is therefore important to consider the individual's soft tissue status and tolerance to load when managing the loading situation. The parameters for determining the soft tissue status in a clinical setting are often related to assessing the pathological condition by morphology (size, shape and structure), or aetiology (the cause, set of causes) of the conditions [3-8].

Moreover, the mechanisms of soft tissue behaviour and risk for damage when exposed to external loads are not yet fully understood. Several studies investigating specific biomechanical material properties *in vivo* have been performed over the years, but further investigations are still needed [9-12]. The multilayer configuration, diverse tissue structures and time dependence are challenging aspects of human soft tissues [9, 10, 13]. So far there is no established standard methodology for obtaining properties of individual-specific soft tissues [10, 14]. Additionally, little reference data for soft tissue materials from living humans are available.

Despite this, various mechanical material properties and material models have been used to represent the biomechanical behaviour of human tissues [9, 10, 13, 15]. The finite element method (FEM) is increasingly applied in

biomechanics to generate material properties, and for analyses of internal conditions of tissues exposed to loads. For these simulations diverse assumptions have been applied depending on the models used, available material properties, geometries and loading conditions. Examples of simplifying assumptions in models of human leg tissues are small strains, incompressibility and that specific tissue types and geometries have been merged together or neglected in the simulation models. For interpretation it is important to know how these simplifications influence the simulation results, but this is so far unclear. Using overly simplified simulations the error could be considerable [14]. There is a need to further explore effects of simplifications in simulation by FEM.

Hence, we need improved understanding of the deformation behaviour of soft tissues when exposed to load, as a compound and as separate tissue types and layers. In order to use simulation models for biomechanical analyses to decrease tissue damage and discomfort, we need further understanding of the influence of tissue representation in FE models for interpretation of simulation results. We need also to address the individual-specific conditions related to tissue behaviour including health related aspects. Thus, techniques to obtain such information on individual-specific level need to be further developed.

1.2. Purpose and aim

Thus, the overall purpose of this research is to improve the understanding of human soft tissue response when the body is interacting with external supports, such as improving methods for determining soft tissue behaviour, and representation in simulation models with FEM.

The specific aim is to investigate aspects of deformation in human soft tissue of the leg when exposed to external loading.

To achieve this aim, different aspects of this multidisciplinary problem are addressed in the context of mechanical conditions and health conditions related to tissue load tolerance. Analyses and measures of individual specific soft tissue behaviour, which include risk factors for pressure ulcers and health conditions, is part of this. The aim is wide, and further delimitations are

required. These will be addressed after the background chapter by the scope, research questions and delimitations in chapter 3.1.

1.3. Outline

A multidisciplinary approach was used, combining engineering, biomechanical and medical perspectives. Some preunderstanding from the engineering field is assumed. However, some concepts in one discipline require explanations for readers from another discipline and vice versa. This is a difficult balance, and the level of theoretical depth therefore varies in the thesis. A nomenclature is also provided to assist the reader. The outline of the thesis is as follows:

Chapter 1 describes the problem and aim of the research. The background, Chapter 2, describes human soft tissue and tissue damage due to load, some aspects of deformation, and introduces to varying extent related aspects, definitions and concepts that are used in the subsequent chapters. Experimental and numerical methods are reviewed as a basis for the research approach. Relations of this work to the industrial product realisation process are also presented here. In Chapter 3 the research questions, the chosen research approach and developed instruments are described. The initial simulation study provided insights to the subsequent experimental study, and these two studies addressed different aspects of deformation. Chapter 4 presents the results per study. In Chapter 5, the findings and methods are discussed in relation to the research questions, leading to the conclusions in Chapter 6. Future work is suggested in Chapter 7. Appendices are provided containing protocols and additional data.

2. Background

2.1. Human leg tissues

This research considers deformation in human soft tissues of the musculoskeletal system, the lower leg in particular. Therefore, a short description of the tissues of the lower leg based on Tortora [16] is introduced to the readers not familiar to human anatomy.

The lower leg is the structures between the knee and ankle and consists of many different tissues. Each tissue type is structured for its function and consists of different types of cells, often in layers.

The skeleton of the lower leg includes the longitudinal bones tibia and fibula. The bone consists of cortical bone and bone marrow, while the joint surfaces of bones are covered by articular cartilage, a fibrous connective tissue with high water content. The bones are attached to each other with ligaments and membranes, made of connective tissues. The soft tissues of the lower leg are here defined as follows: the skin, subcutaneous fat, crural fascia, deep fascia inter-muscular dividers (septum) of connective tissue, intra-muscular fat, muscles, tendons, ligaments, blood vessels, nerves, and lymphatic vessels. They are organized in relation to each other in various ways, depending on the site and individual morphology. The transverse cross section at the height of upper third part on the lower leg is illustrated in Figure 1, based on Netter [17]. This cross section, at approximately the same level of leg height, is in focus for the research presented here.

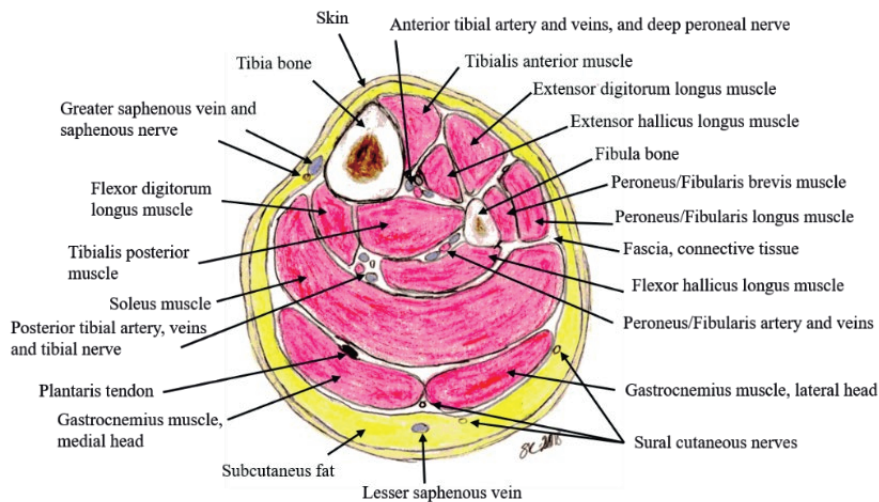


Figure 1 Tissues at the mid-height of a human transtibial transverse cross section, the front of the leg, anterior, is up. (author)

The layers of tissues surrounding and connecting organs, as protecting bags, dividing walls and bands, are the fascia, epimysium, ligaments and tendons made of connective tissues. Fascia is like a sheet or broader band of fibrous connective tissue. A layer of fascia under the subcutaneous fat, the crural fascia (*cruris* Latin; from the leg), covers the internal soft tissues of the leg, with vessels and nerves penetrating it. Deep fascia is dense and irregular, dividing the muscles into groups with similar functions and allow them to move relative to each other. The fascia also provides channels for vessels and nerves. Tendons are fibrous bundles of connective tissues. The muscles and tendons move and stabilize the skeletal structures, and thus facilitate possibilities for physical activities.

Skin and muscle tissue structures are illustrated in more detail in Figure 2. The human skin is a structure of interconnected layers, epidermis, dermis and subcutis/hypodermis (Figure 2 A). The underlying layer (named subcutis, hypodermis or subcutaneous fat) consists mainly of fat cells and connective tissues. Fibrous bands anchor this layer to the underlying crural fascia, while collagen and elastin fibres connect it to dermis. Blood vessels and nerves pass through this layer to dermis.

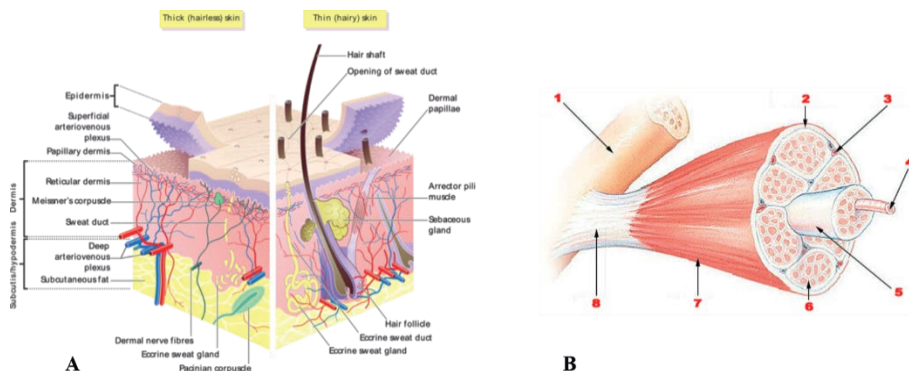


Figure 2 Skin and muscle tissue layers. A: Skin layers of human skin. B: Muscle tissue structure 1. Bone 2. Perimysium 3. Blood vessel 4. Muscle fiber 5. Fascicle 6. Endomysium 7. Epimysium 8. Tendon. (Wikimedia Commons)

There are many muscles between the knee and ankle (examples in Figure 1). Each muscle consists of bundles of muscle fibres in groups, endomysium, divided by fascicles, Figure 2 B. The muscle outer layer, the perimysium, is encapsulated by another thinner layer of connective tissue, epimysium. These two layers can expand when the muscle contracts and shrink when the muscle relaxes or becomes thinner for other reasons. The epimysium will also contribute to sliding between neighbouring tissues.

Larger vessels for blood and lymphatic transportation are flexible tubes with walls of tissue layers of mainly connective tissue and muscle fibres. The nerves are bundles of hundreds to thousands of nerve cells, axons, within a thin protecting cover.

The interaction of human body soft tissue and external supports involves structures and mechanisms on different levels [1, 18]. A multilevel model adapted from Shoham and Gefen [18] and here applied to the musculoskeletal system of the human leg is suggested in Figure 3. ‘Macro level’ relates to the segment and site of the body where the external load is applied. ‘Meso level’ relates to the tissues and organs, e.g. skin, muscles, blood vessels, and the compound of tissue layers at a certain site. ‘Micro level’ relates to the cellular level, with the cell structure for each tissue type, and cellular functions, e.g. metabolism, transmission of substances through the cell membrane, signal substances for body system communication etc. When the body tissues are exposed to external loading, interaction at these suggested levels occur, and

may contribute to tissue damage [1, 3, 18, 19]. This is addressed in the next chapter.

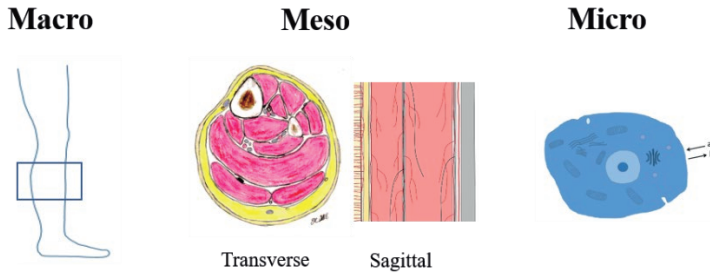


Figure 3 Multistructural model with defined levels, applied to the lower leg structures, adapted from Shoham and Gefen [18]. Macro level: body segment and site. Meso level: organs, tissue types, tissue layers. Micro level: cell types, cell structures, metabolism, transmissions. (illustrations S. Kallin, author)

2.2. Soft tissue damage

Mechanical load on the human body tissues from external supports are present in daily life while seated, standing, walking, lying etc. The tissues respond to the load, and sometimes damage occurs within the interacting tissues, often referred to as pressure ulcers (PU) or pressure sores. Definition of soft tissue damage due to this kind of load, theories of aetiology and known prevalence are important for the understanding of this problem and follow below. Mechanical deformation will be addressed in more depth in next chapter.

2.2.1. Definition Pressure Injuries

Mechanical induced tissue damage can be divided into superficial and deep tissue damage. The National Pressure Ulcer Advisory Panel (NPUAP) recently updated the international definition from pressure ulcer (PU) to pressure injury (PI) and included more factors of aetiology [20-22]:

“A pressure injury is localized damage to the skin and/or underlying soft tissue usually over a bony prominence or related to a medical or other device. The injury can present as intact skin or an open ulcer and may be painful. The injury occurs as a result of intense and/or prolonged pressure or pressure in combination with shear. The tolerance of soft tissue for pressure and shear may also be affected by microclimate, nutrition, perfusion, co-morbidities and condition of the soft tissue.” [21]

Pressure injuries are classified as Stage 1 to 4 Pressure Injury, ‘Unstageable’ and ‘Deep tissue pressure injury’ [21]:

Stage 1 Pressure injury: Non-blanchable erythema of intact skin

Stage 2 Pressure injury: Partial-thickness skin loss with exposed dermis

Stage 3 Pressure injury: Full-thickness skin loss

Stage 4 Pressure injury: Full-thickness loss of skin and tissue

Unstageable pressure injury: Obscure full-thickness skin and tissue loss

Deep tissue pressure injury: Persistent non-blanchable deep red, maroon or purple discoloration

In this thesis the term PI is used accordingly.

2.2.2. Suggested mechanisms and factors

A literature review on the occurrence of pressure injuries while using external supports during locomotion by Mak *et al* in 2010 [1] listed four possible mechanisms: “(a) local ischemia and anoxia resulting from blood-flow occlusion, (b) compromised lymphatic transports resulting in accumulation of toxic substances in the tissues (c) reperfusion injuries concomitant with reactive hyperaemia, and (d) direct mechanical insults to cells that cause cellular necrosis.” ([1] p. 36). All of these are related to prolonged excessive epidermal loading, but it is unclear how these relationships more precisely contribute to tissue damage. Ischemia, or lack of oxygen in tissues, during loading causes cell damage within hours, and compression and shear forces are two factors that are known to cause tissue breakdown [19, 23, 24]. The unloading of tissues is also of importance since it causes reperfusion (refilling of blood into the tissue), oxidative stress and inflammatory response [25]. The loading-unloading situations may make the tissues more susceptible to

damage compared to static loading only [26, 27]. Time is an essential factor for the development of pressure injuries [1, 28, 29]. Mak *et al* [1] pointed out the need for better damage models in future research, such as damage laws on cellular level, load-duration tolerance including shear forces, and specific models for different tissues.

The pressure ulcer conceptual framework by Coleman *et al* in 2014 [3] presents a system of key factors and risk factors, see Figure 4. This framework for PI prevention is further developed from the NPUAP and EPUAP (European Pressure Ulcer Advisory Panel) guidelines [22] based on a systematic literature review on pressure injury risk factors [30] and expert consensus on epidemiological, physiological and biomechanical evidence and risk assessment [6]. A balance model with the mechanical boundary conditions on one side and the individual susceptibility and tolerance on the other side illustrates PI development in Figure 4, and will determine the individual threshold level for tissue damage. Mechanical boundary conditions are characterized by load magnitude and directions by pressure or shear, and friction. Individual specific geometry of tissue layers influences the tolerance to load as well. The framework includes immobility, skin-status and poor perfusion as key factors, and age, diabetes, poor sensory perception, nutrition, and low albumin levels, as indirect risk factors for PI and deep tissue injury (DTI) development, all of which are related to physiology or pathology. In Figure 4, the risk factors are placed on the side of the balance board they mainly contribute to (mechanical boundary conditions or individual susceptibility and tolerance). The balance model in this framework also means that if a risk factor is not present for that person, the person may tolerate higher levels of the conditions on that side.

Additionally, the body mass index (BMI) is a health related parameter that increases the risk of DTI [31] and PI [32]: as the body weight increases the load on external supporting surfaces resulting in increased reaction forces on the tissues. A high BMI may also increase immobility, in itself a risk factor [30]. Blood pressure is a common health measure of blood circulation and the regulatory system [33], and is related to oxygenation, perfusion and thus tissue behaviour [27].

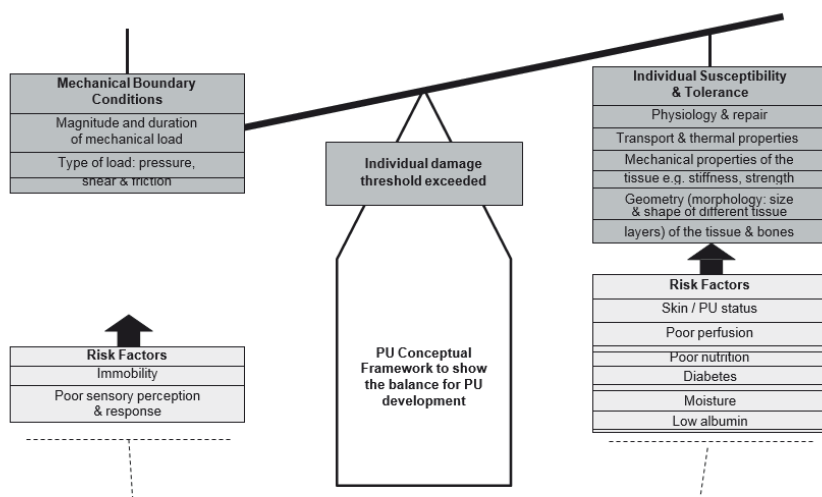


Figure 3 New pressure ulcer conceptual framework.

Figure 4. Coleman *et al* [3] New Pressure Ulcer Conceptual framework, from p.2232, figure 3.

An explanation for DTI aetiology was proposed by Oomens *et al* [19] based on several studies of skeletal muscle, mainly from animal and engineered tissue experiments, with a multi-scale approach combined with FEM. The authors state that slow and moderate mechanical strain will cause cell death in 2-4 hours due to metabolic components, while fast and high strain causes cell death in ten minutes due to the deformation of the cytoskeleton cell structure [19]. A damage threshold for the rat muscle cell at 45% shear strain has been proposed by Ceelen *et al* [23] and a damage risk volume (DRV) measure for muscles at 50% strain level, was defined and applied by Moerman *et al* [34] as the volume of tissue that reached that level of strain. Stecco *et al* [35] reports a damage level of 27% nominal strain for dead human leg fasciae under tensile tests. They defined the nominal strain as elongation divided with the original length.

2.2.3. *Prevalence of soft tissue damage related to PI*

The mean point prevalence of pressure injuries in Swedish hospitals was 13.5% in 2017 [2] and 14.1% in 2018 with 10.6% of PI acquired in hospital [36]. As stated by Coleman, Gorecki *et al* 2013 [30] a risk factor for PI is diabetes, without distinguishing between type 1 and type 2 diabetes. In Europe, 9.1% (66 million persons) of the population aged 18-99 had diabetes of type 1 or type 2 in 2017 [37], and 15% of diabetic patients acquire a foot ulcer during their lifetime [38], while the incidence of foot ulcers increases yearly by 2% [38, 39]. Diabetic foot ulcers increase with peripheral arterial disease (PAD) and infections [40, 41] and can start with a PI. Foot ulcers are well known causes of lower limb amputations in patients with diabetes [42, 43]. In populations with lower limb amputations using a prosthesis, the prevalence and incidence of skin problems are 15-82 % [44-47]. Very few studies on prevalence of skin problems among orthosis-users were found. The reported PI prevalence in this category was 5-37% [48-50].

2.2.4. *Evaluation of soft tissue status and PI*

Evaluation of skin and soft tissue status of the musculoskeletal system in relation to tissue damage varies [30, 51]. Assessments for PI risk may include general skin status for vulnerable skin, existing and previous PI status and sites, perfusion, sensory perception, moisture, nutrition, grade of immobility and diabetes [6, 7, 51].

There is no uniform evaluation method for skin status or soft tissue behaviour in prosthetics and orthotics [5, 44, 52]. Assessment of soft tissue status in this field is mainly based on clinical condition, mobility, physical examination of tissues by palpation and observation, external geometrical measures and neuro-muscular function of the body segment [4, 5, 8, 53-55]. The ISO Standard 8548-2 [8] provides some descriptors for lower extremity residual limbs: by shape, blood circulation, and soft tissue status by amount and texture. The skin status should be described by amputation scar, intact skin or not, and normal or impaired sensation [8]. More recent evaluation recommendations propose the use of either morphology or aetiology [44] and description of the skin problem in more detail [5, 45]. Deeper tissues are not clearly addressed in these assessment recommendations within prosthetics and orthotics. However, pressure injuries related to medical devices (which could

include prostheses and orthoses) are now recommended by the NPUAP to be staged according to their classification [21].

the human tissue status and responses to external loading is related to the mechanical properties and deformation behaviour of the tissues [1, 3, 13]. Thus, deformation is addressed in the next chapter.

2.3. Deformation

To investigate the soft tissue response to loads, the deformation is very important [13]. Thus, some theoretical background is given in the following text based on literature [9, 13, 56-60].

The behaviour of a material or a body when exposed to a load (as in a force or a temperature change), is described by its deformation. Deformation refers to the shape and volume change of an object as a result of loads being applied. Kinematic relationships describe the motions between the original/non-loaded/reference and the loaded/current configuration. If there is no size or shape change of the body, then the displacement of the body is a rigid-body displacement.

Stress is responsible for internal deformation and is defined as force divided by cross sectional area. Stress is represented by a 3x3 matrix σ in a general 3D situation. The stress and strain relationship for a material is described by constitutive equations, which specify the properties of the material. Materials respond differently to loads: the response depends on the material constituents and molecular structure. Constitutive equations to represent material behaviour are developed based on experiments.

To capture the volume and shape change due to an applied load, deformation is measured by strains in different directions. Different strains measures are used depending on the amount of local deformation. These are divided in three categories depending on the theory used:

- Small strain, small rotation theory,
- Small strain, large rotation, large displacement theory,
- Finite strain, large strain, large deformation theory.

When the strains and rotations are small, the deformed state can be assumed to be identical to the undeformed state. This applies to analyses of elastic materials with strains in the range up to 1%, typically. The second category is applicable when strains are assumed to be small, but the rotations and displacements are assumed to be large. Large strain and large deformation theory, as the names reflect, deal with conditions where both the strains and rotations are large. This means that there is a considerable difference between the undeformed and deformed states, which should be considered. This theory is applied to elastomers, materials with plasticity behaviour, fluids and biological soft tissues [13, 57].

The type of behaviour due to the applied load is typically described as elastic, plastic or viscoelastic deformation. In the plastic deformation permanent changes remain after off-loading in contrast to the elastic case. If the strains are large in the elastic behaviour it is said to be hyperelastic. Time-dependent deformation is described by for example creep, stress- or strain relaxations, and stress-strain curve changes with hysteresis shape, i.e. viscoelasticity and viscous deformation. Thus, there is a large variety of constitutive equations specifying material properties, taking into account the amount of deformation and the type of deformation.

Strain measures

When considering the type of deformation, we need to choose the appropriate strain measure. Strain measures are defined in relation to the length of the object, in given directions, during undeformed and deformed states. The strain measure depends on which base is used, the undeformed or the deformed/current shape, and if the squared or unsquared length is used. At small deformations the results will be very similar regardless of strain measure used, but not when deformations are large. Thus, to state which strain theory and strain measure used is important.

Small strain expressed in one dimension:

$$\text{Strain (engineering strain, Cauchy)} \quad \varepsilon = \frac{(L-L_0)}{L_0} = \frac{\Delta L}{L_0} = \lambda - 1 \quad (1)$$

Large deformation in one dimension:

$$\text{Stretch ratio} \quad \lambda = \frac{L}{L_0} \quad (2)$$

$$\text{Logarithmic strain} \quad \varepsilon^L = \ln \lambda \quad (3)$$

$$\text{Green \& St Venant strain} \quad E = \frac{1}{2} \left(\frac{L^2 - L_0^2}{L_0^2} \right) = \frac{1}{2} (\lambda^2 - 1) \quad (4)$$

$$\text{Almansi, Hamel finite strain} \quad e = \frac{1}{2} \left(\frac{L^2 - L_0^2}{L^2} \right) = \frac{1}{2} \left(1 - \frac{1}{\lambda^2} \right) \quad (5)$$

Here L_0 denotes the length of a line element in the undeformed state, and L the deformed length. [13] A positive strain means elongation along the direction of strain, and negative means shortening. The stretch ratio of the line element is said to be extended when $\lambda > 1$, unstretched when $\lambda = 1$ and compressed when $0 < \lambda < 1$.

It is apparent in the literature that different notations tend to be used for the same parameter, e.g. Green strain uses ε_G or E , Euler-Almansi strain ε_E or e , and Young's modulus, an elasticity modulus, also uses E . This can be confusing, hence, in this thesis the name and/or equation number will be used along with the symbol used.

The above strain measures have been expressed in one dimension for simplicity. In two and three spatial dimensions, we use tensor notation and matrices. In tensor notation, indices with letters are assigned to keep track of the directions or dimensions. We refer to these by standard terms, i.e. $i=1,2,3$, $j=1,2,3$, etc. In matrices the directions are noted by indices of x, y and z, or numbers 1,2,3. An example is the Euler-Almansi strain tensor for finite strains often noted as e_{ij} .

Strain energy function (SEF)

Another strategy to analyse strain and deformation is the energy method. It is based on equilibrium and the total energy potential, *TPE*:

$$TPE = \bar{U} - \bar{W} \quad (6)$$

where W is the work done when external forces are applied to the object, causing displacement. U is the strain energy stored in the material due to the work done. [61] The external work is the sum of the forces, F_i , multiplied by displacements, u_i :

$$\bar{W} = \sum_i F_i u_i$$

The strategy is that by minimizing the total potential energy, TPE, we find the unknown displacements. Thus, there are material models developed for determining the strain energy per unit of reference volume (strain energy

density), U , as in the example here expressed for the elastic, small strain condition in tensor form:

$$U = \frac{1}{2} \sigma_{ij} \varepsilon_{ij} , \quad i = 1,2,3 \quad (7)$$

and \bar{U} is found by integrating U over the volume.

The strain energy is often used in material models applied to human soft tissues: indeed the definition of hyperelastic materials is that the stress-strain relationship is derived from a strain energy density.

In the following two chapters, material models for large deformation and experimental investigations of human tissues will be addressed further.

2.4. Material models and parameters for large deformation

A material's behaviour depends on its microstructure and constituents. When properties measured in a material are independent of the direction in which they are measured, the material is isotropic, otherwise the material is anisotropic. An orthotropic material is a type of anisotropic material, with different properties along orthogonal axes. The behaviour can be described as linear or nonlinear, due to the shape of a curve approximated from a range of experimental data points for the studied property. The same material can behave differently depending on conditions and type of load applied, such as behaving linearly elastic when initially loaded, and then nonlinearly as the load increases or continues. [59]

There are many models available for approximations of material behaviour and the number is growing [57]. In this chapter the main linear elastic model and some other models for large deformations will be presented briefly based on [9, 13, 56-58].

Small deformation model

For situations with linear elastic behaviour with small deformation, Hooke's law is used, which shows good representation for many engineering materials with small strain. In Hooke's law, stress σ , is related to Young's modulus E , and infinitesimal strain ε :

$$\sigma = E\varepsilon \quad (8)$$

The strain is expressed by the derivative of the displacement u , for each direction, and the strain matrix in three dimensions is:

$$\boldsymbol{\varepsilon} = \begin{bmatrix} \frac{\partial u_x}{\partial x} & \frac{1}{2} \left(\frac{\partial u_x}{\partial y} + \frac{\partial u_y}{\partial x} \right) & \frac{1}{2} \left(\frac{\partial u_x}{\partial z} + \frac{\partial u_z}{\partial x} \right) \\ \frac{1}{2} \left(\frac{\partial u_x}{\partial y} + \frac{\partial u_y}{\partial x} \right) & \frac{\partial u_y}{\partial y} & \frac{1}{2} \left(\frac{\partial u_y}{\partial z} + \frac{\partial u_z}{\partial y} \right) \\ \frac{1}{2} \left(\frac{\partial u_x}{\partial z} + \frac{\partial u_z}{\partial x} \right) & \frac{1}{2} \left(\frac{\partial u_y}{\partial z} + \frac{\partial u_z}{\partial y} \right) & \frac{\partial u_z}{\partial z} \end{bmatrix}$$

The stress can be written as

$$\boldsymbol{\sigma} = 2\mu \boldsymbol{\varepsilon}(\mathbf{u}) + \lambda \nabla \cdot \mathbf{u} \mathbf{I} \quad (9)$$

where μ is the shear modulus, and $\lambda = \frac{E\nu}{(1+\nu)(1-2\nu)}$ with Young's modulus E and Poisson's ratio ν . \mathbf{I} is the identity matrix. Bold letters represent a matrix form.

This strain, $\boldsymbol{\varepsilon}$, cannot describe large deformations correctly since it assumes the displacements are so small that there is no difference between the undeformed and deformed state. Not even large rotations can be handled. Thus, we need to use a strain measure for large deformations.

Large deformation models

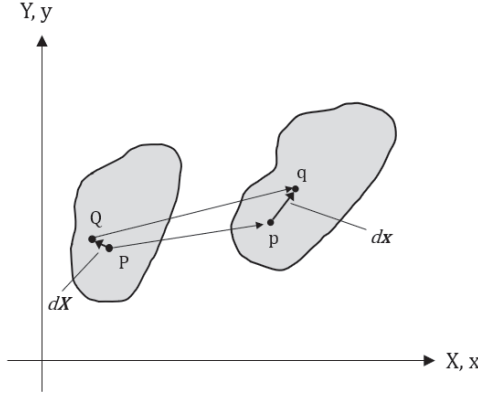


Figure 5 Deformation of a line element in a 2D body, displacement, rotation and elongation. Left undeformed, right deformed body configuration.

Consider local deformation in an object represented in the illustration in Figure 5. The (infinitesimal) line element between two points (P and Q) in the undeformed configuration is denoted by $d\mathbf{X}$ and the same line element in deformed state is $d\mathbf{x}$, (between points p and q) in the figure.

The vector $d\mathbf{x}$ is found by

$$d\mathbf{x} = \mathbf{F}d\mathbf{X}, \text{ where } \mathbf{F} = \frac{\partial \mathbf{x}}{\partial \mathbf{X}} = \begin{bmatrix} \frac{\partial x}{\partial X} & \frac{\partial x}{\partial Y} \\ \frac{\partial y}{\partial X} & \frac{\partial y}{\partial Y} \end{bmatrix} \quad (10)$$

where \mathbf{F} is the deformation gradient, which relates tangent vectors of undeformed and deformed configurations to each other. These tangents describe the rate of change between the states for each point and direction and hence distinguish between the undeformed and deformed conditions. In the notation is this represented by capital letters referring to the undeformed state, and small letters to the deformed state.

The original length of $d\mathbf{X}$ is $dS^2 = d\mathbf{X} \cdot d\mathbf{X}$ and the deformed $d\mathbf{x}$ is $ds^2 = d\mathbf{x} \cdot d\mathbf{x}$.

Then we have

$$d\mathbf{x} \cdot d\mathbf{x} = d\mathbf{X} \cdot (\mathbf{F}^T \mathbf{F} d\mathbf{X})$$

The term $\mathbf{F}^T \mathbf{F}$ in the equation above, is called the right Cauchy-Green deformation tensor, \mathbf{C} , since \mathbf{F} is to the right. \mathbf{C} is a metric tensor, measuring the change in distance under the map \mathbf{X} to \mathbf{x} .

Now we return to the strain measures.

The Green strain, \mathbf{E} , in three dimensions is

$$\mathbf{E} = \frac{1}{2}(\mathbf{F}^T \mathbf{F} - \mathbf{I}) \quad (11)$$

If we use the Almansi strain tensor instead, we have

$$\mathbf{e} = \frac{1}{2}(\mathbf{I} - \mathbf{b}^{-1}) \quad (12)$$

with $\mathbf{b} = \mathbf{F}\mathbf{F}^T$, which is the left Cauchy-Green deformation tensor.

Left and right Cauchy-Green deformation tensors are applied in material models for large deformation and the deformation gradient \mathbf{F} is a very important quantity in large deformation.

Volume change deformation

Another aspect of the deformation gradient is the possibility to calculate the geometrical amount of the local deformation by the determinant of \mathbf{F} . In matrix calculations, the determinant of a matrix, \mathbf{A} , in three dimensions, geometrically represents the volume of the space defined by the vectors in the matrix. The determinant of \mathbf{A} is denoted $\det \mathbf{A}$. In analogy with this the determinant of the deformation gradient \mathbf{F} , $\det \mathbf{F}$, represent volume change due to the deformation, for the geometrical defined element mapped from \mathbf{X} to \mathbf{x} . The determinant of \mathbf{F} is also denoted as

$$\det \mathbf{F} = J \neq 0 \quad (13)$$

where J is sometimes called the Jacobian. The transformation of volume elements from the undeformed to the deformed condition is described by the relationship

$$dv = JdV$$

where J is also described as the volume ratio

$$J = \frac{V}{V_0} \quad (14)$$

The original, reference, volume is V_0 and deformed, current volume V and

$$V_0 = \int dV$$

$$V = \int d\mathbf{F}$$

When $J = 1$ the material does not change volume.

When we have an elastic condition, the change is linear. The determinant of the elastic deformation gradient, expressed by the stretch ratios is in three dimensions, in absence of shear

$$\det \mathbf{F} = J = \begin{bmatrix} \lambda_1 & 0 & 0 \\ 0 & \lambda_2 & 0 \\ 0 & 0 & \lambda_3 \end{bmatrix}$$

$$J = \lambda_1 \lambda_2 \lambda_3 \quad (15)$$

If all the principal stretches, $\lambda_i = 1$, then $J = 1$, and the solid does not change volume.

Stress-Strain relation

The definition of stress by such terms as for example, Cauchy Green \mathbf{C} , or the deformation gradient \mathbf{F} depends on which of the formulations for strain energy potential is used. If the stress is defined as the derivative of strain energy potential with respect to the Cauchy strain, \mathbf{C} , then it is expressed as:

$$\boldsymbol{\sigma} = 2 \frac{\partial U}{\partial \mathbf{C}} \quad (16)$$

Material models for tissue behaviour

The behaviour of biological tissues is complex, also including viscoelastic and viscous aspects [13]. When it comes to deformation of human soft tissue of the muscular-skeletal system, incompressibility or near incompressibility are often assumed [11, 12, 62-65]. Examples of different material models that have been used in calculations and simulations of human soft tissue are linear elastic [66-68], or nonlinear by 2nd order-reduced polynomial [62] or 3rd order polynomials [69], hyperelastic by elastic strain energy functions such as James-Green-Simpson [11, 70, 71], Neo-Hookean [64, 72-75], and nonlinear hyperelastic by Ogden [12, 63, 64, 72] and 2nd order Ogden [11]. These material models apply different parameters and the deformation relationships are summarized in Table 1, and were either obtained from above mentioned studies or from Silber and Then [9].

Table 1 Examples Material models used for human soft tissues

Name	Strain energy function	Eq. no.
Polynomial form	$U = \sum_{i,j=0}^N C_{ij} (I_1 - 3)^i (I_2 - 3)^j + \sum_{i=1}^N \frac{1}{D_i} (J^{el} - 1)^{2i}$ <p>N number of terms.</p> $\mu_0 = 2(C_{10} + C_{01}) \quad C_{ij} \quad D_i = \frac{2}{K_0}$ $I_1(C) = \sum_{i=1}^3 \lambda_i^2, \quad I_2(C) = \sum_{i,j=1}^3 \lambda_i^2 \lambda_j^2, \quad i \neq j$ <p>When N=1 and $C_{11} = 0$ this becomes the Mooney-Rivlin model, When N=2 is used for biological tissues</p>	(17)
Neo-Hookean (polynomial)	$U = C_{10}(\bar{I}_1 - 3) + \frac{1}{D_1} (J^{el} - 1)^2$ <p>$\mu_0 = 2C_{10}$</p> <p>\bar{I}_1: 1st deviatoric strain invariant $\bar{I}_1 = \bar{\lambda}_1^2 + \bar{\lambda}_2^2 + \bar{\lambda}_3^2$,</p> $\bar{\lambda}_i = J^{(-1/3)} \lambda_i$ <p>Hyperelastic, isotropic, incompressible</p>	(18)
Mooney-Rivlin (polynomial)	$U = C_{10}(I_1 - 3) + C_{01}(I_2 - 3)$ <p>$\mu_0 = 2(C_{10} + C_{01})$</p> $I_1(C) = \sum_{i=1}^3 \lambda_i^2 \quad I_2(C) = \sum_{i,j=1}^3 \lambda_i^2 \lambda_j^2, \quad i \neq j$ <p>Hyperelastic, isotropic, incompressible</p>	(19)
Yeoh (reduced polynomial)	$U = \sum_{i=1}^3 C_{i0} (I_1 - 3)^i + \sum_{i=1}^3 \frac{1}{D_i} (J^{el} - 1)^{2i}$ <p>$\mu_0 = 2C_{10}$ and $I_1(C) = \sum_{i=1}^3 \lambda_i^2 \quad D_i = \frac{2}{K_0}$</p> <p>Last term ignored for incompressible materials</p> <p>Hyperelastic, good fit for large strains</p>	(20)
James-Green-Simpson	$U = C_{10}(I_1 - 3) + C_{01}(I_2 - 3) + C_{11}(I_1 - 3)(I_2 - 3) + C_{20}(I_1 - 3)^2 + C_{30}(I_1 - 3)^3$ $I_1 = \lambda_1^2 + \lambda_2^2 + \lambda_3^2, \quad I_2 = \lambda_1^2 \lambda_2^2 + \lambda_2^2 \lambda_3^2 + \lambda_3^2 \lambda_1^2$ <p>Nonlinear, elastic</p>	(21)
Ogden, 1 st order	$U = \sum_{i=1}^N \frac{\mu_i}{\alpha_i} (\lambda_1^{\alpha_i} + \lambda_2^{\alpha_i} + \lambda_3^{\alpha_i} - 3) + \sum_{i=1}^N \frac{1}{D_i} (J^{el} - 1)^{2i}$ <p>$\mu_i, \alpha_i, D_i, \lambda$ material constants are determined by experiments.</p> <p>α thermal expansion, $\lambda_3 = \lambda_1^{-1} \lambda_2^{-1}$</p> <p>When $N = 1$ and $\alpha = 2$ this becomes the Neo-Hookean model. When $N = 2$, $\alpha_1 = 2$ and $\alpha_2 = -2$ this becomes the Mooney-Rivlin model.</p> <p>Nonlinear, hyperelastic, nearly incompressible</p>	(22)
Ogden, 2 nd order	$U = 2 \sum_{i=1}^N \frac{\mu_i}{\alpha_i^2} (\bar{\lambda}_1^{\alpha_i} + \bar{\lambda}_2^{\alpha_i} + \bar{\lambda}_3^{\alpha_i} - 3) + \sum_{i=1}^N \frac{1}{D_i} (J - 1)^{2i}$ <p>$\bar{\lambda}_i = J^{-1/3} \lambda_i, \quad D_i = \frac{2}{K_0}$</p> <p>Nonlinear, hyperelastic, nearly incompressible.</p> <p>Good for large deformation, >5%</p>	(23)
Neo-Hookean (SEF)	$U = C_{10}(I_1 - 3) + K_v \left[(J_2 - 1)/2 - \ln(J) \right]$ $I_1 = J - 2 \operatorname{tr}(\mathbf{F}^T \mathbf{F})/3$ <p>Finite deformation, compressible</p>	(24)

2.5. Experimental investigation of deformation

The material properties of human *in vivo* soft tissues have been studied in depth, using varying methods, populations and outcome measures, e.g. [9-11, 13, 76, 77]. However, the biomechanical behaviour of living soft tissues is complex and not fully understood [1, 9, 10, 13]. The anisotropic material structures, non-linear and hyper-viscoelastic behaviour and large deformation are challenging aspects of human soft tissues [9, 10, 13]. Furthermore, human tissue material properties have been shown to change with physiological conditions such as pathology [1, 65, 72, 78], and also with changing loading conditions due to their adaptive mechanisms [27, 66, 69, 72, 76]. Material properties also vary between and within individuals [11, 69, 72, 76, 79].

Material mechanical properties are usually derived from material response during loads, e.g., deformation measures obtained from tensile or compressive tests [59]. Properties of musculo-skeletal soft tissues have been studied *in vivo* on, for example the upper or lower arm [67, 68, 73, 77], gluteal tissues [12, 63, 64, 72, 76, 80-83], thigh [12, 74-76], intact lower limb [62, 69-71, 84], amputees' residual lower limb [11, 69, 71], and plantar soft tissues [85-93]. Despite the great many studies, no general standard methodology for living soft tissue property determination has been established [10]. In addition, these sets of property data for human populations are limited, since they are based on small samples with insufficient information of health conditions related to soft tissue load tolerance.

However, the indentation method of living soft tissue for property determination is most common among the above-mentioned studies. The indentation method is non-invasive when applied on the skin of living humans and facilitates collection of force-displacement data on the compound of tissues underneath.

A variety of human *in vivo* indentation methods have been used to determine elastic and/or viscoelastic behaviour in different subjects and soft tissue sites of the musculo-skeletal system. Methods have developed from studying the bulk of soft tissues as one homogenous, isotropic layer at the site [66, 70, 71, 84, 94] to investigating between two to five layers of up to three types of tissues [11, 12, 62-64, 68, 72-77]. The indenter geometry has varied in shape and size, the most common was axisymmetric with a tip flat ended cylinder [63, 66, 67, 69-71, 77, 84, 94], and a plate larger than tissues [12, 64, 72, 74,

76, 81, 82]. An asymmetric indenter by a cylinder was used in two studies, applied along the longitudinal axis of the fore arm and lower leg respectively while using the axisymmetric circle shape of the cylinder in the transverse plane [62, 73]. The studies applied different loading and off-loading rates and relaxation scenarios to address the nonlinear behaviour.

Different types of sensors were used to measure the indenter applied force data *in vivo*, for instance a load cell [62, 66, 69, 94, 95], photo elastic sensor [87], and optical fibre sensor [96]. Displacement was measured by different sensors, such as LVDT, linear variable differential transformer, [62, 84, 95] and electromagnetic spatial sensor [97]. Other non-invasive methods have also been used to study human soft tissues *in vivo*, e.g. optical measurements of skin [98] and digital image correlation (DIC) [99].

Medical imaging techniques such as Magnetic Resonance Imaging (MR, MRI) or X-ray Computed Tomography (CT) have commonly been used to collect geometries of internal tissues and to record undeformed and deformed human soft tissue thickness due to load, e.g. in [11, 64, 72, 87, 96, 100-102]. Open-MRI is a version where the magnets are not positioned circular around the body, but above, under and/or at sides. With Open-MRI the person can even sit or stand during the scan. Images from sitting or standing give a representation of geometries which may differ from MR in prone position due to gravity and support surfaces. However, the quality may be lower than with the closed MRI. [103] Tissue geometries in sitting and standing are also relevant when studying effects from external supports. Portnoy and colleagues used standing position in Open-MRI with amputees to capture the residual limb in a plaster-socket in non-loaded and loaded conditions [101, 102] while Linder-Ganz *et al* [64] used it for gluteal studies in sitting position. Both MR and CT give high resolution digital images of internal tissues, with the possibility to discriminate between different geometries of tissues and relative positions, both in two and three dimensions. However, the contrast resolution is up to 40% better in MR than in CT [103]. MR is considered better than CT for imaging the muscular-skeletal system, not exposing the body to radiation. [103] Ultrasound is another common clinical imaging technique, that has been combined with indentation [10]. However, MR and CT currently capture larger volumes of tissue and with higher resolution [103].

The outcome measures vary, as well as the reported tissue-specific data, which complicates comparisons and accumulation of tissue data. A collection of material parameters obtained from studies on human lower limbs (including the gluteal/buttocks, thigh and calf regions) using indentation *in vivo*, is presented in Appendix I. Studies applying exclusively small deformation models or pure viscoelastic behaviour are excluded in that list based on the focus of this thesis.

So far insufficient reference data are available for human soft tissue material behaviour. Sufficient reference data are important for comparison and identification of normal and pathological behaviour and to identify parameters for damaged soft tissue.

2.6. Computer simulations of soft tissue by Finite Element Method

Tissue loads and responses to stresses and strains within the tissue at different postures, can be simulated and analysed using the finite element method (FEM). Geometry, material properties and boundary conditions (e.g. loads) are combined fundamentals in an FE analysis (FEA) and problems are solved numerically. FEM is common in many areas of engineering and various FE software are available in computer aided engineering (CAE), e.g. for simulations during the product development process. Thus, this section begins with a basic introduction to some concepts used in FEM, and then presents briefly applications in tissue biomechanics related to soft tissues and external mechanical loading.

2.6.1. *Finite element method – a brief introduction*

In FEM, the model geometry is divided into small pieces, finite elements, on which the deformations and conditions are locally computed with approximations based on partial differential equations (PDE). Depending on the problem to be solved, the knowns and unknowns are mainly displacements, loads and constitutive relations. The results on the elements are combined to investigate the distribution over the region of interest. [104] Not only is the model geometry important, but also the way it is divided into elements, the mesh, and the element type used for representation (the

discretisation). There are many types of elements, all of which represent the approximation of the problem differently, e.g. continuum, shell, membrane elements, triangular or bilinear elements for two dimensional problems, tetrahedral and hexahedral (brick) elements for three dimensions, or the use of linear or higher order interpolations of the displacements. [104]

The displacements are evaluated at the nodes, points of the element, such as corners and defined points on element sides and in the interior. The number of nodes of the element and where these nodes are placed on the element determines how the degrees of freedom are interpolated over the element domain. The adjacent elements of a solid or plane structure are connected at their nodes, i.e. elements then share nodes and nodal coordinates. The elements of a defined geometrical part are not overlapping, and the deformation is coupled over the element borders. The stiffness and mass of an element is given by integrals which are approximated using sampling points called integration points. These are chosen so as to approximate the integrals sufficiently well; the total number of integration points thus depends on the element type as well as the size of the elements in the mesh, or mesh coarseness. [104]

In general, a coarse mesh would behave stiffer than a finer mesh, if other factors are kept constant. The accuracy will increase with larger number of elements, at the expense of computation time. Choosing type of elements and mesh refinements also requires knowledge of the problem to be simulated, the geometries, understanding of the relevant physics, material properties, loads and constraints. [104]

The Jacobian matrix is used in the FE method to map the nodal coordinates of an element in the undeformed and deformed body, the global element, to a reference element, the parent element, and keeps track of the changes. The element behaviour is described by basis functions dependent on the type of element, e.g. triangular or bilinear (square) in two dimensions. The parent element and nodal coordinates in ξ, η -coordinate system corresponds to the global element in the x, y coordinate system (Figure 6). The relationship between the points in the global element and the parent element is described by mapping functions. If these mapping functions coincide with the basis functions used in the FEM we have an *isoparametric* mapping or transformation. The derivatives of these functions describe the deformation of the parent element at the chosen points and are collected in the Jacobian

matrix, J . This transformation can then be applied to obtain the deformation of the global element. It is easier to compute the integrals on the bilinear parent element than on the global element, thus this method is commonly used in FEM. [104]

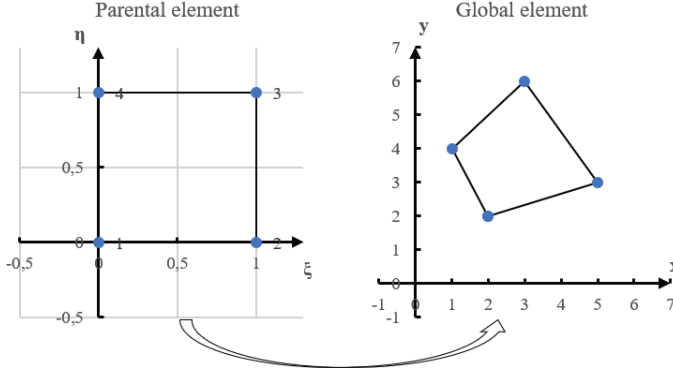


Figure 6 Transformation node-to-node, Isoparametric mapping

Jacobian matrix

$$J = \begin{bmatrix} \frac{\partial x}{\partial \xi} & \frac{\partial x}{\partial \eta} \\ \frac{\partial y}{\partial \xi} & \frac{\partial y}{\partial \eta} \end{bmatrix} \quad (25)$$

And with the chain rule

$$\begin{bmatrix} dx \\ dy \end{bmatrix} = \begin{bmatrix} \frac{\partial x}{\partial \xi} & \frac{\partial x}{\partial \eta} \\ \frac{\partial y}{\partial \xi} & \frac{\partial y}{\partial \eta} \end{bmatrix} \begin{bmatrix} d\xi \\ d\eta \end{bmatrix} \quad (26)$$

Thus

$$\begin{bmatrix} d\xi \\ d\eta \end{bmatrix} = J^{-1} \begin{bmatrix} dx \\ dy \end{bmatrix}. \quad (27)$$

The Jacobian J is the determinant of J ,

$$J = \det J \quad (28)$$

This J measures volume change between reference and physical element in the same way as the determinant of the deformation gradient \mathbf{F} measures physical volume change, cf. eqs. (13)-(15).

2.6.2. FEM in tissue biomechanics

The use of FEM computer simulations has grown in biomedical engineering [105, 106], biomechanics and PI research [1, 79, 100, 101, 106-114]. FEM is in the context of deformation often used to analyse the impact of external

loading on internal human soft tissues, e.g. in the musculo-skeletal-system [15, 72, 100, 101, 115-117], as in the lower limb tissues [11, 15, 101, 109, 114, 118-120]. The concept of patient-specific modelling (PSM) has occasionally been introduced and applied in clinical practice, and is predicted to grow [105]. Computer simulations with FEM are often used to derive material properties by optimization of parameters and reverse engineering from undeformed and deformed tissue geometries while applying chosen material models [12, 72, 74, 88, 120-123].

Geometry

The developed digital models of the anatomy of the individual body tissue's geometries, are often based on images captured by different scanning techniques, such as MR, and CT (see also chapter 2.5). However, the level of geometric detail in soft tissue models of the body segments studied have so far been low. It is common, even in recent studies, to merge (in FEA literature the term *lump* is used) soft tissues together into few layers in two or three types [11, 62, 110] even if individual muscles have separate layers [11, 12]. The level of detail in geometry was developed further with separate regions for skin, fat, muscle, inter-compartment walls, and vessel walls in the leg in [124] and with fat and four muscles of the thigh in [74, 75]. As stated by Moerman *et al* it is of high importance with individual specific geometries of soft tissues in finite element analyses (FEA) [34]. The differentiation of material layers in an FE-model has an impact on the mechanical responses [104]. Thus, it is important to consider how the tissues are geometrically represented, when evaluating the simulation results.

Material properties

The complexity of human soft tissue is a challenging aspect in computer simulations, e.g. by the configuration of tissue layers, and their various behaviour. When tissue types are lumped together in FEA, they are assigned one material type and material property, for simplicity and computational reasons. It is common to model the soft tissues in two or three material types, such as skin, fat, skin/fat, and muscle, even if individual muscles have separate layers [11, 12, 74, 75]. In contrast to those, the model reported by Rohan *et al* in 2015, used separate properties for skin, fat, muscle, inter-compartment walls of connective tissue, and vessel walls to study effects of compression stockings [124].

Many material models are available in FEM software and have been applied to models of human tissues, as described in chapter 2.4. The specific mechanical material properties need to be determined before applying the material models. Experimental data and optimisation by reverse engineering to find the parameters have been used, as described in chapter 2.5. In reverse engineering the material models are chosen, and the material properties of related parameters determined. Differences in identified material properties, e.g. for the transtibial tissues in Appendix I, highlights the importance of representative material properties and models in specific simulations.

Boundary conditions

The loading (forces, temperature load etc), contact conditions (friction, bonded, slip etc), and known boundary displacements, are set by boundary conditions according to the chosen situation for the simulation. Examples of boundary conditions for soft tissue situations, such as interface contact stresses on the skin, have been addressed for instance by physical measurements of surface pressure [65, 119, 125, 126], by indentation as explored in chapter 2.5, and by change in positions of external supports [76, 127, 128]. Challenges remain in defining realistic boundary conditions, e.g. external loads, anatomical displacements of interacting tissues, shear forces and friction between tissue layers and/or external supports and loads on blood vessels. Contact pressures can also be set as outcomes from the simulation, as recently reported by Cagle *et al* for interaction between prosthetic liners and residual limb skin in amputees [110].

Verification

These kinds of computer simulation models are useful tools but need to be calibrated, verified and validated for their representativeness of the problem at hand [15, 104, 129, 130]. Experiments of tissue behaviour can be used for such validation and verification [1, 13, 14, 114].

2.7. Position in the Industrial Product Realisation context

Knowledge about soft tissue behaviour when exposed to loads is important for decisions regarding body-interacting products, such as standardized products as well as custom made products. Thus, processes within product realisation are involved.

The process in industrial product realisation (IPR) is considered a broad concept which includes product and production development as part of the innovation and product life cycle (Figure 7), as described by Säfsten and Johansson in 2005 [131]. To realise an idea of a product to meet set goals, there have to be strategies, research, development and planning prior to the production. Understanding of the user and usage of the product is essential.

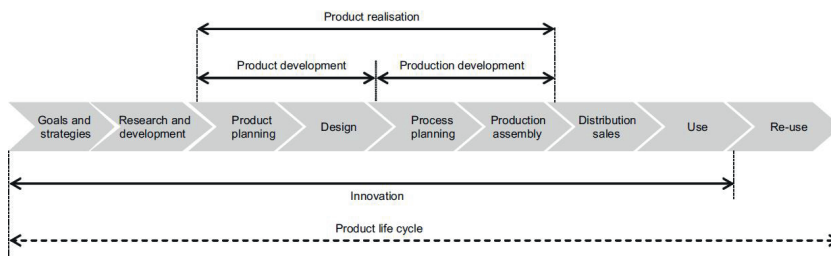


Figure 7 The product realisation process: part of the innovation process and product lifecycle (fig 1.3. p.6. in [131] from Säfsten and Johansson, 2005)

Examples of standard products interacting with human body segments are chairs, car seats, shoes, handheld tools/machines and sports-gear. Examples of customized or individually custom-made products to assist and improve the biomechanical functionality for the individual are prostheses, orthoses and wheel chairs.

The applications of knowledge of soft tissue behaviour and deformation in the product development process in product realization for products interaction with the body are suggested in Figure 8 (modified from exhibit 2-2, p.14 in [132]). Suggested parts involved are highlighted in bold letters under each phase of the process. Briefly it can be described as follows. In planning of a new product, we look at research, development and new technologies, and

continue with investigating the predicted user and usage. Different concepts of designs are developed and evaluated, in relation to the interaction with the user and usage. Options and requirements are refined, and a detailed design is decided including production possibilities. In industry, prototypes of the product are tested in different ways and further improvements are implemented, before the production begins. Computer simulations are often applied during the process. With knowledge of soft tissue behaviour and representative simulation models, the prediction ability contributes to refinements during the development process, as well as failure assessments in case of breakdown of a used product. This should eventually contribute to prevention and decrease of PI.

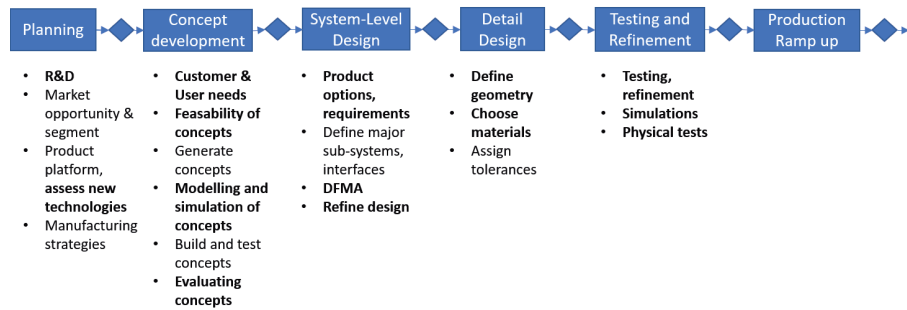


Figure 8 Product development process related to soft tissue material properties (R&D research and development, DFMA design for manufacturing) Adopted and modified from exhibit 2-2, p.14 in [132]

2.8. Rationale

Soft tissue response to loads is complex, as the framework by Coleman *et al* shows [3]. The research regarding human soft tissue behaviour has focused mainly on mechanical responses in small samples and used diverse methods and behaviour representation. Techniques for measuring deformation in specific tissue layers at the site on the living human are not established. The individual specific situation is important and since there is a lack of data it is hard to compare outcomes between studies. Some differences in tissue response between healthy subjects and subjects with a pathological condition have been reported [69, 72], which highlights the need for health-related descriptors when reporting human reference data.

The simulation models that have been used for investigation of soft tissue internal conditions due to loads, or to obtain material parameters, are simplifications of the problem studied. The simulation models are simplified in geometry, material property representation and contact conditions, and use a diversity of material models, boundary conditions and deformation measures. It is unclear how these simplifications influence the results and how accurate the simulation represents the situation studied. Thus, it is difficult to compare results, interpret, generalize and apply to a clinical situation.

It is especially important to understand the individual's soft tissue status and tolerance to load, when managing a body-interacting product such as prosthesis or orthosis. Present clinical assessment tools are not capable of assessing deep tissue status and their response to external load. Hence, there is a need for improved analyses and measures of individual-specific soft tissue behaviour, which include risk factors for pressure injuries whether pathological conditions are present or not. Since tissue deformation in live humans is complex, there is a need for research that includes both mechanical and biological aspects. This research and thesis attempt to do so.

3. Research approach

3.1. Scope and delimitations

The problem of soft tissue damage is complex and a multidisciplinary approach should be useful to increase the possibilities for exploration and understanding. This research addresses several aspects of the PI framework by Coleman *et al* [3], which are marked by red boxes in Figure 9. The approach combines mechanics, material science, biomechanics, medical imaging techniques, and FEM.

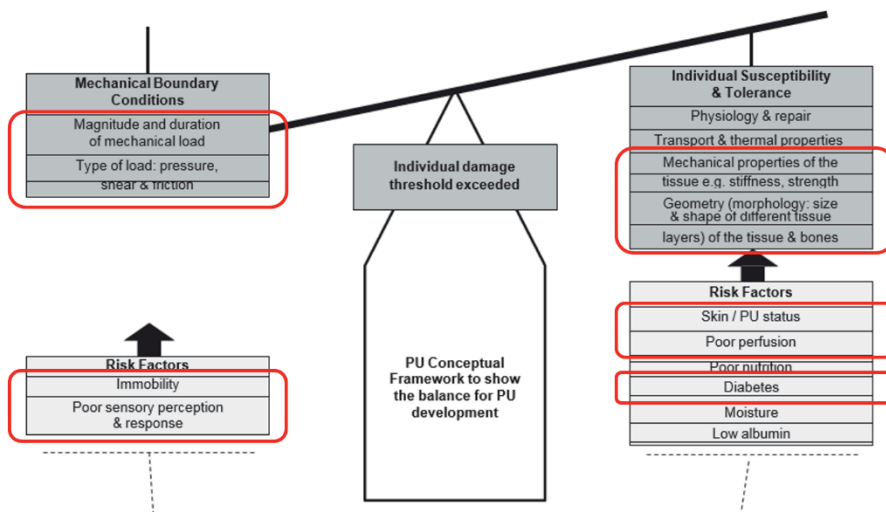


Figure 3 New pressure ulcer conceptual framework.

Figure 9 Application of the PI framework by Coleman *et al* [3] (p.2232, figure 3) to this research. Addressed aspects are marked with red boxes.

The overall aim of this research is to investigate aspects of deformation in human soft tissue of the leg when exposed to external loading.

This aim was addressed by the following research questions (RQ):

RQ 1. How does differentiation of soft tissues in a simulation model influence internal strains and stresses analysed by FEM?

With focus on the representation of fascia tissue separately compared to when combining fascia with muscle tissue in a model of the lower leg

RQ 2. How could individual-specific internal soft tissue deformation be measured in separate tissues *in vivo* under established health condition?

With focus on indentation induced mechanical deformation in relaxed tissues of the posterior lower leg in an individual subject while including health condition and soft tissue assessment

RQ 3. What are the individual-specific deformations of human *in vivo* soft tissue such as skin, muscles, fat, connective tissues, and vessels?

With focus on the measures developed in RQ2, and obtained from the relaxed tissues of the posterior lower leg in a subject without pathology

In this research, the lower leg has been addressed at the macro and meso levels in Figure 3. The soft tissues skin, subcutaneous fat, superficial and deep fascia, individual muscles and large blood vessels are included. Aspects of mechanical conditions as well as individual specific health and the leg's soft tissue condition related to pressure injury tolerance are addressed, see Figure 9.

Several factors were excluded in order to focus the research. Examples of delimitations related to the complexity of the studied problem were time dependence, dynamic loading, muscle activity monitoring including modelling of such activity. Skin moisture, thermal properties or reactions to thermal load were also excluded. Thus, viscosity and thermodynamics were not addressed. Blood flow was not measured as such, only indirectly by blood pressure and skin examination.

The research was part of the multidisciplinary research project PEOPLE, *PrEvention Of Pressure uLcers and dEep tissue injury by optimization of body tight external supports*. PEOPLE is a collaborative project between the School

of Engineering and the School of Health and Welfare at Jönköping University, and three companies in the field of prosthetics, orthotics and medical technology: Ottobock Scandinavia, Össur HF and Hotswap Nordic. The project is jointly financed by the partners and the Jönköping Regional Research Programme, Sweden.

3.2. Research perspective and strategy

The research addressed conditions when human soft tissue is exposed to load. The research perspective is positivistic with deductive reasoning [133].

Different research designs have been used in this work to address the aim and RQs. Consequently, the research in this thesis is divided into two studies. To address RQ1 the Study I was developed, a computer simulation with FEM, to study the effect of different material representation of soft tissue on internal mechanical conditions.

Study II was developed as part of a larger study design for investigation of live human soft tissue deformation and damage. Study II addressed RQ2 and RQ3 in a case study with physical experiment to investigate deformation behaviour in live human soft tissue exposed to load, under established health conditions determined by survey techniques.

An overview of the research approach is presented in Figure 10, while the respective study's design, chosen methods and instruments are presented in separate chapters below. Ethical considerations are addressed in chapter 3.5.

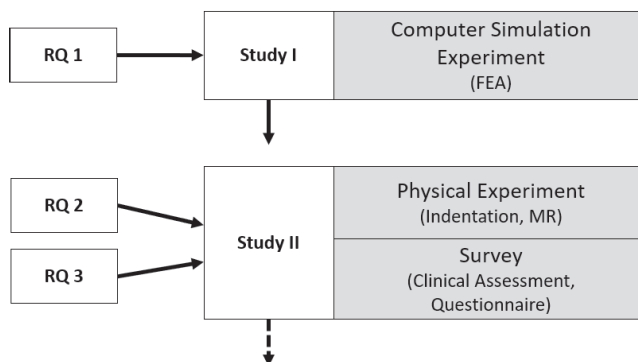


Figure 10 Overview research approach. Note: RQ= research question. FEA= finite element analysis, MR= magnetic resonance

3.3. Study I

3.3.1. *Research design*

As addressed in Chapters 2.2, 2.5 and 2.6, previous studies performing FEA of the lower limb tissues used quite simplified models with few layers and/or tissues lumped together [15, 101, 114, 118-120]. This raised the question as to whether it is necessary to include tissues on a more detailed level, and research question RQ1 was formulated.

The study design was a simulation experimental study using computer models and comparisons for sensitivity analysis.

The simulation study using FEA was performed with the aim to investigate the mechanical effects of two sets of representations of lower leg soft tissues exposed to external load. In this study five soft tissue types and the skeletal bones were represented with respective anatomical regions and material properties. The two sets of soft tissue materials compared were representing the six tissue types separately or with the fascia and muscle combined. The hypothesis was that there would be clear differences in mechanical outcomes of tissue stresses, strains and computed contact pressures between the two material sets used in the models.

A manuscript is generated based on this study, available at arXiv.org, to be submitted [134].

The simulation models and FEA are described below, structured by model geometries and mesh, material properties, boundary conditions, analysis scheme and chosen output.

3.3.2. *The Finite Element Model*

The geometry for the leg model was developed from an generic anatomical illustration of the lower leg transverse plane, (a trans-tibial cross section, page 98 in [17]). The two-dimensional model included separate regions for skin, subcutaneous fat, superficial and deep fascia, muscles, blood vessels and bones, (Figure 11). The dimensions of the leg model were adjusted to adult size.

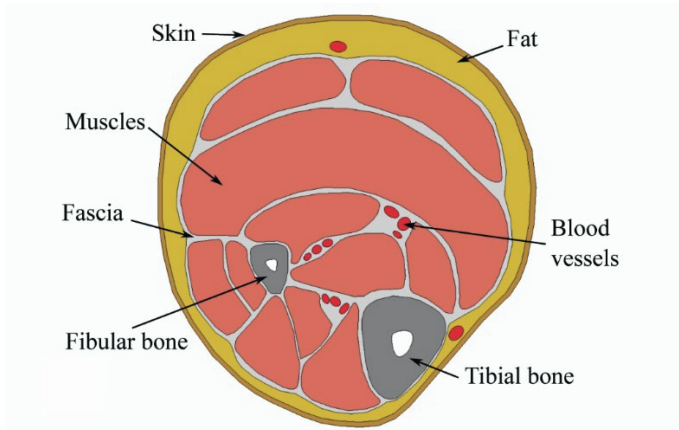


Figure 11 The FE model geometry for the trans-tibial cross-section of a human adult, divided in separate regions according to anatomical tissue type. Each tissue type is here assigned a colour, as labelled.

As loading conditions, transtibial prosthetic socket designs were chosen as an example of FEA application for tissue deformation studies (see also 2.6.2). A transtibial prosthesis is an artificial leg substitute for transtibial amputees. The prosthesis consists of a hard socket with a liner on the residual limb, a pylon as lengthening and connections to a prosthetic foot. The transfer of load between the residual limb skeleton through the soft tissues and the prosthetic socket is provided by the geometrical shape of the hard socket and the liner and padding inside the hard socket in conjunction with the type of anchoring system to the limb. Different trans-tibial socket designs have been used over the years, as presented by Fergason and Smith, 1999 [135]. The patella tendon bearing concept (PTB) changed into the total contact and later into total surface bearing designs. The total contact concept socket applied pressure on weight tolerant areas and provided contact without load bearing on intolerant areas including the distal end of the residual limb. The total surface bearing concept on the other hand, required weight bearing contact all over, distributed pressures more evenly, however with more on tolerant areas but no off-loading of bony regions. The type of liner used in total surface bearing sockets contributed to force distribution and socket-skin interaction. The third concept, the hydrostatic socket, was based on fluid dynamics by Pascal's principle which states that the pressure at a point in an incompressible fluid at rest in a closed container is the same in all directions. A pressure change at one region will be transmitted without loss to the whole fluid. The hydrostatic

socket would not have specific weightbearing areas, instead equal pressure uniformly distributed over the whole limb area, but slight relief at tibia distal end and fibular head [135].

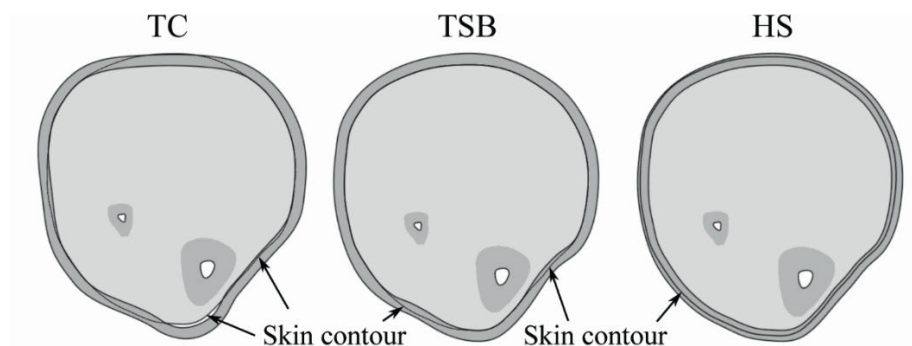


Figure 12 The cross-section geometries of socket models and limb overlap. The socket designs: TC = Total contact concept, TSB = Total surface bearing concept, HS = Hydrostatic concept. Sockets and bones are represented by dark grey, soft tissues by light grey. The contours of the limb and socket models are shown by black lines.

In this FEA study the definitions of these three prosthetic concepts by Fergason and Smith [135] were used for geometries, named total contact socket (TC), total surface bearing socket (TSB) and the hydrostatic socket (HS). The socket concepts were not evaluated, only used as different load cases. The models for the socket designs were created from the skin external line of the leg cross section model and a socket material thickness of 4.5 mm, simulating a check socket cross-section at that site of the leg, thus a 2D test. The shapes of the three sockets' cross-sectional designs were determined by the author according to the literature [135] and clinical practice. The socket models overlapped the leg model in accordance to clinical practice, as illustrated in Figure 12. The area inside the HS socket-cross section was reduced 5% as a possible amount according to clinical practice of 3-6% volume reduction depending on an individual's tissue conditions.

The software Abaqus 6.14-3/Standard (Dassault Systèmes) was used for building the model. The choice of elements was based on the assumption of plane strain, and were of types: 8-node biquadratic plane strain quadrilateral, hybrid, linear pressure, and 6-node quadratic plane strain triangle, hybrid, linear pressure elements (CPE8H and CPE6H in Abaqus [136], respectively).

The limb model mesh contained 26 330 elements, while the socket models around 3000 elements each.

3.3.3. *Material properties*

To study the effect of having differentiated tissue layers or combining two of them together, two sets of the materials were used in the analysis, called the separate and combined set respectively. In the separate set, each of the tissue type regions (see Figure 11) had separate material properties, while in the combined set muscle and fascia tissue regions shared the same properties based on a combination of the two, while the other tissues had unchanged material properties. Selected material properties per tissue type listed in Table 2, were retrieved from literature, while the combined material property of fascia and muscle were obtained by a calibration analysis with optimisation of material parameters, as described later in the chapter.

The availability of material data for live soft tissue in a human leg is limited. Thus, an inclusion guide for choosing data was made. Data for each tissue type should be based on experimental data, retrieved from compression experiments and be available in the transverse plane if possible, due to the 2D plane of the FE model. If optimisation with FEM had been used to retrieve parameters, the continuum material representation was chosen. The soft tissue data with parameters for the Ogden first order model was preferred, when available. The Ogden model for slightly compressible materials was chosen since it is considered good for large deformations, accounts for non-linear behaviour and is commonly used to model human soft tissues. However, blood vessels and bones were chosen as linear elastic materials, due to their different structure. The reason for using few models was to keep the variation in material models low.

The Ogden strain energy potential is expressed by equation 22 in Table 1 as

$$U = \sum_{i=1}^N \frac{\mu_i}{\alpha_i} (\lambda_1^{\alpha_i} + \lambda_2^{\alpha_i} + \lambda_3^{\alpha_i} - 3) + \sum_{i=1}^N \frac{1}{D_i} (J^{el} - 1)^{2i} \quad (22)$$

where U is the strain energy per unit of reference volume, μ_i are shear moduli in direction i , α_i and D_i are material constants, N is the order of the equation, λ_i are the deviatoric principal stretches and J^{el} is the elastic volume ratio.

The polynomial strain energy potential is expressed in Yeoh form by equation 20 in Table 1 as

$$U = \sum_{i=1}^3 C_{i0}(I_1 - 3)^i \quad (20)$$

when incompressibility is assumed. Here C_{i0} are material dependent parameters, I_1 is the first deviatoric strain invariant as $I_1 = \lambda_1^2 + \lambda_2^2 + \lambda_3^2$, $\bar{I}_1 = J^{-2/3}I_1$, where J is the total volume ratio, and λ_i are the principal stretches.

Thus, in the separate material set the skin, fat muscle and fascia were modelled as hyperelastic, isotropic materials by strain energy potentials using the Ogden or Yeoh model. Skin, fat and muscle regions were represented by the Ogden first order model, with properties obtained for skin and fat from Payne *et al* [137], and muscle from Al Dirini *et al* [12], while the fascia was represented by the Yeoh model. The Yeoh model was chosen based on a curve fitting process of human crural fascia experimental data extracted from figure 3 in Pavan *et al* [138]. In order to determine parameters and coefficients, the curve fitting was performed using the free software Hyperfit 2.X (Faculty of Mechanical engineering, Institute of solid Mechanics, Mechatronics and Biomechanics, Brno University of Technology Czechia). The vessels and blood were represented together as linear elastic material. The chosen properties depend on the blood pressure and volume. With the Young's modulus of 10 kPa the maximum pressure in the vessels was predicted to be 14.7 kPa, after the contact was established between socket and skin. This pressure, equivalent to 110 mmHg, was in the range of normal blood pressure. The tibia bone was assumed to be linear elastic and isotropic, with a Young's modulus of 11.8 GPa based on transverse loading of the tibial bone [139]. The fibula bone was assumed to have the same properties.

The socket material, glycol-modified polyethylene terephthalate (PETG), was chosen based on its use in prosthetic check sockets, and material data for the use in this context were obtained from Gerschutz *et al* [140].

Table 2 Material properties

Material for tissue region	Material model	Parameters and coefficients	Reference
Skin	Ogden 1 st	$\mu_1 = 220.0 \text{ kPa}$, $\alpha_1 = 12$ $D_1 = 9.12 \times 10^{-8} \text{ Pa}^{-1}$	[137], [141]
Fat	Ogden 1 st	$\mu_1 = 1.700 \text{ kPa}$, $\alpha_1 = 26$ $D_1 = 1.18 \times 10^{-5} \text{ Pa}^{-1}$	[137], [142]
Muscle*	Ogden 1 st	$\mu_1 = 1.907 \text{ kPa}$, $\alpha_1 = 4.6$ $D_1 = 1.05 \times 10^{-5} \text{ Pa}^{-1}$	[12]
Fascia*	Yeoh	$C_{10} = 4.91 \text{ MPa}$ $C_{20} =$ 13.59 MPa $C_{30} =$ 18.97 MPa	Modified from [138]
Combined Muscle-Fascia**	Ogden 1 st	$\mu_1 = 12.0 \text{ kPa}$, $\alpha_1 = 14$ $D_1 = 1.67 \times 10^{-6} \text{ Pa}^{-1}$	
Blood vessels	Linear, elastic	$E = 10.00 \text{ kPa}$ $\nu = 0.49$	
Cortical bone	Linear, elastic	$E = 11.80 \text{ Pa}$ $\nu = 0.394$	[139]
Sockets, PETG	Linear, elastic	$E = 459 \text{ MPa}$ $\nu = 0.4$	[140]

*Note: D_1 is computed from μ_1 and $\nu=0.495$, according to equation 3.273, p.85, chapter 3 in Silber and Then [9]. *separate material properties used in the detailed set, **combined material properties used for the fascia and muscle regions in the combined set.*

For tissue configuration comparison purposes, a second material set was composed containing the same materials except for fascia and muscle, since they are often lumped (merged) together as one tissue type. Different strategies could be applied to represent the lumped tissues' material property: a) fascia is also assigned muscle properties (i.e. fascia is ignored), or b) find a combination of the two materials' properties. In this study, strategy b) was used when the two tissue types muscle and fascia were assigned the same material property which was a combination of both. The Ogden model was chosen for this new material property since muscle tissue had the largest area of the two. In order to find the parameters for the combination of the fascia and muscle properties, a specially designed calibration simulation was performed as an indentation test (Figure 13). As reference, the limb model with the separate tissue properties was exposed to a displacement load, and the reaction force-displacement data at a point on the skin surface were

collected for the reference curve. Then, the fascia and muscle regions were assigned the new material, and a heuristic optimization process was performed by systematically altering the coefficients of the new material, repeating simulations and compare the new reaction force-displacement curves to the reference, until a good curve fit was reached (right-hand graph in Figure 13). The two material sets were now resulting in the same reaction force during the displacement. The final coefficients were determined for the material called Combined Muscle-Fascia, and used for both the fascia and muscle regions, see Table 2. The material set using the combined muscle-fascia material while the other regions kept their properties was called Combined in the following analyses.

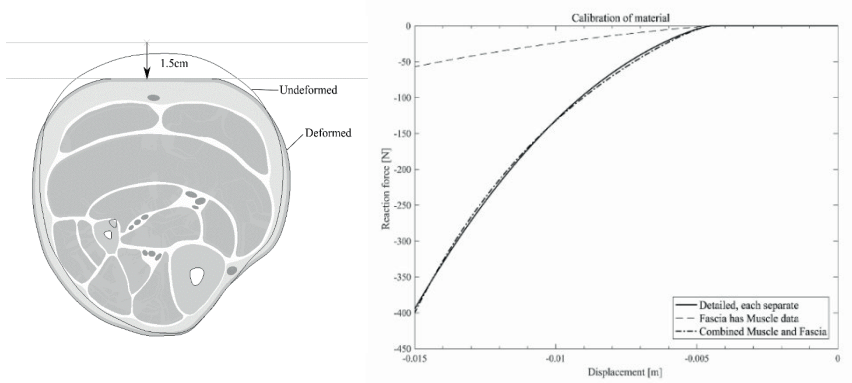


Figure 13 Calibration of material data sets. Left: Calibration model and applied displacement, Right: Reaction force-displacement curves with varying properties for muscle and fascia.

3.3.4. Boundary conditions

In the limb model, the inner border of the tibia was fixed, while the other regions could move. The fibula bone was free to move, which occurs in trans-tibial residual limbs without a bone bridge [143, 144]. The socket models overlapping the limb model were generating load, and no additional load was applied. This overclosure of models was gradually solved by a contact algorithm over multiple steps. The contact surfaces were pushed apart until the overlapping penetration disappeared. As the overclosures were resolved,

stresses and strains appeared in the socket and the limb cross-sections. Discretization was used for surface to surface contact conditions, which considered the shape of both surfaces in the region of contact. The coefficient of friction for the skin-PETG socket interface was assumed to be 0.4 [145]. The internal regions of the limb model shared nodes and thus no further contact conditions were applied.

With these constraints the 2D analysis did not include body weight nor any dynamic load from walking etc. The three different socket shapes were used for generating different loads and internal effects.

3.3.5. *Procedures for analyses*

The software Abaqus 6.14-3/Standard (Dassault Systèmes) was used for building the model and running analyses with an implicit solver. This software for computer-aided engineering (CAE) provides a high level of complexity and control of simulations.

In total six FEA runs were performed, displayed in Table 3, with two per socket type; one with the detailed material set and one with the combined set applied to the limb model. This test scheme was chosen to explore the effects of changing level of differentiation in tissue models under varying loading conditions.

Table 3 Test scheme for FEA: Material set and Socket condition

Loading condition by socket type	Material set condition		Comparison Relative change
	A Separate	B Combined	
1. TC	A1	B1	A1, B1
2. TSB	A2	B2	A2, B2
3. HS	A3	B3	A3, B3

The chosen output for comparisons included distributions of stresses, strains and contact pressures. The logarithmic strain (3) was used. The analyses of results were grouped by the type of output measures.

The sites of maxima and minima of stresses and strains per tissue type were evaluated to determine absolute maximum magnitudes and to identify extreme values or singular nodal values to ignore. The maximum level was determined when at least five nodes from two adjacent elements reached that level in absolute value. These evaluations were performed in order to determine

magnitude values for comparisons to investigate the outcome differences between the used material sets. The relative change with the separate material set condition (A) as reference was used for comparisons, according to

$$Relative\ change(x, x_{reference}) = \frac{x - x_{reference}}{|x_{reference}|} \quad (29)$$

3.4. Study II

3.4.1. Research design

Study II addressed RQs 2 and 3 focusing on individual-specific *in vivo* behaviour of human soft tissues when exposed external load. Since tissue's load tolerance seems individual-specific and related to health condition [3], a selection of health parameters were included for reference. The study addressed aspects in the framework for pressure injury development [3] as marked in Figure 9.

A case study design was used with one subject. Data collection techniques included a quasi-experiment provoking mechanical load on tissues and survey by self-reported questionnaires and clinical assessment protocol.

An overview of the process within the PEOPLE project for addressing mechanical and biological aspects of the PI framework is shown in Figure 14. The parts addressed by Study II is marked with a red frame. Based on Study II, when geometrical and tissue property data exist, individual-specific FE models can be developed, and simulations verified. The overall goal of the whole process, when several subjects with diverse health conditions have been studied, is to determine both mechanical and biological parameters of importance for soft tissue behaviour and then develop simulation models for optimization of individual specific products.

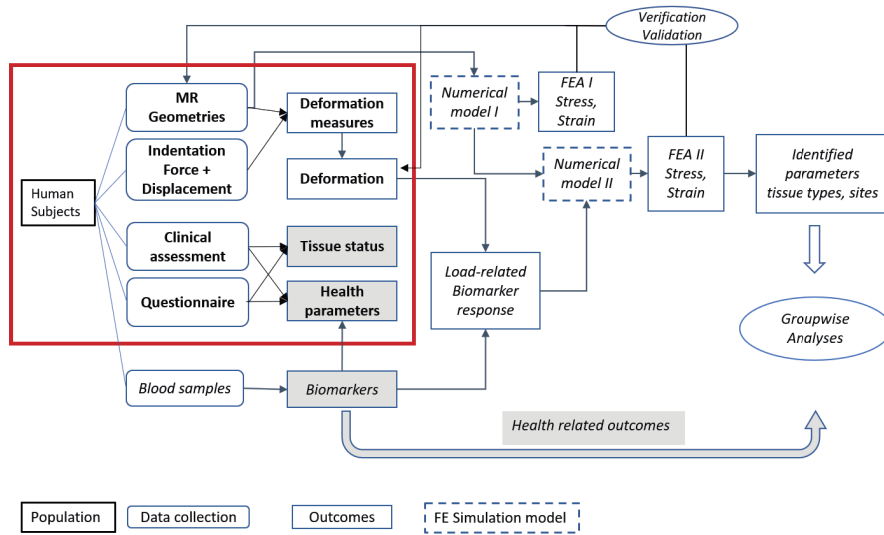


Figure 14 Schematic process of research, as part of PEOPLE. Red border mark included parts in Study II. Note: MR: magnetic resonance, FE: finite element, FEA: finite element analysis

In Study II, individual-specific mechanical deformations of soft tissue layers in the lower leg were obtained from geometries collected by MR and controlled loading using a specially developed indentation equipment. A questionnaire for self-reported health and a clinical assessment protocol were used. Health data from the questionnaire provided information regarding the individual's status in general and on the day of testing. The skin, soft tissue condition, neuro-muscular function and blood pressure were physically assessed.

Except for the indentation intervention, the chosen methods, such as MR, blood pressure, and clinical physical assessment, are commonly used diagnostic methods in health care. These were selected based on literature reviews of research in soft tissue properties, PI/DTI, prosthetics and orthotics and on experience within the research group.

The case study was performed with one healthy subject to investigate the feasibility of the methods. The recruited subject gave informed written consent before participation. The data collection was performed on day 1, with follow-up day 2 and 4. Ethical considerations are addressed in Chapter 3.5.

Further descriptions of the methods are presented in the following subchapters.

3.4.2. Equipment for deformation by indentation in MR

Geometries of the leg tissues were captured by a MR scanner of type 1.5 Tesla, Optima MR450w, GE Medical systems, provided by Aleris Röntgen Jönköping, Sweden. The scanner was operated by a radiology technician. Deformation was induced by an applied force through indentation on the calf posterior tissues. The non-loaded and loaded tissue states were obtained by MR technique. The indentation equipment was developed for the study and is described below.

A force-displacement instrument, TIM, Tissue Indenter Measurement (Figure 15), was developed for this study in collaboration with Hotswap Nordic AB, Jönköping, Sweden. The construction of TIM was restricted due to compatibility with MR and ethical considerations related to risk of harm during management. It was important that the loading device could be controlled manually, adjusted to the individual's comfort, and safe, i.e. not lose control due to break down/flaws in the control system. The indenter should be attached to a frame fixated on the limb to restore same position in non-loaded and loaded condition. In the loaded condition the indenter should be locked at a chosen position, with the measuring systems then detached. The indenter was T-shaped, with a half cylinder of length 70 mm and radius 10 mm.

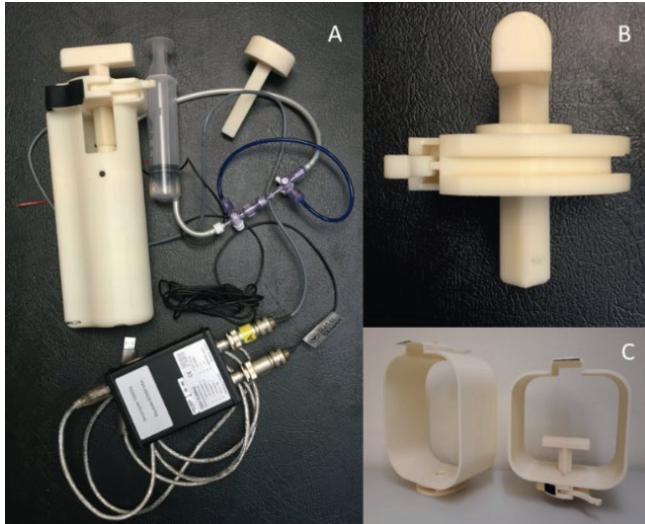


Figure 15 TIM Tissue Indenter Measurement device for indentation and force-displacement data. A: TIM device with two indenters (T-half cylinder and puck versions), water syringe and transducer. B: Indenter (T-version, radius 10 mm) in locking mechanism, lateral view. C: TIM attachment frames of two sizes and the T indenter and locking mechanism assembled

In TIM, a load sensor (KM26z) and a displacement sensor (linear potentiometer) with range 0-150 mm (LRW2-F-X-S) were connected to a closed water pressure system including a polymer piston and a water syringe to control the indenter movement while measuring force and displacement. Reaction force and displacement sampling rate was 10 kHz with baudrate 625 kbit/s transformed via the measurement amplifier (GSV-3USBx2). The load sensor, displacement sensor and measurement amplifier came from ME-Systeme, Hennigsdorf, Germany, www.me-systeme.de. An in-house developed software in Matlab 2016b, (MathWorks, Natick, MA, USA) processed the TIM measurements. The indenter, housing, locking mechanism and fixation frames of two sizes (Figure 15) were manufactured in the thermoplastic material Acrylonitrile butadiene styrene, ABS, (ABSplus-P430 from Stratasys Ltd, www.stratasys.com) by additive manufacturing (3D-Printer fused deposition modelling FDM, machine model: Dimension SST1200ES, Stratasys Ltd, US, www.stratasys.com) at the School of Engineering, Jönköping University, Sweden.

The load cell was first separately calibrated by CA Mätsystem, Täby, Sweden, a SWEDAC accredited laboratory. The measured force was then calibrated at the School of Engineering, Jönköping University, with TIM assembled and the puck-shaped indenter (Figure 15A) carrying the weights. Calibration on the day for data collection was performed with a solid steel cylinder (mass 1000g, manufactured at the School of Engineering, Jönköping University) and the puck-indenter at the MR clinic.

Friction at the interface of skin and indenter, μ_s , was measured using a small box of the same ABS material as the indenter, a cylinder of solid steel, and a dynamometer (Sauter FL100, Sauter GmbH, Balingen, Germany) attached to the box with a hook. The total mass for the box and steel cylinder was 515.4 g. The box and steel cylinder were manufactured at the School of Engineering, Jönköping University.

A body support assembly including an individual specific leg-shell was developed to ensure that the same leg position of non-loaded and loaded conditions were captured by the MR scans (Figure 16). It consisted of an ABS thermoplastic base plate (thickness 6 mm) with attached foam cushions for bilateral thigh and foot supports and straps. A rectangular cut-out on the side of the base plate gave room for application of TIM. The hips were positioned in 20° flexion, and the tibia crest was horizontal. The foot support cushions held the feet in a neutral position, supporting the back of the heels with 22 cm between heel centres. This position allowed the calf tissues to be relaxed, non-loaded, and with space for TIM. A polypropylene U-shaped shell stabilized the foot cushions. The foot cushion position could be adjusted relative to the subject's height to achieve a controlled and comparable leg position during the different testing conditions. An individual specific plaster shell was made and placed anteriorly on the leg to fixate hip and knee angles and for attaching the TIM frame. A flat cushion under the thorax and pelvis was used for comfort. The frame for fixating TIM was mounted on the plaster shell at the point of load application by fixing it to a 8 mm thick plastic plate in the plaster over the tibial crest (Figure 16, Figure 17). The indenter was, with this TIM fixation, applied vertically and perpendicularly to the tibia crest at the thickest part of posterior soft tissues of the calf. The goal was to apply force perpendicular to skin surface and bone axis. A reference point of the TIM centre position in the MR images was defined by attaching a vitamin E capsule

to the top of the frame which would be detected on the MR scans. With this equipment the same body position was achieved for MR scans and TIM measurements, in non-loaded and loaded conditions.



Figure 16 Body support, leg fixation and TIM with frame fixture. Subject prepared for MR scanning

3.4.3. Clinical assessment

A clinical assessment protocol was developed to capture conditions in the lower leg (Appendix II). In summary, it consisted of different body and segment structural measurements, range of motion and muscle strength, neurological status, circulatory items (e.g. skin temperature, skin colour and pulses), and soft tissue conditions. Pain was documented based on palpation and questions to the subject. Potential skin problems present were classified according to the NPUAP/EPUAP International Classification of Pressure Ulcers [7, 21, 146]. Soft tissue structures, shape and behaviour were assessed by inspection and palpation, and described both according to ISO 8548-2 [8] and new descriptor terms also related to material properties.

The new descriptors were divided into five characteristics with scale levels:

- I. **Thickness:** Thin / Normal / Thick
- II. **Firmness:** Compact / Muscular / Oedema / Stiff
- III. **Flaccid:** Atrophic / Rich of fat / Paralytic

- IV. **Elasticity** (returning to initial shape): Low resistance / Moderate resistance / High resistance
- V. **Plasticity** (remaining shape change): Small elongation or compression / Moderate / Large

A goniometer, tape-measure, calliper, monofilament (10g), tuning fork and reflex hammer were used. The surface temperature of the skin at several sites from proximal to distal lower limb, and at the site of the indentation, was measured during the clinical assessment using a laser thermometer (Optris MS Plus, Optris GmbH, Berlin, Germany).

Blood pressure was measured at upper arm (brachial) and ankle respectively, with a manual cuff and a laser doppler probe. The ankle and brachial pressures were collected for the Ankle Brachial Pressure Index (ABPI), a clinical measure related to blood circulation and ischemia in the lower limb and used for diagnostic purposes [147].

The clinical assessment protocol was developed iteratively, in collaboration with experienced CPOs (certified prosthetist-orthotist) and tested on persons with neuromuscular pathologies by two CPOs.

3.4.4. Questionnaire

A self-reporting questionnaire was constructed to collect information on current health conditions (Appendix III). The intended target group included persons without pathologies, persons using a prosthesis or orthosis, and persons with type 2 diabetes. The questionnaire consisted of demographic information and then three parts with subsections, as displayed in Table 4. Both generic and targeted items were included.

Table 4 Questionnaire structure

Part	Subsection	Instrument	Source
I	A.Health and function in daily life.	RAND-36, Swedish version	Register Centrum SydOst http://rcso.se/patientmedverkan/prom/generiska-instrument/rand-36sf-36/
	B.Diseases, infections, other health conditions	Background variables, items constructed for this study	unpublished
	C.Other circumstances	Background variables, items constructed for this study	unpublished
II	D.Assistive devices	Combined from SwedeAmp National register and constructed items based on literature	http://www.swedeamp.com/ and [45, 47, 148-150]. Adapted by S. Kallin (author)
	E.Leg and feet function and status	OPUS Orthotics and Prosthetics Users' Survey, section BFF plus two items* constructed for this study	OPUS [151-154], * unpublished
	F.Problems and pain due to prosthesis or orthosis	NPUAP/EPUAP International Classification of Pressure Ulcers and items constructed for this study.	[7, 21, 45, 146] Adapted by S. Kallin (author)
III	G.Follow-up after indentation	Questions constructed for this study	S. Kallin (author)

RAND-36 is a validated instrument that measure health-related quality of life [155] and was chosen to facilitate comparisons of participating subject's

health conditions with populations from other studies. Part I-B contained health questions regarding inflammatory diseases and infections, and were constructed by a member of the research team based on previous research on biomarker responses [156]. Part I-C contained items on sensitive skin, sensation in lower extremities and medication. Part II contained items related use of prosthesis or orthosis and were excluded in this case study. The subject's experience during the indentation test and the 3 days after, was addressed in Part III.

The development process of items in the questionnaire for this research incorporated experience from the target population and the prosthetist/orthotist profession. It was iteratively tested for content and face validity.

3.4.5. *Human subject*

For this case study, a subject without pathology was of interest before recruiting individuals who are to a higher degree exposed to external loads and/or with increased risk for PI/DTI.

Inclusion criteria for recruitment was physically healthy persons aged 25 to 65 years. Current pressure injuries of grade I-II elsewhere than the indentation site were accepted.

Exclusion criteria were: inability to walk independently, immunological disease, diagnosed and medicated circulatory conditions, dermatological pathology, vulnerable skin, eczema, current pressure injury of grade III or worse, pregnancy during the last 12 months due to influence on connective tissue properties, long-term or current severe pain. Also, implants with magnetic ferrite or electronics were excluded for incompatibility with the MR.

One healthy subject was recruited for data collection with the developed experimental set up in this study. The recruited subject was a 27 years old male, height 189 cm and body mass 86.0 kg.

3.4.6. *Data collection procedure*

The data collection, including position preparations, was held at an MR clinic on day 1, with a total duration of 6 hours, with follow-up at a health clinic on day 2 and a phone call on day 4. The clinical assessment and indentation measurements were conducted by a certified prosthetist-orthotist (the author).

Blood pressure was monitored by a nurse and the MR scanning was performed by a radiology technician.

The protocol sequence for day 1 is displayed in Appendix IV while a description is provided here.

Day 1 Clinical assessment and blood pressure for the base line conditions were obtained initially. The skin at the site of indentation was untreated during the tests. Skin temperature and friction skin/TIM indenter was measured at baseline.

The determined body position for the MR and TIM data collection was prepared and secured as described in chapter 3.4.2. Before the first MR scanning the subject had a relaxing period of 15 minutes to walk etc.

Non-loaded and loaded conditions were captured by MR and TIM. The load by TIM was applied (Figure 17) and measured outside the MR room.



Figure 17 Loaded condition. The TIM frame connected anteriorly to the plaster shell. The TIM mounted to the frame and the T-shaped indenter applied. Body support was moved sideways to facilitate TIM to be mounted and collect measurements.

The applied load was limited to a duration of 30 minutes static load while not exceeding 30N, in order to comply with the proposed limit of pressure-time loading by Gefen [28, 29]. The force was assumed to be constant in the line of action through the tissue layers. The indenter was locked and fixed, and the magnetic sensitive section of TIM dismounted before the MR scanning of the loaded condition.

A body coil was placed over the legs to improve the signals and MR image quality compared to when only the tunnel coil is used, while keeping the

scanning duration shorter for the sake of subject's comfort. Two MR image sets per condition were captured consisting of 30 slices each: one set with T1 weighted (T1 Tra) and one set of STIR (short T1 inversion recovery, with suppressed fat signals). The latter was primarily used for identification of blood vessels. Both sets were transversal scans with 4 mm slices, no axial gaps and a field of view (FOV) of 40 cm to capture both legs and with resolution of 512. An additional set of images in longitudinal direction was captured per condition to determine the indenter position in relation to tibia proximal end, and corresponding slices in the non-loaded set. The first MR scanning duration was 20 minutes and the second lasted 10 minutes.

Repeated blood pressures were collected, once just before first MR non-loaded condition, once after the second scanning with indentation applied, and after removal of indentation force another three times: at 5, 60 and 120 minutes after, see Appendix IV. The subject's comfort was carefully monitored during the whole process. The skin at the indentation site was inspected repeatedly after TIM was removed.

Day 2 The follow-up on the day after the indentation test included assessment of the lower limb, questionnaire items and blood pressure.

Day 4 follow-up was carried out by a phone-call. If the subject experienced load-related symptoms further clinical assessment were prepared, including appointment with a medical practitioner, if wished. If unexpected pathology was suspected in the data, the research team should consult a physician for further actions.

3.4.7. Data processing

Identification of anatomy

Tissue displacements, strains in tissue layers by stretch ratios, volume change and a local deformation gradient determinant ($\det \mathbf{F}$) were chosen deformation measures. Thus, a selection of geometrical landmarks' coordinates and measurements had first to be identified and collected from the MR images. The MR images were analysed in MediaViewer (GE Healthcare) and Mimics Research 20.0 (Materialise, Leuven, Belgium). The DICOM (Digital Imaging and Communications in Medicine) coordinate system was used, with positive x-axis towards the left side of body, a positive y-axis in the posterior direction, and a positive z-axis in the proximal direction. Identification of tissues in the MR image depends on the resolution and image quality. The voxel size became $0.7813 \times 0.7813 \times 4.00 \text{ mm}^3$ with the resolution 512 and FOV of 40 cm.

Since the soft tissues of the calf should be non-loaded, air space was present between the lower legs and the MR table. Because of this, the images were unevenly illuminated. In order to improve the illumination of images for analyses, image filtering processes were applied and evaluated in the open source image processing package Fiji, which is developed for different types of medical images (<https://imagej.net/Fiji>). The illumination could be evened, but at the expense of structural details. With various kinds of filters, the skin disappeared, internal muscles' and vessels' borders and thin connective tissues became undetectable, while tissue layers with larger contrasts were exaggerated and became thicker. Thus, the raw images were used for analyses, without image pre-processing.

Deformation data

The corresponding transversal MR image slice of the non-loaded condition to the image slice at centre of the displaced indenter in the loaded condition was identified by distance measures from corresponding landmarks in sagittal view. The pair of corresponding MR images in transverse plane is shown in Figure 18, A before indentation, and B with indenter applied.

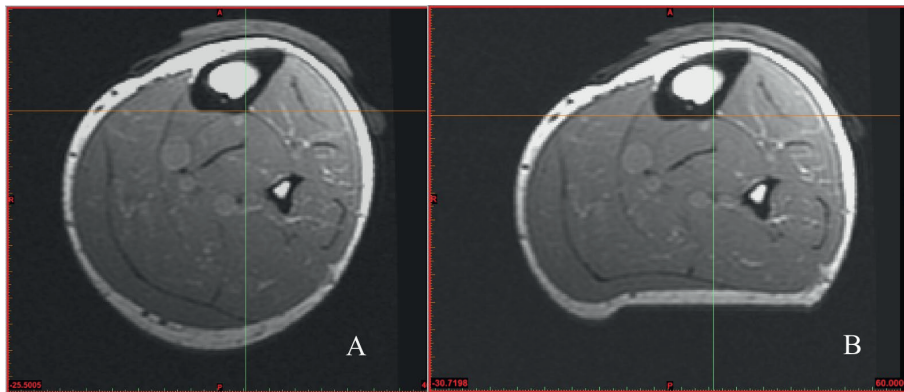


Figure 18 MR images of non-loaded (A) and loaded (B) conditions at the slice of indenter apex. The visible y and x axes intersect at the centre, the origo, of the defined local coordinate system.

Deformation measures were obtained by analysing the MR images in Mimics Research 20.0 software. The following items were identified in both conditions to be used for further analyses: a) sagittal distance between the tibia plateau and maximum indentation, b) reference points on the tibia and fibula

defining centre, an origin for a local coordinate system and lateral bone side angles, c) the centre line of TIM indenter along the y-axis of image, d) separate tissue border positions along the centre line of the indenter along the y-axis, e) a local internal quadrilateral polygon on the lateral aspect of gastrocnemius muscle's lateral head, and f) the skin outer boundary was marked for the limb cross-sectional area which was then calculated by the Mimics software.

The coordinates of the defined reference points were obtained to calculate distances, displacements and stretch ratios (eq. 2). The bone angles were control measures for correspondence between the two image slices. The area measures and slice thickness gave the data for the volume ratio J (eq. 14).

The local internal quadrilateral polygon (e), marked on a muscle region close to the indenter, was chosen based on the ease of identifying the same corner points in the non-loaded and loaded conditions. Based on the local test-element coordinates, FEM was applied on this 2D test-element with isoparametric mapping. The local deformation gradient \mathbf{F} and the deformation determinant J^{FEM} was computed in the centroid of the element, using Matlab 2016b (MathWorks, Natick, MA, USA). The analysis process was as follows.

The centroid of the parent element in the ξ, η -coordinate system was determined at $\xi=1/2, \eta=1/2$ when $0 \leq \xi \leq 1$ and $0 \leq \eta \leq 1$.

The basis functions, $\varphi(\xi, \eta)$, for the bilinear parental element, with the nodes $i=(1,2,3,4)$ were then:

$$\varphi_1 = (1 - \xi)(1 - \eta)$$

$$\varphi_2 = \xi(1 - \eta)$$

$$\varphi_3 = \xi\eta$$

$$\varphi_4 = (1 - \xi)\eta$$

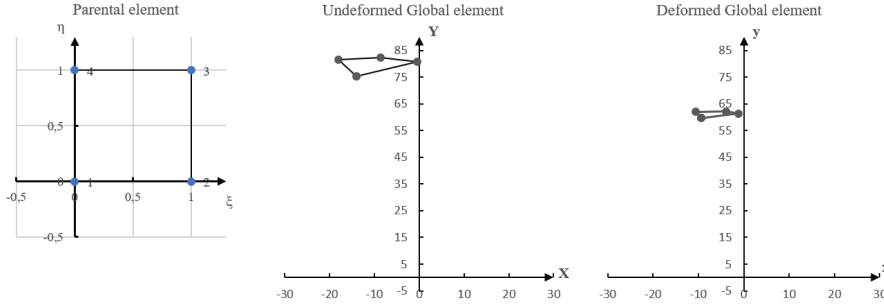


Figure 19 Mapping from parent to global domain. From left to right: parent element, undeformed and deformed test element from the data set.

At large deformation the analysis needs to include both the undeformed element and the deformed element. Isoparametric mapping was used (Figure 19). This was processed in three steps: 1) compute the change, derivatives, on the parental element, 2) transform that by isoparametric mapping to the undeformed global element, and then to the global deformed element. 3) The deformation gradient on the global deformed element can then be computed, and finally the determinant of the deformation gradient can be determined for the deformed global element. The defined nodal coordinates of both undeformed and deformed element were known and used for the numerical solution, X, Y , and x, y respectively. Shape functions for the global elements are noted $\phi(x, y)$.

- 1) Change on the parental element in 2D by partial derivatives of the basis functions:

$$\begin{aligned}\frac{\partial \varphi_i}{\partial \xi} &= [(\eta - 1) \quad (1 - \eta) \quad \eta \quad -\eta] \\ \frac{\partial \varphi_i}{\partial \eta} &= [(\xi - 1) \quad -\xi \quad \xi \quad (1 - \xi)]\end{aligned}$$

- 2) Mapping X and Y to ξ and η , by $X = \sum_{i=1}^4 X_i \varphi_i$ and $Y = \sum_{i=1}^4 Y_i \varphi_i$

And transformation, Jacobian matrix,

$$J = \begin{bmatrix} \frac{\partial X}{\partial \xi} & \frac{\partial X}{\partial \eta} \\ \frac{\partial Y}{\partial \xi} & \frac{\partial Y}{\partial \eta} \end{bmatrix}$$

$$\begin{bmatrix} \frac{\partial \phi_i}{\partial \xi} \\ \frac{\partial \phi_i}{\partial \eta} \end{bmatrix} = \mathbf{J}^T \begin{bmatrix} \frac{\partial \phi_i}{\partial X} \\ \frac{\partial \phi_i}{\partial Y} \end{bmatrix}$$

where ϕ refer to the functions for the global element,

$$\text{and the gradient of the global element is } \nabla_X \phi_i = \begin{bmatrix} \frac{\partial \phi_i}{\partial X} \\ \frac{\partial \phi_i}{\partial Y} \end{bmatrix} = \mathbf{J}^{-T} \nabla_\xi \phi_i$$

- 3) The determinant of the deformation gradient on the deformed element is

$$\det \mathbf{F} \approx J^{FEM} = \det \begin{bmatrix} \sum_{i=1}^4 \frac{\partial \phi_i}{\partial X} \cdot x_i & \sum_{i=1}^4 \frac{\partial \phi_i}{\partial Y} \cdot x_i \\ \sum_{i=1}^4 \frac{\partial \phi_i}{\partial X} \cdot y_i & \sum_{i=1}^4 \frac{\partial \phi_i}{\partial Y} \cdot y_i \end{bmatrix} \quad (30)$$

TIM data

External force and displacement data from TIM were analysed in Matlab 2016b, by force-time, displacement-time and force-displacement. Time was here applied for identification of corresponding events, not time-dependence behaviour.

Friction data for the interface skin-TIM indenter were analysed, mean force calculated, and the kinetic friction determined.

Clinical assessment

BMI was calculated by

$$BMI = \text{body mass}/(\text{height})^2 \text{ [kg/m}^2\text{]} \quad (31)$$

Ankle brachial pressure index, ABPI, was obtained by the ratio ankle systole/arm systole.

The functional status and determined tissue conditions were collected for descriptive use in this study. Geometrical measures were collected for image identification and descriptive purposes.

Questionnaire data

Data was manually transferred to a digital file. Only Part I-A from RAND 36 were processed with scores in the eight domains: PF Physical functioning, RP

Role limitations due to physical health, BP Bodily Pain, GH General health perceptions, VT Energy/Vitality, SF Social functioning, RE Role limitations due to emotional health, and MH Mental health.

3.5. Ethical considerations

This research has considered the ethical principles to respect autonomy, do good, not harm, be justice [157] and the World Medical Association Declaration of Helsinki [158].

Study I was using a simulation model based on a generic illustration of human anatomy of the lower leg. This was a chosen strategy to not involve a human subject unnecessarily.

Study II is part of the research project PEOPLE that involves persons, dealing with sensitive personal information and biological material from humans. Ethical approval was obtained for PEOPLE by Linköping Regional Ethical Review Board (No 2015/397-31) according to the Swedish Act (2003:460).

The use of provocation studies in medicine is common, and ethically justified by the possibility to increase knowledge of pathophysiology, treatments and diagnostic utility [159]. In the PEOPLE project the outcomes are expected to increase knowledge and understanding of pressure injuries and for decreasing and prevention of those when optimizing products. Study II combined existing and developed data collection techniques in a new protocol and applied it for feasibility initially on one subject without pathology.

Recruitment of the participant was handled by the author, using advertisement to respect the individual's autonomy. Written and oral information was given. Written informed consent was obtained before participation, emphasizing the voluntariness and possibility to withdraw without giving reason or suffering negative consequences. Participant was insured by the project and offered a small remuneration.

The indentation test used in Study II were expected to give none to minor soreness in the tissues during the tests and 2-3 days after. The indenter was manually controlled to decrease the risk of unexpected force application due to equipment failure and to respond to participant's comfort. MR scanning is a clinical procedure and information given accordingly. Possible discomfort

during MR scanning was considered and diminished. The test could be stopped at any time.

Answering the questionnaire was considered no risk of harm to participants. There was a risk that a pathological condition not previously known to the subject could be detected or suspected based on the findings in the collected data. If this would occur, an appointment with a physician (free of charge to the subject) was prepared for in collaboration with a health centre.

All collected data (such as sensitive personal information according to Swedish Act (2003:460) and (1998:204)) were handled confidentially and secured to avoid unauthorized access for protection of participant. The results are presented in such a way as to prevent the risk of identifying the participant.

An agreement between the partners in PEOPLE project regulates issues like the interests of parties, collaboration, use of data, immaterial rights, publications and ownerships including after the end of the agreed period. Financial support is regulated in the agreement. The data is owned by the School of Engineering, Jönköping University. There is no conflict of interest identified.

4. Results

In this chapter the results are presented per study in relation to the research questions (RQs). Results from the FEA simulation of a lower limb model, study I, with comparisons of soft tissue responses depending on material representations, are first presented. Individual specific physical deformation of soft tissues in the lower leg and clinical measures are then presented for study II.

4.1. Study I

Study I addressed RQ1:

RQ 1. How does differentiation of soft tissues in a simulation model influence internal strains and stresses analysed by FEM?

With focus on the representation of fascia tissue separately compared to when combining fascia with muscle tissue in a model of the lower leg

The simulation exposed the limb models to three socket designs while the material representation of soft tissues was altered using two material sets. The Separate set and the Combined set accounted for fascia and muscle tissues in diverse ways. The ranges of maximum magnitudes per outcome are presented shortly to report the level of those outcomes. The results of comparisons by distribution and by relative change are presented grouped by the effective stress (vonMises) and shear stress, while the logarithmic strains as absolute maximum principal strain (AMP) and shear strain. The influence of the material sets on the computed contact pressures at the interface of skin and PETG socket are also presented per condition, which represent the effective load.

4.1.1. Comparisons of stresses and strains

The stresses and strains in the soft tissues changed considerably with the Combined set, compared to when the Separate set was applied, for the three socket conditions. The distributions of internal stresses (Figure 20) and strains (Figure 21) per material set and socket condition showed changes of sites for maximum values and of magnitudes. Magnitudes of determined maximum

effective stress per tissue type ranged between 0.91 kPa found in vessels to 1120 kPa in fascia regardless material set and socket condition. Determined maximum shear stress ranged between 0.28 kPa in vessels to 500 kPa in fasciae. For absolute principal strain (AMP) per tissue type the determined maximum ranged between 5.7% in fasciae to 49.5% found in muscle, while for shear strain that ranged between 8.0% in vessels to 84.1% also found in muscle tissue. The high-end levels in these ranges were all found in results from the conditions with Separate material set. The identified magnitudes of maxima data are provided in Appendix V.

The sites for maximum effective stress were found in fascia with the Separate set while in skin with the Combined material set applied, regardless socket condition. The sites for maximum strains were found in muscles with the Separate set for all sockets. When the Combined set was applied, the sites for strain maxima varied by socket condition: in TC and HS both strain measures maxima were found in fat. In the TSB condition the AMP was found in muscles while maximum shear strain was found in vessels.

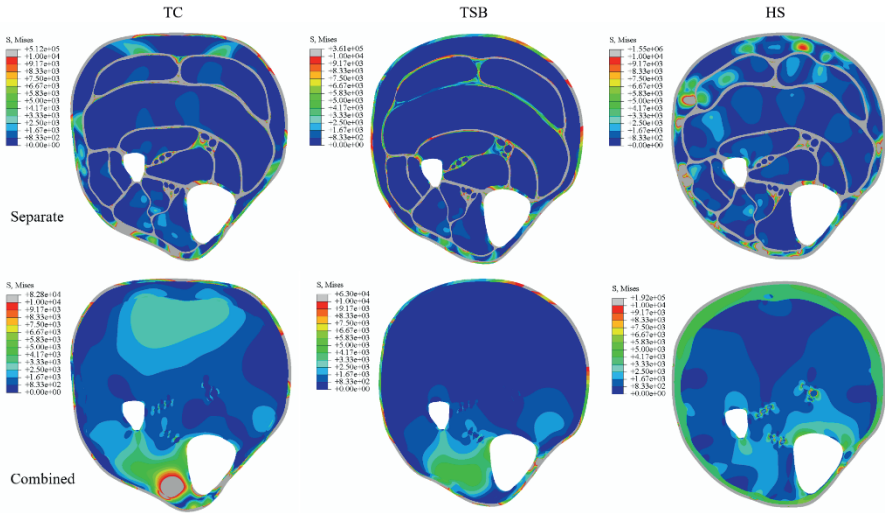


Figure 20 Effective Stress S (vonMises) in [Pa], displayed distribution per material set and socket design. Upper row: Separate set, lower row: Combined set. Socket designs: TC Total Contact, TSB Total Surface Bearing, HS Hydrostatic. Coloured scale limited to 0-10 kPa, with grey over 10 kPa.

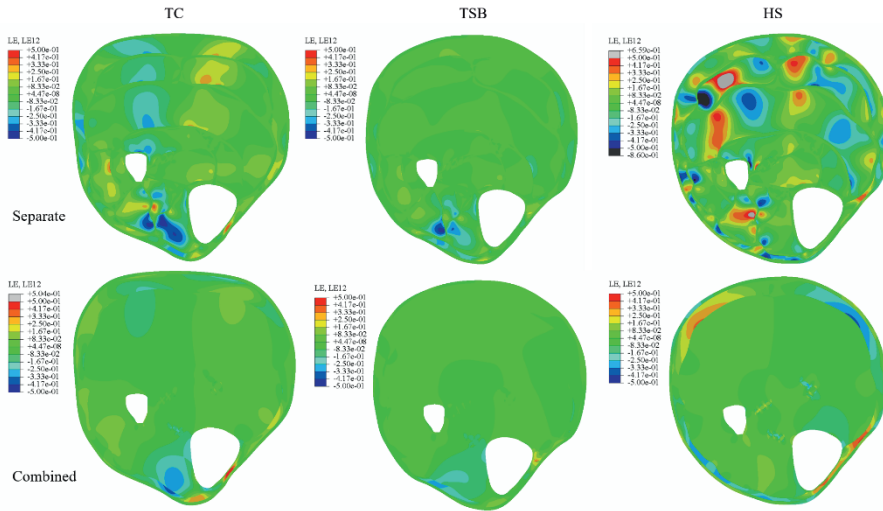


Figure 21 Shear Strain distribution per material set and socket design. Upper row: Separate set, lower row: Combined set. Socket designs: TC Total Contact, TSB Total Surface Bearing, HS Hydrostatic. LE12 Shear strain. Coloured scale limited to $\pm 50\%$, with black below -50% and grey above 50% . Negative and positive show opposite strain directions.

The comparisons of maximum values per tissue and per site, by relative change in percent (eq.29) with the Separate set as reference, are displayed in Table 5, Table 6, Figure 22, Figure 23 and Figure 24. The relative change of maximum stresses per tissue type and socket condition increased the most by 459% for effective stress and decreased the most by -599% for shear stresses in muscles with TC socket, when using the Combined set, compared to the Separate.

The relative change of strains increased the most by 202% for shear strain in fat with the HS socket and decreased the most by -253% for shear strain in vessels with the TC and HS socket conditions. Comparisons per material set at their respective sites of maximum in each tissue type, (noted as Max Separate and Max Combined) showed even larger increase and decrease, and other distribution of the changes over the tissue types (Figure 23, Figure 24).

Table 5 Relative change of stresses for comparison Combined to Separate set

Tissue	Site	Socket	TC		TSB		HS	
			Effective stress	Shear stress	Effective stress	Shear stress	Effective stress	Shear stress
Skin	Max Separate		51%	40%	13%	216%	-5%	6%
	Max							
	Combined		51%	40%	13%	216%	78%	6%
Fat	Max both		51%	40%	13%	216%	15%	6%
	Max Separate		-73%	74%	-7%	34%	-89%	100%
	Max							
Muscle	Combined		367%	294%	124%	152%	54%	68%
	Max both		17%	250%	19%	234%	-64%	117%
	Max Separate		40%	-212%	164%	-160%	-79%	112%
Fasciae	Max							
	Combined		837%	-853%	507%	-245%	1224%	-22800%
	Max both		459%	-599%	173%	-165%	23%	23%
Vessel	Max Separate		-99%	99%	-99%	99%	-100%	-100%
	Max							
	Combined		270%	92%	78%	49%	-40%	88%
Vessel	Max both		-93%	97%	-93%	98%	-98%	-99%
	Max Separate		0	-22%	47%	83%	2%	132%
	Max							
Vessel	Combined		339%	-445%	47%	83%	938%	-1400%
	Max both		35%	-251%	47%	83%	72%	-221%

Note: TC: total contact, TSB total surface bearing, HS hydrostatic. Effective and shear stress.

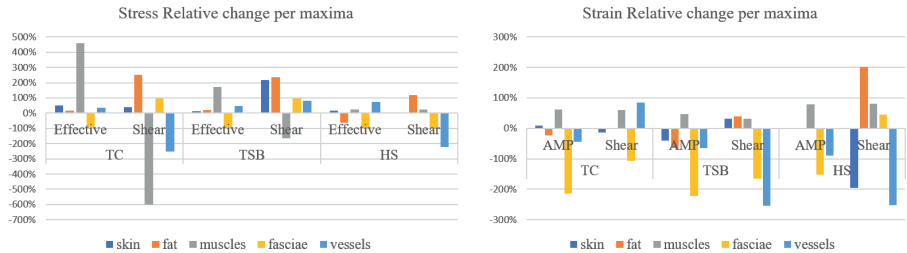


Figure 22 Relative change of maxima, per tissue type, for Combined set compared to Separate set. An increase with Combined set is displayed by positive change in percent. Left: Stresses. Right: Strains. TC Total Contact, TSB Total Surface Bearing, HS Hydrostatic. Effective stress, shear stress, MPA maximal principal absolute value, shear strain



Figure 23 Relative change of stresses per sites of maxima and tissue types. Separate set as reference. Upper panels display full ranges, lower panels show limited ranges. An increase with Combined set is displayed by positive change in percent. Left: Effective Stress. Right: Shear stress. TC Total Contact, TSB Total Surface Bearing, HS Hydrostatic. Max Separate: at site for maximum with the Separate set. Max Combined: at site for maximum with the Combined set.

Table 6 Relative change of strains for comparison Combined to Separate set

Socket		TC		TSB		HS	
Tissue	Site	AMP	Shear strain	AMP	Shear strain	AMP	Shear strain
Skin	Max Separate	-15%	33%	10%	-14%	1%	-196%
	Max						
	Combined	-250%	33%	10%	-14%	1%	-196%
Fat	Max both	-40%	33%	10%	-14%	1%	-196%
	Max Separate	-55%	37%	-17%	12%	23%	78%
	Max						
Muscle	Combined	-69%	39%	-23%	-57%	-36%	28%
	Max both	-64%	39%	-23%	-1%	0%	202%
	Max Separate	74%	54%	62%	61%	89%	103%
Fasciae	Max						
	Combined	21%	11%	35%	51%	-10%	-15900%
	Max both	47%	31%	61%	60%	78%	81%
Vessel	Max Separate	-10%	-47%	-60%	-29%	23%	-45%
	Max						
	Combined	-12833%	-1360%	-9070%	-4409%	-1511%	1250%
Vessel	Max both	-223%	-164%	-215%	-107%	-152%	46%
	Max Separate	-12%	-32%	-44%	79%	-34%	120%
	Max						
Vessel	Combined	-172%	-417%	-44%	93%	-874%	-1310%
	Max both	-66%	-253%	-44%	86%	-89%	-253%

Note: TC: total contact, TSB total surface bearing, HS hydrostatic. AMP Absolute maximum principal



Figure 24 Relative change of strains per sites of maxima. Separate set as reference. Upper panels display full ranges, lower panels show limited ranges. An increase with Combined set is displayed by positive change in percent. Left: Strain Absolute Maximum Principal, AMP. Right: Shear strain. TC Total Contact, TSB Total Surface Bearing, HS Hydrostatic. Max Separate: at site for maximum with the Separate set. Max Combined: at site for maximum with the Combined set.

4.1.2. Comparisons of contact pressures

The computed skin-socket interface contact pressure changed in magnitude per material set used, and by site of maximum by socket condition (Figure 25). The relative change of maximum contact pressures increased with the Combined set in all socket conditions, by 134%, 58% and 37% for TC, TSB and HC respectively. The distribution of contact pressures at the skin-socket interfaces in the six conditions are displayed in Figure 25.

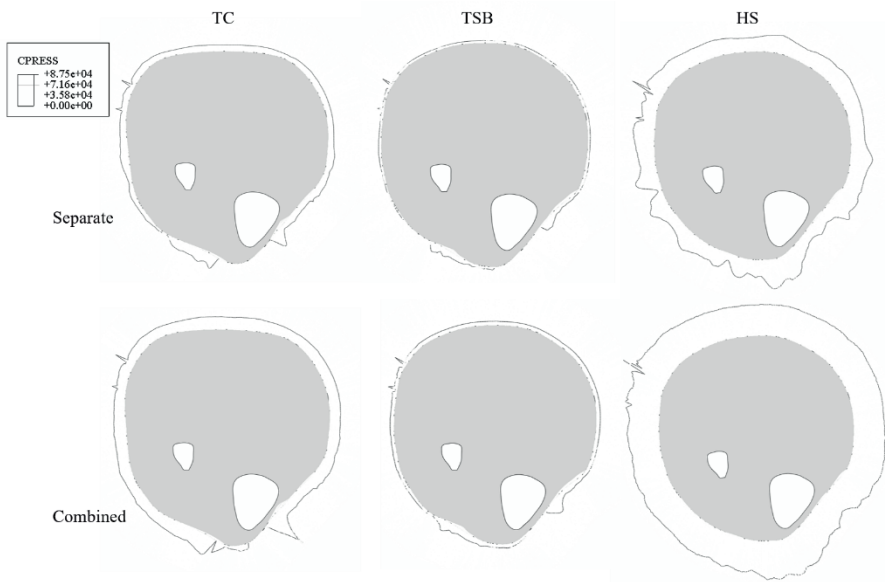


Figure 25 Contact pressure distribution [Pa] at skin-socket interface with three socket designs and two material sets, Separate and Combined set. The magnitude of the contact pressure is represented by the line and its distance from the grey limb model. TC Total contact, TSB Total surface bearing and HS Hydrostatic. The spikes at lateral/posterior region were excluded from comparison, as they are singular nodal values due to border definition.

4.2. Study II

Study II addressed the research questions RQ 2 and 3 demonstrated with one subject without pathology:

RQ 2. How could individual-specific internal soft tissue deformation be measured in separate tissues *in vivo* under established health condition?

With focus on indentation induced mechanical deformation in relaxed tissues of the posterior lower leg in an individual subject while including health condition and soft tissue assessment

RQ 3. What are the individual-specific deformations of human *in vivo* soft tissue such as skin, muscles, fat, connective tissues, and vessels?

With focus on the measures developed in RQ2, and obtained from the relaxed tissues of the posterior lower leg in a subject without pathology

The data collection techniques in this study were controlled indentation in MR, a questionnaire for self-reported health and a clinical assessment protocol. Tissue types and layers on meso level were identified in the transverse plane of the relaxed lower leg.

The outcome measures of the case study were subject-specific deformations of identified soft tissues in terms of displacements, stretch ratio λ , Jacobian determinant J , local deformation gradient determinant $\det \mathbf{F}$ and external reaction force-displacement data. Individual specific numerical results are provided.

The subject-specific health conditions were studied in terms of self-reported health, functional status and clinical measures of soft tissue status. These are here presented prior to the deformation results to provide insights of the subject's health conditions and soft tissue status related to the tissue response, as suggested in Figure 9 framework for PI development.

4.2.1. Subject specific health conditions

The subject was a 27 years old male, height 189 cm, weight 86 kg and BMI of 24. Self-reported health by RAND36 was in respective domain scored PF 100, RP 100, BP 70, GH 65, VT 50, SF 75, RE 67, MH 60. The subject reported no immune system related diseases, inflammation nor sensory defects, no diabetes of any type and was not smoking. Subject reported the skin to be moderate irritable if exposed to wear.

Neuromuscular function of the lower extremities was good bilaterally, with full range of motion, muscular strength of M5 and sensation of S4 on the Medical research council (MRC) scale. Subject was physically active and exercising at least three times per week.

The circumferential measure of the left leg at the site of indenter application was 380 mm, the depth (anterior-posterior) 110 mm and width (medio-lateral) 120 mm. Volume was normal. The skin of the lower leg was without remarks. Lower leg soft tissues were also evaluated by manual palpation in terms of thickness, structural aspects, and elasticity/plasticity. Each tissue type was considered normal in relation to age and BMI. Details of tissue conditions is presented in Table 7. Skin temperature at the site for indenter was at baseline 30.2°C.

Table 7 Results palpation of lower leg soft tissues

Tissue	I: Thickness	II: Firmness	III: Flaccid	IV: Elasticity	V: Plasticity
Skin	Normal	Compact	Rich of fat	Moderate	
Subcutaneous fat	Thinn				
Muscle	Normal	Muscular		Moderate	
Relaxed					
Muscle	Normal	Muscular		Moderate	
Contracted					
Tendons, ligaments	Normal	Compact		Moderate	
Forefoot pads	Normal	Compact		Moderate	
Heel pad	Normal	Compact		Moderate	
Other					

Note: Application II or III, IV or V. Levels: I: Thinn / Normal / Thick, II: Compact / Muscular / Oedema / Stiff, III: Atrophic / Rich of fat / Paralytic, IV: Low resistance / Moderate resistance / High resistance, V: Small elongation or compression / Moderate / Large.

Blood circulation evaluated by skin coloration, pulses and skin temperature was consider normal. The blood pressure was varying during the test at repeated measures from baseline to 2 hours after offloading, displayed in Figure 26 (test sequence described in Appendix IV). The brachial pressure and the ABPI were respectively 138/75 mmHg and 1.0 at baseline, 122/59 mmHg and 1.13 just before indenter was applied, and 140/80 mmHg and 1.04 when measured after MR with load still applied. Brachial blood pressure data 5 minutes after off-loading was missing, while the ankle pressure decreased to

125 mmHg. The last brachial blood pressure was 118/72 mmHg 2h after off-loading.

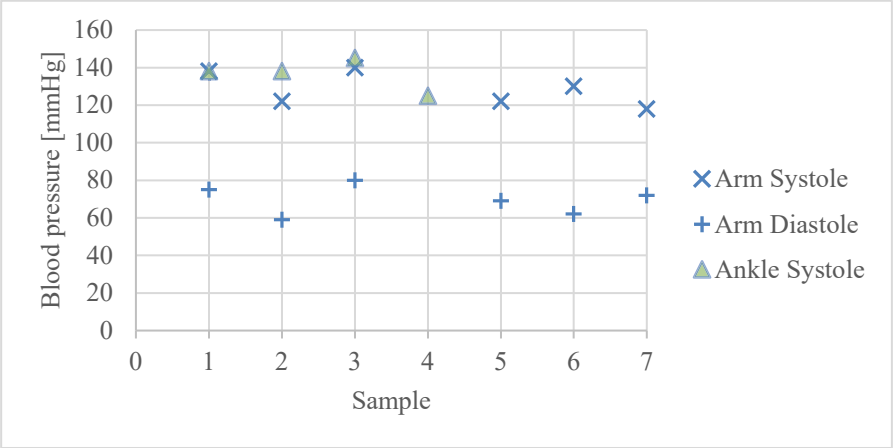


Figure 26 Blood pressure data in supine position. Systole in arm and ankle, and diastole in arm. Sample points: 1. Baseline. 2. Preload, in position before MRI. 3. Loaded, after MRI. 4. Post load 5 minutes. 5. Post load 15 minutes. 6. Post load 60 minutes. 7. Post load 2 hours. Data from arm at point 4 were by mistake not obtained.

4.2.2. Deformation measures from image analyses

The indentation site was identified at 52% of tibial length from the proximal end of tibia. The angles of the x- and y-axes of the indenter corresponded to the DICOM coordinate system, however in the opposite direction of the y-axis. The angle between the lateral side of the tibia bone and the y-axis in transversal plane was 36.5° for the non-loaded condition and 4 degrees less in the loaded condition. The analyses on the subject identified 5 soft tissue types on meso level with 14 separate layers. Tissue geometries were identified, see examples in Figure 27.

Displacement

The tissues posterior to tibia were displaced by the indenter, most in y-direction and slightly in x-direction, thus additional reference points along parallel y-axes were defined (Figure 28). There were mostly larger displacements in superficial layers than in deep layers. The tissue layers

posterior to the Tibia bone moved 3 to 22.6 mm due to the indentation, the posterior skin surface the most. The tissue specific displacement measures in the y direction are displayed in Table 8.

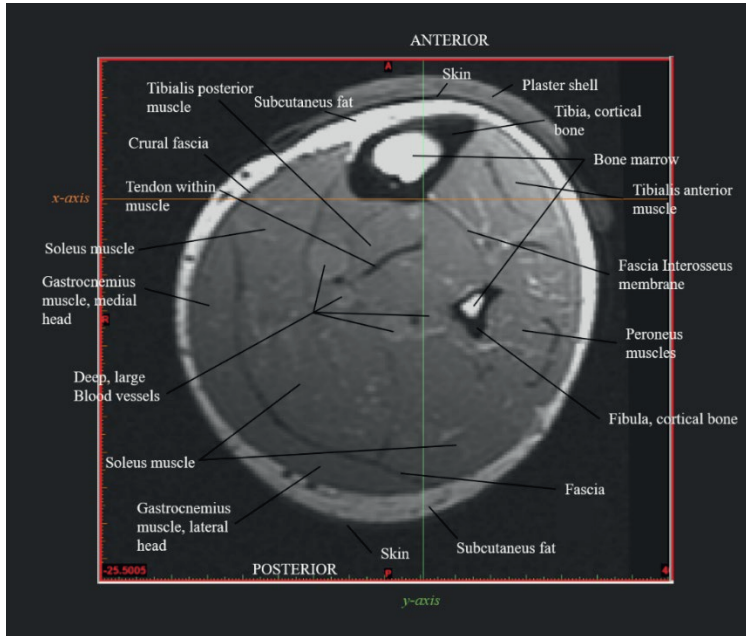


Figure 27 Examples of identified tissues in MR image of no-loaded condition at the level of indentation. MR image had y-axis positive direction downwards, towards posterior side.

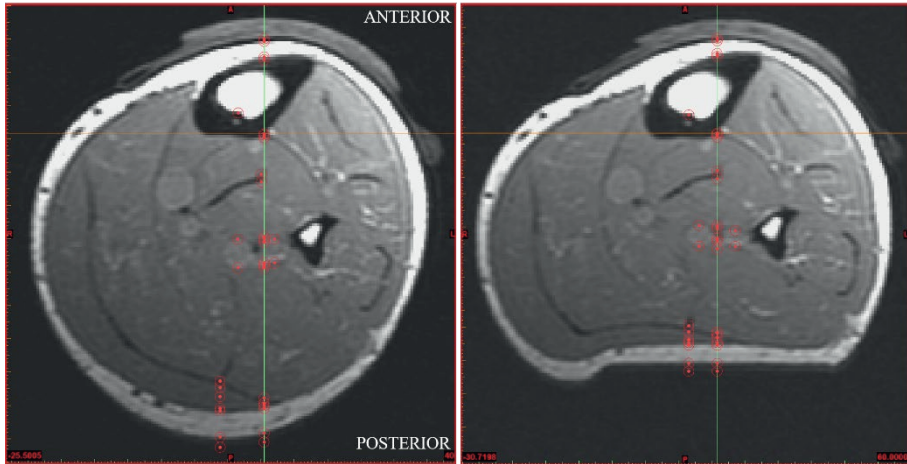


Figure 28 Corresponding MR images with identified tissue reference points as red dots in circles. The local coordinate system is displayed by orange line for x-axis, green line for y-axis, intersecting at the defined origin. Left: Non-loaded. Right: Loaded, indenter applied. Additional points medial and lateral to the y-axis are displayed, along parallel $y(x(n))$ axes.

Table 8 Displacement of posterior border of tissues posterior to the Tibial bone

Tissue superficial to deep. at posterior border	Displacement [mm] At $y(0)$ through centre of TIM	Displacement [mm] at $y(n)$
Skin posterior	-21.0	-22.6*
Fat posterior	-20.6	-21.9*
Fascia posterior to. Gastrocnemius	-18.7	-20.3*
Gastrocnemius lateralis, lateral aspect	-18.7	-20.3*
Fascia posterior to Soleus	-19.5	
Soleus	-19.5	
Lateral artery posterior inner wall		-4.6**
Lateral artery anterior inner wall		-2.3**
Lateral vein posterior inner wall		-6.2***
Lateral vein anterior inner wall		-3.9***
Tibialis posterior	-3.2	
Tendon internal of tibialis posterior	-0.7	

Note: $y(0)$ when $x=0$, * medial to $y(0)$ -axis with y -axis through the mid conjunction of the fascia-branch in the Soleus muscle, ** lateral artery at $x(n)$ lateral to $y(0)$, *** lateral vein $x(n)$ medial to $y(0)$, see Figure 28. Negative values due on the image coordinate system.

Stretch ratio

The stretch ratio along the y-direction, $\lambda(y)$, varied by tissue type from 0.38 to 1.26. The skin, fat and muscles stretch ratio varied with their respective position in relation to the applied indenter and were more compressed closer to the indenter, Figure 29. The stretch ratio for the posterior compound of soft tissue, from skin surface to tibial bone, was 0.77. Large deformation strain measures in one dimension, based on Equations (2)-(4), were compared for the tissues with notable stretch and grouped per tissue type in Table 9.

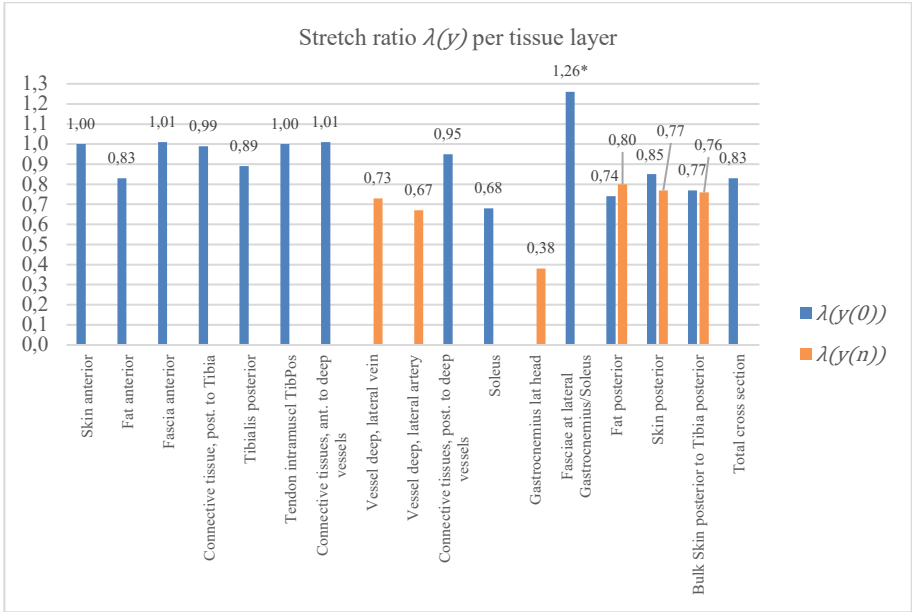


Figure 29 Stretch ratio in y, per tissue layer with $y(0)$ at the centre of TIM indenter, $y(n)$ at secondary positions $x(n)$ (see Figure 28 and Table 8). From left to right: tissue layer in the position order from anterior to posterior in Figure 28. * double layers of connective tissue due to indentation, difficult to identify separately.

Table 9 Strain measures in y-direction per tissue

Tissue layer	λ	E	e
Skin posterior	0.85	-0.14	-0.19
Skin posterior *	0.77	-0.20	-0.34
Fat anterior	0.83	-0.16	-0.23
Fat posterior	0.74	-0.23	-0.41
Fat posterior *	0.8	-0.18	-0.28
Tibialis posterior	0.89	-0.10	-0.13
Soleus	0.68	-0.27	-0.58
Gastrocnemius lateral head *	0.38	-0.43	-2.96
Vessel deep, lateral vein *	0.73	-0.23	-0.44
Vessel deep, lateral artery *	0.67	-0.28	-0.61
Connective tissues, posterior to deep vessels	0.95	-0.05	-0.05
Bulk Skin posterior to tibia posterior	0.77	-0.20	-0.34
Bulk Skin posterior to tibia posterior *	0.76	-0.21	-0.37
Total cross section	0.83	-0.16	-0.23

Note: λ : stretch ratio, E : Green & StVenant Strain, e : Almansi finite strain. Included tissues with $\lambda \neq 1$ * along a parallel y-axis, $y(x(n))$, see Figure 28

Area and volume

The cross-sectional area was 116 cm² and 108 cm² in non-loaded and loaded condition respectively and the slice thickness 4 mm. The Jacobian determinant J , volume ratio (eq.14), was 0.931; the compound of the leg at that level was compressed 6.9% by the applied indentation.

Local deformation was evaluated in a muscle region close to the indenter, at the lateral head of muscle gastrocnemius (Figure 30). The deformation by the Jacobian determinant J^{FEM} (eq.30) computed for the local test-element centroid was 0.204 which means that the element was in its centre compressed 79.6%.

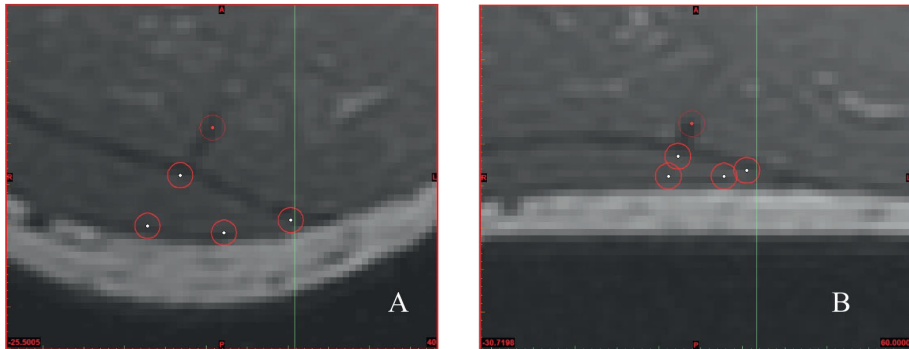


Figure 30 The local bilinear test-element's defined nodes are marked white. A Non-loaded condition. B Loaded condition. The y-axis through the local origo displayed by green line, and the point in fascia for determination of direction of the medial nodes of the element is also displayed for reference.

4.2.3. *Force-displacement by TIM*

The TIM device measured force and displacement and the indenter could be locked in position. TIM could be separated in two sections to dismount the electronics and magnetic components, with the indenter locked in position to be MR compatible. The developed body supports, frame for TIM fixture and leg fixation provided same body position in non-loaded and loaded situation. The set-up, TIM measures and MR protocol provided documentation of the non-loaded and loaded tissue conditions of mechanical nature. The displacement of the indenter at the locked position was 19.6 mm with an applied force of 27 N.

The individual specific friction coefficient μ_s , for the indenter material/skin interface was 0.54 for this subject at the site of indentation.

4.3. Geometry model from MR data in Study II

The MR images in Study II were also processed to build an individual-specific geometry model for future finite element analyses. Skin, subcutaneous fat, fascia, septum, separate muscles, intramuscular tendons, large vessels, and cortical bones were identified, and separate regions defined in Mimics Research 20.0 (Figure 31, A). The tissue regions, segments, were first defined by windowing functions, and then adjusted manually on each slice. The muscles were segmented using the muscle segmentation module in Mimics and then adjusted manually. From these segmentations, specific files of the 3D surfaces were created in the 3-Matic module and imported to the ANSA pre-processor software (BETA CAE Systems, Switzerland). In ANSA was preparatory work of the tissue segments' surfaces started (Figure 31, B) in order to create FEA models for future material parameter optimization and validation to the experimental findings, according to the larger research project, see Figure 14.

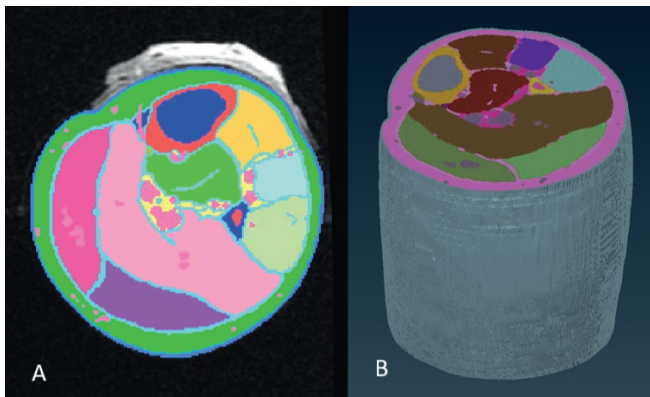


Figure 31 Digital 3D model from MR images: A Segmentation of tissues in Mimics 20.0 (Materialise, Belgium), top slice displayed, B: Surface model in ANSA (BETA CAE Systems, Switzerland) from STL-files created in 3-Matic (Materialise, Belgium).

5. Discussion

This research investigated several aspects of soft tissue deformation related to pressure injuries in Figure 9. Soft tissue deformation was studied on human anatomy in several layers and tissue types in the transverse plane in both studies. The research combined disciplines to explore human tissue behaviour from different perspectives. This chapter discuss the studies with respect to the research questions while incorporating methodological aspects. Generalizations are not possible at this stage due to the novelty of the methods and the limited sample. Future implications to the industrial product realisation process are then elaborated upon.

5.1. Influence of differentiated tissue representation in FEA

Understanding of the influence of different model representations is important for interpretation of results from FEA simulations and clinical applications. How the tissue differentiation in a leg model would influence the outcome was thus of interest, RQ1. The simulation study (study I) addressed the effect of differentiation of 4 and 5 soft tissue types respectively, in a lower limb cross section model, by variation of fasciae and muscle properties.

5.1.1. *Influence on stresses, strains and contact pressures*

The limb model represented more layers of different tissue types than many previous FEA studies of the lower extremity [11, 12, 62-65, 74, 75, 101, 110, 120] and defined tissue layers similar to those of Rohan *et al* [124]. The distribution and magnitudes of stresses and strains changed with the alternate muscle and fascia properties (Figure 20, Figure 21, Appendix V). The relative change varied over both tissue types and applied load conditions. The difference in resulting stresses, strains and contact pressures between the two used material sets were considerable, in several cases exceeding a hundred percent relative change and in a couple of cases even thousands of percent relative change comparing the same site (Table 5, Table 6, Figure 22, Figure 23, Figure 24). The stress was higher in fascia in the Separate set, than when

muscle and fascia had combined properties (Figure 20 and Appendix V). When muscle and fascia had same material property, this combined property was stiffer than the muscle property and softer than the fascia property (Table 2, Figure 13). Thus, the fascia property was stiffer in Separate set, which could explain the increase in stresses and decrease in strains in this tissue. With the separate set, the muscle tissue property was less stiff than in the combined set, which explains the strain behaviour with larger muscle strains in Separate set conditions than in the Combined set conditions.

The overall largest strains were found with the separate material set in the HS socket design, at the lateral head of gastrocnemius muscle, by 49% and 84% muscle principal and shear strain respectively (Figure 21 and Appendix V). In contrast, with the same socket load but with combined fascia-muscle material the principal and shear strains reached maxima of 10% and 16% respectively in muscle regions but at other sites. For the combined set highest strains in muscle tissue were 16% and 31% respectively, with the TC socket. Surrounding tissues were also affected by the change in properties of muscle and fascia. For example, the distributions in Figure 20 show that fat responded with higher effective stress all around in the HS condition with the Combined set, compared to the Separate set where smaller localised areas showed higher levels of stress.

The geometries of the differentiated limb tissues and the sockets in the FE models were asymmetric (Figure 11, Figure 12) which may contribute to the diverse changes. The thin fascia divides muscles and vessel-nerve tracks into different shaped pockets (Figure 1). However, in the model the tissue layer regions were intact with constant mesh through all simulations. With the separate properties of muscle and fascia tissues (Separate set) the fascia represented a relatively small portion of the limb cross sectional area, while the muscle regions had larger area. The dividing effect was apparent in the results with the Separate set and diminished with the Combined set.

The contact pressures between the sockets and skin surface were also influenced by the muscle-fascia representation. Thus, these choices of model representation influenced through the depth of the leg cross-section. However, whether the simulations represented an over- or underestimation of tissue's stresses, strains and contact pressures were not evaluated. That should be important to study in future verifications of simulation models for patient-specific-modelling.

The amount of relative changes showed that it did matter to represent fascia tissues separated from muscle tissues, there were notable differences. Thus, the hypothesis was supported.

5.1.2. *Discussion of the simulation model*

Model in two dimensions (2D)

The transverse 2D plane, the cross section of the leg, was used for the model of loading effects on different structures. In this plane several tissue types and layers can be identified and studied, through the whole depth of the leg. The assumption of isotropic materials complies better with the transverse plane than the longitudinal plane due to the structure and directions of fibres and cell layers [13]. The 2D case is less demanding on modelling and computational resources, and was deemed enough for the purpose of study I. However, a 3D model with relevant geometries and material properties would be an improvement for the future.

Geometry and material property

The geometrical model of the lower leg was based on an anatomical illustration by Netter [17], and the tissue properties were obtained from literature based on experiments (Table 2). Hence, neither the geometry nor the material properties were from one individual person. Since the study addressed whether it mattered to have separate fascia and muscle tissues in the model, a standard geometry from literature with clearly defined structures - a generic anatomical model - was considered sufficient. Such an anatomy illustration demonstrates the configuration of tissues with defined structures and regions. However, individual variation of geometries and material properties exists in reality [13].

The material data for compression in transversal direction was used based on the loading situation chosen. Since compression data for the Ogden model for human skin and fat were not found, these properties were obtained from studies on pig (Table 2, [137, 141, 142]). To what extent these non-human material data influenced the results have not been investigated here, however, skin, fat, vessel and bone material properties were kept constant during the simulations.

Regarding the fascia and muscle material properties a calibration test was developed to determine the data for the combined fascia-muscle-material (Figure 13). The calibration test demonstrated that if fascia was given the

muscle tissue property, as if fascia was ignored, the response for the compound was softer than with the defined two sets. Hence, fascia was accounted for in both of them, either as a separate tissue or in combination with muscle tissue, as displayed to the right in Figure 13. The model with five tissue types (skin, fat, muscle-fascia, vessels, bones) were considered the simplified model, with the Combined set. Moreover, a few studies comparing effects using different material properties in a FE model of human leg have been found [62, 74, 75], but none done with these tissue layers.

Elements and mesh

A diversity of element types are found in the biomechanical FE studies (chapter 2.6.2, Appendix I). Comments on element and mesh choices seem to be rare in biomechanical FEA (chapter 2.6.2, [109]) despite their influence on the solving process and results [104].

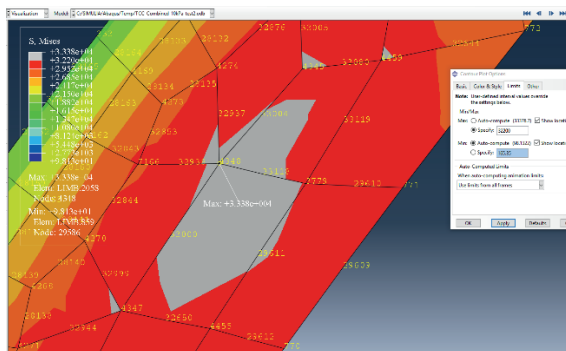


Figure 32 Example evaluation maximum effective stress found at nodes in elements with small-angled corners. Numbers in the elements indicate nodal identities. Example from fat region in TC Combined set condition. CAE Software Abaqus 6.14-3/Standard (Dassault Systèmes).

The chosen elements in Study I were of continuum type, accounted for plane strain, were second order using quadratic interpolation, reduced integration, and hybrid (to deal with incompressible behaviour), which introduced variables into the solution of the problem to handle different aspects [104, 136]. The mesh was refined with smaller elements in regions with thin or small defined tissue layers and consisted of at least two rows of elements. The tissue layer regions had constant mesh through all simulations, for differentiation. When the limb model was loaded by the geometries of sockets, some elements were distorted with resulting small corner angles. This was accounted for

when analysing the results and identifying the magnitude levels: peaks were identified, assessed and ignored if only situated at very small corner angles. The limits for the colour-coded scale of the outcome were adjusted to display at least 5 nodes to determine the maximum or minimum level of that measure. An example for such situation is given in Figure 32 from fat with the Combined set in the TC condition when effective stress was analysed. The grey colour in the image indicates area above the set limit.

Boundary conditions

The tibia was fixed while fibula could move, to correspond to clinical findings in amputees [143, 144]. No longitudinal or dynamic cycling load, as during standing or walking, were applied. Only geometrical constraints by the three socket shapes were applied as loading conditions. These socket concepts were chosen as clinically relevant applications for the FE simulation. However, in the clinical situation the socket shapes are individual-based and depends also on the socket concept and the CPO's judgement of modifications for that individual. Thus, socket geometries will vary within a chosen socket concept category even for the same individual prosthesis user. The main reason for choosing these three socket shapes and only the geometry as loading generation was to keep the simulation less complicated and reduce the risk of concurrent influence from different sources.

The contact condition of friction in the model between skin surface and PET-G socket inner surface was applied, obtained from literature [145]. The contact was solved by iterative computations to reject overclosure. The contact pressure was computed in the solving process, and not defined and applied as known boundary conditions. This feature of the study showed that the contact pressure is a consequence of the load on those interacting materials and should not be defined in advance.

Comparisons

The differences in stresses, strains and contact pressures due to the two ways of representation of tissues was of interest. Thus, the comparison was investigated by the relative change of maxima, per tissue and per site of the maximum value for that tissue under the applied loading condition. The separate material set was used as reference. There was no golden standard simulation to refer to, outcomes would vary with simulation models, and no standard model has been established. Repeated simulations with same

conditions will replicate the results, and is thus not applicable for repeated measures comparisons. Comparisons using means of values for several tissue types would be in conflict with the purpose of the study, and was thus not applied. Using means of relative change per tissue type could be an option, but here it was only three pairs per tissue type and outcome measure, thus too small a base for means comparison. Moreover, for mechanical reasons, the peak values are of interest when evaluating effects by simulations, for risk analyses and optimization purposes and not overall means. Hence, in this study the peak values (i.e. maxima of stresses, strains and contact pressures) were compared per tissue type and site of this peak value.

The material representation was in focus for this study. Thus, comparisons of socket designs based on these simulations were not of interest, nor clinically relevant.

5.2. Process for measuring individual-specific soft tissue deformation in separate tissue layers *in vivo* under established health conditions

Individual-specific tissue health status, morphology and deformation measures are important for material behaviour and tissue damage investigation. The developed case study included several of the dimensions in the framework regarding pressure injury development by Coleman *et al* [3]. Study II demonstrated a process to measure soft tissue deformations due to indentation under established health conditions in one subject (illustrated by the red box in Figure 14). The process obtained subject-specific health conditions, strain data for 14 layers of 5 tissue types in the lower leg, and volume changes of the transverse compound and in specific muscle tissues. The strain was determined by stretch ratio, λ , a relative measure of the material behaviour in a selected direction. Volume change as measured by the determinant of deformation gradient investigates compressibility of the defined region. The developed process is discussed below divided in data collection techniques and developed data analyses for individual-specific results.

5.2.1. Data collection techniques

Tissue geometries by magnetic resonance images

Magnetic resonance imaging requires expensive equipment and special operating skills, which are resource demanding. However, the quality of the MR images is better than ultrasound images and MR does not expose the body to radiation as CT does [103]. We collaborated with a clinic providing a MR tunnel scanner for full body in prone positions. The determined body position was developed to enable leg scans of participants with different physical conditions e.g. transtibial amputation, muscle weakness or paresis, to facilitate a consistent position. The transverse plane of the leg tissues was in focus, however, the MR scan provided sagittal and frontal plane image sets that here were used for identification purposes. These three planes (example in Figure 33) built the base for the 3D digital model with different tissue layers in Figure 31.

The resolution of MR images and the obtained intensities from different tissue types influenced the identification of tissue borders and specific reference points to use. When a voxel contains more than one type of tissues, the emissions from these influence the intensity, called the partial volume effect [103]. In this study the voxel size was $0.7813 \times 0.7813 \times 4.0 \text{ mm}^3$. Thin layers, such as connective tissues surrounding muscles, were difficult to detect, while fasciae and septum were thicker and easier to differentiate. The image quality by smaller voxels, could be increased by thinner slices or smaller FOV. However, thinner slices require longer scan time, and smaller FOV would exclude the opposite leg which here was used for tissue identification purposes. Portnoy *et al* [102] used FOV for single leg with voxel size $0.1 \times 0.1 \times 4.0 \text{ mm}^3$, while Senghe *et al* had image resolution of 256 and voxel size of $1.18 \times 1.15 \times 1.00 \text{ mm}^3$ [11]. Both studies identified fewer tissue layers than was done in Study II. Moerman *et al* had FOV of 12.0 cm for the upper arm case with a voxel size of $0.94 \times 0.94 \times 2.0 \text{ mm}^3$ [96]. Thus, Senghe *et al* and Moerman *et al* obtained thinner slices but larger pixels than our case study. For improvement of future identification of tissue borders with the here presented set up and same MR equipment, the FOV could be smaller, excluding the opposite leg, and the slice thickness reduced to 2 or 3 mm however kept within the comfortable scanning duration for the subject. This should refine the voxel size and decrease the partial volume effect.

Other aspects of the image quality were the illumination and contrasts. The captured images had uneven illumination probably due to the distance between the leg, the MR table and body coil covering the lower legs. This caused further difficulties of identifying tissue types and borders. The uneven illumination problem was addressed during the analysing process as described in chapter 3.4.7. Radiologists were consulted during the tissue identification process to verify analyses and for benchmarking.

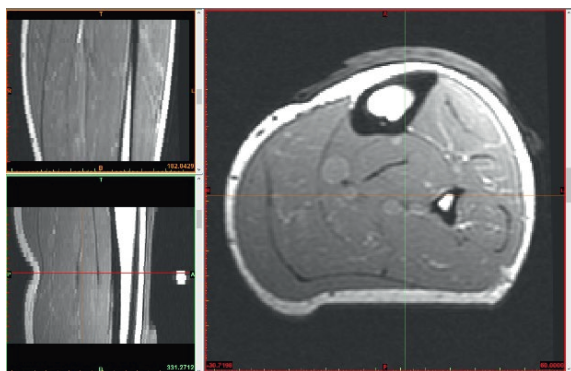


Figure 33 Example MR data of the loaded condition in three planes. Images analysed in Mimics Research 20.0 (Materialise, Leuven, Belgium).

Force and displacement measurement by TIM

The TIM instrument and fixation equipment were developed for this study. The shape of the TIM indenter tip was designed by the author, CPO, based on clinical experience and estimations of diverse subjects' comfort in relation to the load to be applied (force and time). The axial asymmetric indenter with radius 10 mm and length 70 mm was larger and the applied force higher than in most of the studies listed in Appendix I, but the estimated contact pressure lower. Frauziols *et al* used a larger radius of the cylinder, (radius of 15 mm, length 50 mm), and applied it along the longitudinal axis of the leg [62], while in Study II the TIM indenter was applied along the transverse plane. A larger radius might reduce the stretch of the skin in tangential direction. This effect was assumed neglectable in the chosen plane and range of x-positions used.

Force was chosen as the determining factor for the indentation, based on the pressure-time loading recommendation by Gefen [29]. The force sensor was calibrated by a certifying body before mounted in TIM. The displacement of the indenter was recorded by the linear potentiometer. After TIM was

assembled and connected to the in-house developed data processing program TIM was only calibrated for the load registration. Displacement should have been calibrated simultaneously. The load was calibrated on site before data collection with the subject. The indenter position for skin contact was visually determined during the data collection, and that displacement was held constant for a period of time before the progression of displacement to the defined force limit. Friction in the internal piston of TIM restricted the free reverse movement of the indenter but was considered not influencing the on-loading process.

Applying a reconditioning protocol when loading tissues has been proposed by for instance Huang *et al* [10] and Silver-Thorn [69], in contrast to the earlier study by Vannah & Childress [84]. The exclusion of preconditioning protocol in Study II was a conscious choice, since the intervention with one indentation run was deemed essential at the time. Preconditioning may also be considered in the future with a device with more sensitive off-loading capability, especially if viscoelastic properties should be studied.

The friction coefficient at the skin-indenter interface was collected for information of loading conditions and for further future analyses of the contact conditions.

The assembled TIM instrument should be calibrated for both load and displacements at each data collection occasion. Calibration weights were developed and used, but no displacement calibration device.

Improvements for more sensitive off-loading and relaxation data could provide additional features of TIM.

The TIM fixation frame together with individual plaster shells may be possible to apply on both lower and upper limbs. The TIM may also be attached to other frames and applied on other body segments, hence capture tissue deformation due to indentation on different body regions.

Indentation during MR

The design of TIM and the fixation frame were compatible with MR and enabled data collection of multilayer tissue geometries under fixed known load. The loadcell and potentiometer could be separated from the fixation frame after the indenter was locked in the decided position (Figure 15, Figure 16, Figure 17). However, on-loading and off-loading during MR were not possible with current design.

In order to keep the body position consistent in non-loaded and loaded condition, the body position was defined and support equipment developed. The soft tissue of the leg was only affected by the TIM indenter and the anterior plaster shell. Thus, posterior tissue had space to change shape and was only partially confined. With the supporting cushions, stabilizing plaster shell and foot support, the tissues of interest could be relaxed during the whole scanning procedure. Muscles in relaxed and activated states were expected to respond differently to indentation, as experienced in clinical practice of muscle palpation. However, it would be tiresome for the subject to keep muscle contraction during the time of indentation and the second MR scan. Additionally, for future data collection with subjects with pathological conditions including amputation, the muscle contraction state would be difficult to obtain. Hence, the relaxed state was chosen.

Health measures and clinical assessment

Health conditions and risk assessment of the individual susceptibility to pressure injury is a major part of pressure injury prevention [3, 6]. Possibilities for comparisons between studies depend on which subjects tested, source of experimental data, instrumentation and measures used. Information on the participating subjects' soft tissue conditions are not described in such detail in previous studies of tissue properties (Appendix I). The main information reported has been age, gender and the health conditions described as healthy, abled bodied, physically active, with diagnosis as diabetes (not defining which type of diabetes) and if amputation was caused by trauma or vascular disease. Participants in the indentation studies in Appendix I had no reported skin problems. The health items reported were not consistent, thus they limit the comparisons between studies. In consequence, demographic data and health conditions were included in Study II, obtained by the questionnaire and clinical assessment protocol. They addressed aspects corresponding to the PI framework by Coleman *et al* [3] including the blood pressure data and the prosthetics and orthotics clinical field. Since individual-specific aspects influence the tissue load-tolerance [3] it was important to include individual-specific health and tissue conditions to know under which situation the deformation data were obtained. The intention was a protocol which could cover different health and tissue conditions.

However, assessment methods for the conditions of soft tissues seem to vary between professions and within prosthetics and orthotics clinical practice. No

golden standard exists [5]. Experts in the field argue for a multidisciplinary approach to handle patients with vascular disease in risk of amputation and collaboration in assessments of the conditions in the lower limbs [160]. The clinical assessment protocol constructed for this study intended to address soft tissue conditions of the leg in more detail than the ISO 8548-2 [8] reflects, with available tools commonly used in prosthetics and orthotics clinics (chapter 3.4.3 and Appendix II). Tissue consistency was assessed by palpation and subjectively estimating types of soft tissues' thickness and properties as compact, loose, elastic and plastic, since palpation is a subjective technique commonly used within orthopaedics [4]. The protocol was pilot tested by two CPO on two subjects with polyneuropathy and post-polio respectively.

The protocol included brachial and ankle blood pressure monitoring which required movements of the foot for cuff application. Consequently, the leg was moved between MR scans. The body positioning equipment was designed to account for movements between MR scans.

The questionnaire (Appendix III) for self-reported health included the validated RAND-36 and a part of the validated OPUS questionnaires as well as Swede-Amp items and new constructed items (Table 4). There was no validated instrument available covering the content we wanted to include in relation to the PI framework. The questionnaire was tested for content and face validity with individuals with and without pathologies and with CPOs and was found sound. More aspects of the individual's conditions related tissue conditions and PI development were included with the clinical assessment protocol and the questionnaire, than previous assessment methods [5, 8, 160].

The questionnaire and the clinical assessment protocol included many items and were primarily designed for research. The novelty of the tissue property descriptions require objective verification. In order to investigate the validity and reliability of the assessment protocol and questionnaire, further studies designed for that purpose are required.

5.2.2. *Analyses of data*

Deformation

The deformation measures, based on tissue displacements due to indentation, were explored on the compound tissues and on specific tissue layers and regions, through the leg, thus on macro and meso level. The chosen items

measured how deformable and compressible the tissues were in the defined direction at these sites with the applied load in this individual subject.

In previous indentation studies different indenters, applied force, deformation measures and material properties were reported, which made it difficult to compare results between studies (chapter 2.5 and Appendix I). To address this limitation, the developed analyses of tissue deformation in Study II were performed on both full compound level and on tissue layer levels. Tissue layers' displacements (Table 8), stretch ratio (λ), and equivalents of two strain measures (Table 9) were included, and may be used as reference measures. We chose to analyse the stretch ratio as the main measure since this is a relative measure of the tissue layer's deformation, and can be applied in different material models and strain measures (chapters 2.3 and 2.4). The stretch ratio per tissue layer requires medical images of the undeformed and deformed state, with indentation applied during the image capture. The equipment and protocol we developed for the study provided such conditions. However, the stretch ratio as such is not commonly reported in studies that used the indentation method, hence limits the between-study comparisons to date.

The volume and area changes were also analysed for compressibility. The computed volume ratio J on compound, the deformation gradient \mathbf{F} and the Jacobian determinants (J and J^{FEM}) on a local region, based on the physical displacement measures in MR images, were measures not found in the reviewed studies of deformation in chapter 2.3. With these measures the right and left Cauchy-Green deformation tensors can be computed for the local element based on \mathbf{F} and determination of the Green-StVenant and Almansi strain tensors respectively, see eq. (9) and (10). However, the application of FEM by the element at a defined local region and related reference points presented an approximation of the deformation at that selected region. The smaller the test-element is, the more accurate the computed \mathbf{F} , J and J^{FEM} will be. The technique could in principle be applied to any region of interest. In this work the technique was described and demonstrated in muscle tissue on a bilinear element that was quite large in comparison with FE analysis applied in simulations on the lower leg muscle tissue in transverse plane [117, 120, 124] including in study I. Thus, the test-element should need to be considered and adjusted to similar sizes and shapes when comparing results between the presented technique and FE computations in a FEA simulation software. The

MR image resolution influenced the possibilities to define reference points for the local element, hence the element size was chosen of practical reasons. The soft tissues' deformation was assessed in the transverse plane for this study. The asymmetric indenter shape made it possible to obtain stretch ratios in y-direction at several x-positions.

We used two states (non-loaded and loaded) for the deformation measures, and not stepwise loading-displacement-measurements nor exploring the viscoelastic behaviour due to constraints in the instrumentation and the participant's comfort. The two-state analysis limited the results to a linear assumption of the relationship. Stepwise loading with tissue geometries documented at several steps should give more data for analyses of tissue deformation and may detect nonlinearity [69, 84]. With the developed set-up and instruments, this should have required longer time in the fixed body position and in MR which may have caused the participant discomfort. Based on comfort, the time restrictions for static load and provided MR scans, the chosen set-up was judged sufficient for analyses in this study.

The evaluation of individual tissue's displacements, thickness change and compressibility by volume change due to deformation based on indentation and MR images was considered straight forward.

Health conditions and clinical status of subject

Validated instruments were part of the questionnaire and clinical assessment, and those items analysed accordingly. The RAND-36 was analysed to provide possibilities of comparisons to larger populations. Blood pressure data and ABPI were analysed for general condition, for assessment of circulation status in the lower limb and for monitoring during the indentation test including for safety reasons.

It was not established in Study II if the new tissue descriptors reflected the tissue conditions more accurate than that standard items did.

Study II was a case study with one healthy subject. The results described the subject and the individual-specific health conditions at this stage, hence not analysed further. Generalisations based on this study were not possible.

5.3. Individual-specific soft tissue deformation measured in separate tissue layers *in vivo* under established health conditions

5.3.1. Deformations

The applied force of 27N for the locked indentation duration was below the computed safety level of 30N based on Gefen [28, 29]. Displacement data from TIM were missing from the initial phase of the on-loading process, and indenter position at the contact skin-indenter not captured. Thus, displacement by TIM in study II was not used for deformation measures. The individual-specific force-displacement-time data from TIM were not further analysed, due to the scope of study.

The tissue deformations for this subject under the current conditions (load 27N and displacement 21 mm), showed that the compound of soft tissues was compressed.

The skin, fat and muscle tissues were most affected by the indentation, with λ between 0.38 - 0.89 and large strains (Green/StVenant strain $E > 10\%$, Almansi strain $e > 13\%$), and thus the large deformation theory should be used when modelling them. Strain in the connective tissues were small (Figure 29) with λ close to 1 and down to 0.95 corresponding to -5% in E and e (Table 9). Hence, soft tissue deformation measures were provided, and individual-specific soft tissue reference data reported for one healthy subject. However, studies with several subjects and loading conditions are needed to investigate and explore the parameters and their variation between individuals with their respective health conditions. However, compressibility should be addressed when material representations are considered in FE simulations for this subject's tissues at this site.

The strain measured by Stecco *et al* [35] of 27% strain for dead human leg fasciae was obtained from tensile tests. However, compressive tests and tensile tests are not providing the same properties [59]. The assumption of incompressible connective tissues is supported for the current conditions and subject by the results from study II.

The age, gender and bodyweight of the subject as well as the site of the indentation in study II corresponded to subjects and indentation site in the study by Vannah *et al* [84]. The displacement of the posterior calf tissue

compound corresponded to the 21.2 mm reported by Vannah *et al* [84]. However, they used a smaller indenter which imply a larger contact pressure on the skin surface than the TIM indenter with larger area would cause. Moreover, the displacement measurements with TIM were not calibrated; hence the quality of that data was not assured but reported, and the data were not used for further analyses.

Displacements of individual-specific tissue borders were determined in the y-direction, however also sometimes noted in the x-direction. Thus, the secondary reference points along parallel y-directions at different x-positions were identified to document tissues of interest (Figure 28). The x-direction deformation was included in the FEM numerical results for the local element in the muscle gastrocnemius lateral head (Figure 19, equation 30 and Figure 30). These displacements and sliding effects may be explained by the structure of layers that should be able to move independently, such as muscles, tendons, vessels and nerves, and the asymmetric shape of tissues and bones. Muscles can slide with respect to surroundings, due to their protective layers of connective tissues and the interstitial fluid between those layers. This is a function that facilitate muscles to contract, relax, and work independently of the adjacent tissues. The tibial and fibular bones act as counter force to the indenter force but are not parallel to the indenter surface, thus may contribute to the sliding effect on tissue layers.

For this subject in the defined position the angle between the lateral side of the tibia bone and the y-axis in transversal plane was 4° less in the loaded condition than for the non-loaded condition. When analysing the MR images, and photo documentation from the data collection, it was discovered that the plaster shell had moved distally 16 mm. This change in position of the plaster shell as well as the tibia rotation may have occurred when the ankle blood pressure data was measured, since the foot was lifted to apply the cuff. However, the corresponding images of non-loaded and loaded conditions were selected based on the distance from the tibial proximal end. Hence, the longitudinal corresponding position was found. The rotation and sliding of tissues might have been influenced, but the changed angle of tibia by 4° was deemed small, with little effect on the y-direction.

These kinds of rotations and sliding of tissues were not reported in the previous indentation-in-MR studies (Appendix I). The possibility to identify such tissue rotation and sliding in both y- and x-directions should be beneficial for further analysis of tissue behaviour due to loading.

5.3.2. *Health measures and clinical findings*

The subject was healthy, physically active, and had no PI-related conditions. The tissues at the site of indentation had normal and healthy conditions according to the items assessed (Table 7). The new tissue descriptors were applied, however each describing term was not applicable for each tissue type. The blood pressure was within normal range [161]. This confirmed the selection of a subject from the population with no pathology.

The blood pressure and ABPI varied during the experiment (Figure 26). The participant had the ankles in approximately the same height above the floor as the heart when the first set was taken. Thus, the ABPI at baseline should be 1 for a normal healthy person [161], which it was. However, when blood pressure was taken with the legs in defined positions for MR scans, the ankles were above heart level, and lower ankle systole pressure than arm systole could be expected. The ankle systole pressure showed approximately the same level though. Additionally, the brachial systole was missing just after the off-loading, and the ankle systole not captured during the recovery period. Thus, the ABPI could not be evaluated at these sample times. The blood pressure seemed to decrease during the relaxing period after the MR and indentation was finished. The variation noted in the obtained blood pressure data may be due to many reasons including to the whole situation with possible psychological effects as well. Thus, the effect of the indentation on the blood pressure couldn't be evaluated for this case. Further investigations in such conditions and with several subjects should be required for exploration of influence of indentation on blood pressure.

5.4. Contribution

Different aspects of this research have been discussed in relation to the research questions in the previous sections of this chapter. An effort to summarize the contributions is made below and in Figure 34.

This research used a multi-disciplinary approach that addressed mechanical and health related aspects of tissue deformation. Instruments, techniques and protocols that addressed several aspects of the framework by Coleman *et al* [3] were developed. Both primary key factors and risk factors for PI were addressed (Figure 9). This approach has not been found elsewhere.

During the review of previous studies it was found that FEA applied to human musculo-skeletal system used simplified models, both regarding material properties and geometries. However, comparisons with different material properties or models for the same geometries and boundary conditions were not found. The leg model in Study I considered 6 tissue types in their respective anatomical regions which was an improvement from previously reported studies. Study I showed the importance of distinguishing between tissue layers, and that the internal mechanical conditions clearly changed depending on how muscle and fascia layers were represented. The results support the choice to represent fascia separately done by Rohan *et al* [124].

Study I gave insights regarding the importance of tissue layers in FEA modelling, which then influenced the level of tissue layer detail in Study II. The identification and determination of deformation measures of differentiated tissue layers and types were thus relevant and performed in Study II. Techniques for investigation of mechanical deformation in several specific tissue layers at a site in the live human leg were developed and demonstrated for feasibility on one healthy subject. The protocol for the individual specific health conditions included general health and soft tissue conditions at superficial and deep tissue levels. New soft tissue descriptors for the clinical assessment were developed and demonstrated. The clinical assessment protocol did not reveal how the soft tissues responded to loads, however the TIM indentation during MR with the analyses of mechanical deformations did.

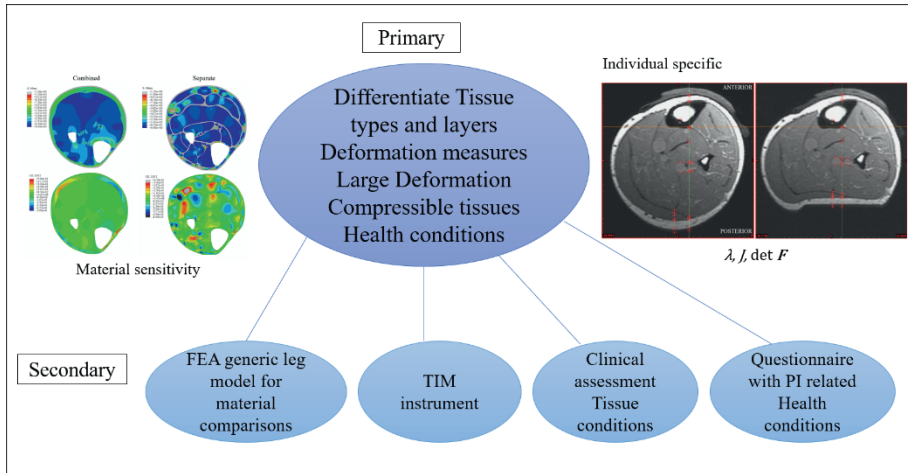


Figure 34 Schematic overview of contributions by primary and secondary levels, from study I and II. FEA: finite element analysis, TIM: Tissue Indenter Measurement, PI: pressure injury

This thesis is to my knowledge the first to report on individual specific deformation measures for the identified 14 tissue layers and 5 soft tissue types (skin, subcutaneous fat, fasciae, muscles and deep blood vessels), and including health conditions to this extent. It is also new to report deformation with these different strain measures simultaneously. Deformation was measured by stretch ratio, volume ratio and deformation gradient and determinant from displacements of tissues obtained by indentation during MR. For this subject (a healthy male of age 27), the skin, fat, muscles and deep blood vessels were compressed, but connective tissue in fascia and tendons were not. The volume change investigated on compound level and the amount of deformation in the lateral head of gastrocnemius showed compressibility. Thus, the multidisciplinary approach addressed more aspects than was found in other studies of the material properties of soft tissues in living humans.

However, it is not possible to draw generalisations to other situations or subjects. Further studies with representative samples including several subjects and evaluations of techniques used are needed.

5.5. Implications

5.5.1. *Tissue configurations in FE simulations*

The large relative changes in outcomes between the two used material sets in the FEA in Study I highlight the importance of a model's configuration and careful interpretations of the simulation outcomes. Interpretations could be over- and under-estimations depending on the model used, since FEA results depend on the simulation model's geometries, material properties and boundary conditions [104]. Increased differentiation of soft tissues could be part of developments of representative models of soft tissues applied to individual-specific simulations for clinical purposes. Study I imply that it matters to differentiate fascia tissues from muscle tissues.

The use of a standardised geometrical model, such as the anatomical illustration used in Study I, could provide a base for comparisons of material representations, as a reference model.

Moreover, verification and validation of computer simulations in biomechanics need further attention [14]. When individual-specific tissue properties are determined by FEA or individual-specific tissue loading effects are studied, that individual's geometries and properties of tissue types are important. Thus, an individual-specific FE model with differentiated tissue types of skin, subcutaneous fat, fascia, muscle and vessels in their respective layers could be used.

5.5.2. *Individual specific tissue deformation in vivo*

Further research on material properties of live human tissues under different health conditions are needed for investigations of tissue tolerance to loads. Investigations of material properties and material model representation for the individual case are needed. It should be of benefit to develop more reference data and guidelines for use of material models for simulation of different human related conditions, as well as for refinement, validation and verification of representative simulation models.

The demonstrated protocol with TIM during MR and tissue layer-specific deformations seems promising for these purposes. The presented measures might be used for assessment of material behaviour, for comparisons of measurement methods and to verify numerical models and individual specific

simulations with FEA. Material models could then be evaluated, e.g. estimations of difference between models that assume incompressible tissues and material models that account for compressibility.

With several subjects could data be analysed and compared more, according to the type of data and the research questions of interest. Comparisons between the mechanical properties obtained by the measures from indentation and the clinical assessment results from several subjects with different health conditions would further explore aspects of these issues and evaluate validity of the methods.

The asymmetric indenter shape may also provide possibilities for studies in sagittal and frontal plane (Figure 33), i.e. investigation of anisotropic behaviour. The indenter is also possible to position in longitudinal direction, as done by Frauziols *et al* [62]. That could provide deformation measures in a selection of stacked slices.

The contact area of the indenter may be calculated from medical images with good resolution and contact pressure from TIM computed.

5.5.3. *Product realization process*

This research is related to the product realization process and the product development process as presented in chapter 2.7. With knowledge of individual specific conditions and tissue damage mechanisms, it should be possible to predict and reduce tissue damage and optimize the product-tissue interaction. The technique for deformation measures of soft tissues presented here could be implemented in product development processes in the future. When soft tissue material parameters have been determined for the individual, these could be implemented in material models and simulations using FEA to predict behaviour during external loading conditions. The FEA models would represent soft tissue on meso level with diverse layers and types. Individual-specific stresses and strains could be analysed in the different layers of soft tissues exposed to different loads, geometries and materials.

Investigating user conditions and interaction between user and product, here included in the questionnaire and clinical assessment protocol, are related to the human factors during the design phase [132] as part of the product development, e.g. design concept generation. With more data from several

individuals with diverse health conditions and body configurations, this might be applied to mass produced products as well as individual specific, unique products.

During the design phase it is not only the interaction with the soft tissues of the user and the durability of the product that is of interest, but also the manufacturability [132]. Different materials, components and assemblies can be evaluated by computer simulations based on realistic tissue deformation data of the user group. Other aspects of manufacturability are quality, flexibility, lead times and production cost [131, 132] which influence the choice of concept and production strategies. Knowledge of living soft tissue behaviour should be of benefit in evaluations, verifications of methods and testing of products.

Implementation of this research to develop the clinical prosthetic/orthotic process might be possible and is here suggested in Figure 35. My vision is that this research in the future will contribute to a diagnostic protocol for prosthetists and orthotists, by clinical assessment of the patient's status of defined important tissue parameters, evaluate the risk level of tissue damage and take relevant action.

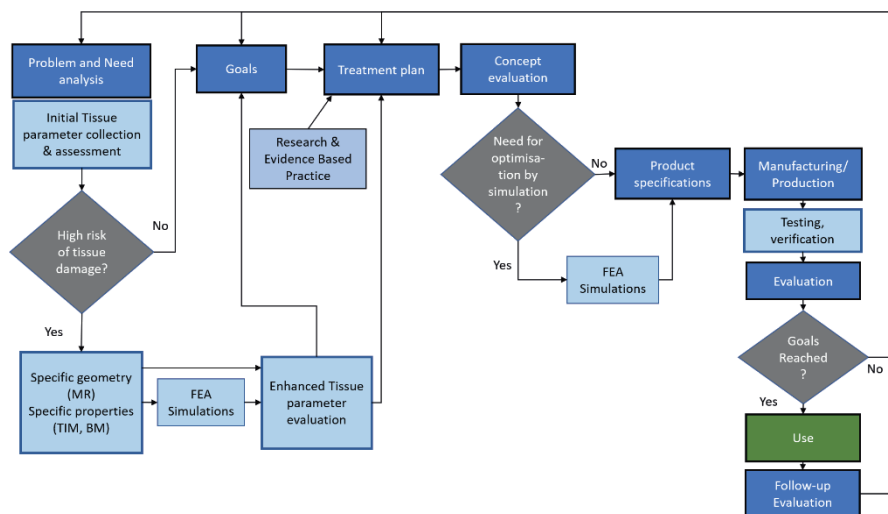


Figure 35 Algorithm of Clinical process incorporating assessment of tissue properties and suggested steps addressing soft tissue parameters based on current research. MRI: magnetic resonance imaging, TIM: tissue indentation measurement, BM: biomarkers, FEA: finite element analysis

Consider the process illustrated in Figure 35. During the problem and user need analysis, the tissue status, health condition and biomechanical situation

is evaluated. The tissue deformation parameters should be assessed. If an individual specific FEM simulation is needed for additional risk assessment or for product design decisions, the algorithm steps required and simulations for optimizations of material models and product should be performed. If the risk level is low, the extensive investigation with MR and FEA simulation is not needed, and the process could continue along the shorter path. In this way the identified soft tissue status and material parameters with the aim to reducing the incidence of soft tissue damage, e.g. PI, DTI and user discomfort, also will have impact on resource use in the product realization process. Improved knowledge of risk for soft tissue damage and simulations should require fewer produced prototypes, test devices/products, to hopefully reduce need for adjustments of the product at use e.g. shape changes due to discomfort, and lead to fewer iterations to reach a good product for the user. This may require less time/appointments/visit to the prosthetic/orthotic clinic for adjustments and increase time of use of the product, which might be more effective for the user in terms of health, social activities, economical cost, energy consumption etc. Hence, this relates to the three pillars of sustainability: environmental, social, and economical sustainability [162]. Knowledge gathered by clinical experience and simulations could be merged, and influence decision making in the whole product realization process.

6. Concluding remarks

Based on the used generic anatomical model for FEA simulation, differentiation of skin, fat, muscle, fascia, vessels and bones tissue layers with related material properties influenced the FEA results. The various relative changes demonstrated that it mattered how the muscle and fascia were represented. FE models should be differentiated by tissue types, geometries and material properties and the results interpreted considering the model representation. Applying the same anatomical geometries, a standard model, when comparing and evaluating different material models should be possible. Further research on representative models and the refinements of them as well as reference data of material properties for live humans are needed.

The experiment demonstrated that it was possible to analyse transverse deformations in individual live leg tissue layers of skin, fat, fascia, separate muscles and vessels when applying indentation during MR, under established health conditions.

Assessing individual specific deformation of leg tissues could include several factors related to pressure injury development;

- the mechanical boundary conditions by magnitude of compression force applied and interface friction,
- individual-specific response to load in specified tissue layers' geometries, deformation measures as displacements, stretch ratio and volume change on compound level and within a tissue region,
- risk factors for pressure injuries by physical health and pathologies related to PI, mobility, skin status, circulation and sensory ability.

The deformation investigation for one healthy male under the current conditions of indentation showed that

- the different soft tissue types of the leg cross section, except for connective tissues, were compressible on meso and macro level,
- large deformation theory should be applied for simulations of the layers of the tissues skin, fat, muscle and vessels compressed in this particular leg.

Several deformation measures based on displacements of tissue layers could be obtained. With these relative measures, comparisons between studies should be improved. Hence, the contribution of data by the selected measures to a reference data set should be possible, and future comparisons between studies may be improved. The individual-specific outcomes of these deformation measures could be applied in material models and simulations for the individual-specific conditions.

The combined results suggest that the mechanical deformation of the human lower leg soft tissues should be investigated per tissue types and layers and represented by separate material behaviour instead of combined types and layers.

Multidisciplinary collaborations seem beneficial for this field of research.

7.Future work

This research has shown some progress in methods for investigation of tissue deformation. During the process of this research questions were raised as well as insights of shortcomings, need for better understanding and more investigations. The potential for development is large, and below are suggestions for future work.

Develop the method and protocol

With high medical image resolutions in future data collections, the accuracy of tissue layer identification and displacement measures could be increased.

Further investigations of medical images for deformation measures in all three dimensions are needed in order to address anisotropy.

Data collection could be extended by preconditioning, stepwise loading and off-loading for better understanding of tissue behaviour.

The indenter equipment TIM could be further developed to obtain time-dependent deformation measures.

For clinical purposes the questionnaire and the clinical assessment protocol should be tested for validity and reliability.

Furthermore, repeated measures on the same subject over time in longitudinal studies could be of interest for within-subject variation.

More macro and meso level data from live humans

Investigations of individual specific deformation in several subjects with matching and with different health conditions are needed. Variation between participants, tissue type and site could be investigated for deeper understanding of live human tissue deformation on macro and meso level.

Determine individual specific material properties and material models

Further research is needed with focus on material properties and models.

Verification and validation of individual specific simulation models and material properties are needed. A simulation model was here initiated based on study II, see chapter 4.3.

Which material models to choose in specified simulations are not yet determined, and no golden standard exist. Thus, research comparing different material model's effects and prediction ability of the behaviour in the individual specific case is needed.

Investigations of soft tissue damage and risk levels

Provoking loading of tissues and mechanical and biological responses should be combined for investigations of tissue damage. Different types of tissue investigations may be needed to study the micro-level response to identify tissue damage and risk levels.

Sammanfattning

Förståelse för deformation av mänsklig vävnad är viktig för prevention och minskning av vävnadsskador från belastning av externa produkter, t.ex. för trycksårsprevention. Experimentella data för mänskliga vävnaders mekaniska materialegenskaper är begränsade. Dessutom verkar vävnaders tolerans mot belastning bero på individ-specifika förutsättningar och förhållanden, inklusive hälsotillstånd. Prediktering av mekaniskt vävnadsbeteende med hjälp av finita element (FE) modeller finns, men dessa simuleringar använder förenklade modeller och materialrepresentationer. Det är oklart hur förenklingarna påverkar resultaten. Strategier för att undersöka mänskliga vävnaders reaktion på belastningar behöver förbättras för ökad förståelse av vävnadsdeformation.

Denna avhandling syftar till att undersöka aspekter av deformation i mänsklig mjukdelsvävnad i nedre extremiteten när de utsätts för extern belastning. Avhandlingen fokuserar på vävnadsrepresentation i FE-simulering och individspecifik deformation av levande vävnad under kända hälsotillstånd.

För att undersöka påverkan av olika representationer av vävnader i FE simulering utformades en strategi med en generisk flerskiktmodell av ett underben. Två materialuppsättningar användes, där hud, fett, kärl och ben representerades separat medan fascia och muskelvävnader hade separata eller kombinerade materialegenskaper. Belastningssituationer med tre olika protesgeometrier användes och jämförelser av resultaten med de två olika materialuppsättningarna analyserades. Den relativa förändringen i resulterande spänningar, töjningar och kontaktkrafter var betydande mellan de två sätten att representera vävnaderna, oavsett belastningssituation. Således var modellen känslig för hur muskel- och fascia-vävnader var representerade. En experimentell strategi för att undersöka deformation i mjukdelsvävnader i underbenet hos en person med specifikt hälsotillstånd utvecklades och demonstrerades i en fallstudie. Ett instrument för vävnadsbelastning (tissue indentation measurement, TIM) designades så att mekanisk deformation kunde fångas i magnetisk resonanstomografi (MR). Ett frågeformulär och ett kliniskt bedömningsprotokoll omfattade hälsotillstånd relaterade till trycksårutveckling. De undersökta deformationsmått var förskjutning och töjning per vävnadsskikt, volymförändring med volymkvot respektive

deformationsgradient och dess determinant i ett definierat element i ett muskelområde. Individspecifika resultat för en frisk man visade att skikten av hud, fett, muskler och kärl komprimerades och hade stora töjningar, medan bindvävsskikten var inkompressibla och hade små töjningar.

Dessa resultat tyder på att deformation av mjukdelsvävnader i underben hos människor bör undersökas på vävnadsnivå per vävnadstyp och per vävnadsskikt, och representeras med separata materialbeteenden i modeller, istället för sammanslagna vävnadstyper och skikt.

Detta arbete har relevans för utökning av materialdata för mänskliga vävnader hos personer med olika hälsotillstånd och för verifiering och validering av simuleringsmodeller.

References

- [1] A. F. T. Mak, M. Zhang, and E. W. C. Tam, "Biomechanics of Pressure Ulcer in Body Tissues Interacting with External Forces during Locomotion," in *Annual Review of Biomedical Engineering, Vol 12*, vol. 12, M. L. Yarmush, J. S. Duncan, and M. L. Gray, Eds. (Annual Review of Biomedical Engineering, 2010, pp. 29-53.
- [2] Sveriges Kommuner och Landsting SKL (Swedish Association of Local Authorities and Regions). Mätning av trycksår i slutenvården: Resultat trycksårsmätningar 2017 (Measurement of pressure ulcers in hospital care) [Online]. Available: <https://skl.se/halsasjukvard/patientsakerhet/matningavskadorivarden/matningtrycksar.2125.html>
- [3] S. Coleman *et al.*, "A new pressure ulcer conceptual framework," *Journal of Advanced Nursing*, vol. 70, no. 10, pp. 2222-2234, 2014.
- [4] R. McRae, *Clinical orthopaedic examination*, 6. ed.. ed. Edinburgh, New York: Churchill Livingstone/Elsevier, 2010.
- [5] M. J. Highsmith and J. T. Highsmith, "Skin Problems in the Amputee," in *Atlas of amputations and limb deficiencies : surgical, prosthetic, and rehabilitation principles. Vol. 2, Lower limb, management issues*, vol. 2, J. I. Krajchich, M. S. Pinzur, L. B. K. Potter, and P. M. Stevens, Eds. 4. ed. / editors Joseph Ivan Krajchich ed. Rosemont, Ill.: American Academy of Orthopaedic Surgeons, 2016, pp. 677-696.
- [6] S. Coleman *et al.*, "Developing a pressure ulcer risk factor minimum data set and risk assessment framework," *Journal Of Advanced Nursing*, vol. 70, no. 10, pp. 2339-2352, 2014.
- [7] E. E. Haesler, "Prevention and Treatment of Pressure Ulcers: Quick Reference Guide. ," National Pressure Ulcer Advisory Panel, European Pressure Ulcer Advisory Panel, Pan Pacific Pressure Injury Alliance, Osborne Park, Western Australia 2014, Available: www.internationalguideline.com , www.npuap.org , www.epuap.org.
- [8] *ISO 8548-2 Prosthetics and orthotics - Limb deficiencies - Part 2: Method of describing lower limb amputation stumps*, 1993.
- [9] G. Silber and C. Then, *Preventive biomechanics: Optimizing support systems for the human body in the lying and sitting position*. 2013, pp. 1-372.
- [10] Y.-P. Huang, *Measurement of soft tissue elasticity in vivo : techniques and applications*. Boca Raton : CRC Press, 2015.
- [11] D. M. Sengeh, K. M. Moerman, A. Petron, and H. Herr, "Multi-material 3-D viscoelastic model of a transtibial residuum from in-vivo

- indentation and MRI data," (in English), *Journal of the Mechanical Behavior of Biomedical Materials*, Article vol. 59, pp. 379-392, Jun 2016.
- [12] R. M. A. Al-Dirini, M. P. Reed, J. W. Hu, and D. Thewlis, "Development and Validation of a High Anatomical Fidelity FE Model for the Buttock and Thigh of a Seated Individual," (in English), *Annals of Biomedical Engineering*, Article vol. 44, no. 9, pp. 2805-2816, Sep 2016.
 - [13] Y.-C. Fung, *Biomechanics : mechanical properties of living tissues*, 2. ed. ed. New York ; Berlin: New York ; Berlin : Springer-Vlg, 1993.
 - [14] H. B. Henninger, S. P. Reese, A. E. Anderson, and J. A. Weiss, "Validation of computational models in biomechanics," *Proceedings of the Institution of Mechanical Engineers Part H-Journal of Engineering in Medicine*, vol. 224, no. H7, pp. 801-812, 2010.
 - [15] M. Freutel, H. Schmidt, L. Durselen, A. Ignatius, and F. Galbusera, "Finite element modeling of soft tissues: Material models, tissue interaction and challenges," *Clinical Biomechanics*, Review vol. 29, no. 4, pp. 363-372, Apr 2014.
 - [16] G. J. Tortora and S. R. Grabowski, *Principles of anatomy and physiology*, 9. ed.. ed. New York: New York : John Wiley & Sons, Inc, 2000.
 - [17] F. H. Netter, *The CIBA Collection of Medical Illustrations Part I Anatomy, Physiology, and Metabolic Disorders, A compilation of paintings prepared by Frank H Netter, M.D.* (The CIBA Collection of Medical Illustrations). Summit, New Jersey: CIBA GEIGY Corporation, 1987.
 - [18] N. Shoham and A. Gefen, "Deformations, mechanical strains and stresses across the different hierarchical scales in weight-bearing soft tissues," *Journal of Tissue Viability*, vol. 21, no. 2, pp. 39-46, May 2012.
 - [19] C. W. J. Oomens, D. L. Bader, S. Loerakker, and F. Baaijens, "Pressure induced deep tissue injury explained," *Annals Of Biomedical Engineering*, vol. 43, no. 2, pp. 297-305, 2015.
 - [20] J. M. Black *et al.*, "Pressure Ulcers: Avoidable or Unavoidable? Results of the National Pressure Ulcer Advisory Panel Consensus Conference," *Ostomy Wound Management*, vol. 57, no. 2, pp. 24-+, Feb 2011.
 - [21] National Pressure Ulcer Advisory Panel. (2016, 10 January). *National Pressure Ulcer Advisory Panel (NPUAP) Pressure Injury Stages (3rd ed.)*. Available: <http://www.npuap.org/resources/educational-and-clinical-resources/npuap-pressure-injury-stages/>
 - [22] European Pressure Ulcer Advisory Panel and National Pressure Ulcer Advisory Panel, *Prevention and treatment of pressure ulcers : clinical practice guideline : international guideline* (Pressure ulcer prevention

- & treatment). Washington, D.C.: National Pressure Ulcer Advisory Panel, 2009.
- [23] K. K. Ceelen *et al.*, "Compression-induced damage and internal tissue strains are related," *Journal of Biomechanics*, Article vol. 41, no. 16, pp. 3399-3404, 2008.
 - [24] A. Gefen, "Risk factors for a pressure-related deep tissue injury: a theoretical model," *Medical & Biological Engineering & Computing*, vol. 45, no. 6, pp. 563-573, 2007.
 - [25] R. Taylor and T. James, "The Role of Oxidative Stress in the Development and Persistence of Pressure Ulcers," in *Pressure Ulcer Research Current and Future Perspectives*, D. Bader, C. V. Bouten, D. Colin, and C. Oomens, Eds. Heidelberg, Germany: Springer-Verlag Berlin, 2005, pp. 205-232.
 - [26] S. Tsuji, S. Ichioka, N. Sekiya, and T. Nakatsuka, "Analysis of ischemia-reperfusion injury in a microcirculatory model of pressure ulcers," *Wound Repair And Regeneration: Official Publication Of The Wound Healing Society [And] The European Tissue Repair Society*, vol. 13, no. 2, pp. 209-215, 2005.
 - [27] A. F. T. Mak, Y. Yu, L. P. C. Kwan, L. Sun, and E. W. C. Tam, "Deformation and reperfusion damages and their accumulation in subcutaneous tissues during loading and unloading: A theoretical modeling of deep tissue injuries," *Journal of Theoretical Biology*, vol. 289, no. 0, pp. 65-73, 11/21/ 2011.
 - [28] A. Gefen, "How much time does it take to get a pressure ulcer? Integrated evidence from human, animal, and in vitro studies," *Ostomy Wound Management*, vol. 54, no. 10, p. 26, 2008.
 - [29] A. Gefen, "Reswick and Rogers pressure-time curve for pressure ulcer risk. Part 2," *Nursing standard (Royal College of Nursing (Great Britain) : 1987)*, vol. 23, no. 46, pp. 40-44, 2009.
 - [30] S. Coleman *et al.*, "Patient risk factors for pressure ulcer development: systematic review," *International Journal Of Nursing Studies*, vol. 50, no. 7, pp. 974-1003, 2013.
 - [31] J. J. Elsner and A. Gefen, "Is obesity a risk factor for deep tissue injury in patients with spinal cord injury?," *Journal of Biomechanics*, Article vol. 41, no. 16, pp. 3322-3331, 2008.
 - [32] H. Sookyung *et al.*, "Body Mass Index and Pressure Ulcers: Improved predictability of pressure ulcers in intensive care patients," *American Journal of Critical Care*, vol. 23, no. 6, pp. 494-501, 2014.
 - [33] R. Korthuis, *Skeletal muscle circulation*. San Rafael (CA): Morgan & Claypool Life Sciences, 2011.
 - [34] K. M. Moerman *et al.*, "On the importance of 3D, geometrically accurate, and subject-specific finite element analysis for evaluation of

- in-vivo soft tissue loads," *Computer Methods in Biomechanics and Biomedical Engineering*, vol. 20, no. 5, pp. 483-491, Apr 2017.
- [35] C. Stecco, P. Pavan, P. Pachera, R. De Caro, and A. Natali, "Investigation of the mechanical properties of the human crural fascia and their possible clinical implications," *Surgical and Radiologic Anatomy*, vol. 36, no. 1, pp. 25-32, Jan 2014.
 - [36] Sveriges Kommuner och Landsting SKL (Swedish Association of Local Authorities and Regions). Resultat mätningar 2018 [Online]. Available: <https://skl.se/halsasjukvard/patientsakerhet/matningavskadorivarden/matningstrycksar.2125.html>
 - [37] International Diabetes Federation, "IDF Diabetes Atlas," International Diabetes Federation, Brussels, Belgium ISBN: 978-2-930229-87-4, 2017, Available: <http://www.diabetesatlas.org>.
 - [38] J. Lewis and A. Lipp, "Pressure-relieving interventions for treating diabetic foot ulcers," *The Cochrane Database Of Systematic Reviews*, vol. 1, p. CD002302, 2013.
 - [39] S. D. Ramsey *et al.*, "Incidence, outcomes, and cost of foot ulcers in patients with diabetes," *Diabetes care*, vol. 22, no. 3, pp. 382-387, 1999.
 - [40] L. Prompers *et al.*, "High prevalence of ischaemia, infection and serious comorbidity in patients with diabetic foot disease in Europe. Baseline results from the Eurodiale study," *Diabetologia*, vol. 50, no. 1, pp. 18-25, 2007.
 - [41] L. Prompers *et al.*, "Prediction of outcome in individuals with diabetic foot ulcers: focus on the differences between individuals with and without peripheral arterial disease. The EURODIALE Study," *Diabetologia*, vol. 51, no. 5, pp. 747-755, 2008.
 - [42] W. J. Jeffcoate and K. G. Harding, "Diabetic foot ulcers," *The Lancet*, vol. 361, no. 9368, pp. 1545-1551, 5/3/ 2003.
 - [43] P. C. Leung, "Diabetic foot ulcers - a comprehensive review," *Surgeon-Journal of the Royal Colleges of Surgeons of Edinburgh and Ireland*, vol. 5, no. 4, pp. 219-231, Aug 2007.
 - [44] K. M. Bui, G. J. Raugi, V. Q. Nguyen, and G. E. Reiber, "Skin problems in individuals with lower-limb loss: literature review and proposed classification system," *Journal Of Rehabilitation Research And Development*, vol. 46, no. 9, pp. 1085-1090, 2009.
 - [45] H. E. Meulenbelt, J. H. Geertzen, M. F. Jonkman, and P. U. Dijkstra, "Determinants of skin problems of the stump in lower-limb amputees," *Archives Of Physical Medicine And Rehabilitation*, vol. 90, no. 1, pp. 74-81, 2009.
 - [46] H. E. J. Meulenbelt, J. H. B. Geertzen, M. F. Jonkman, and P. U. Dijkstra, "Skin problems of the stump in lower limb amputees: 1. A

- clinical study," *Acta Dermato-Venereologica*, vol. 91, no. 2, pp. 173-177, 2011.
- [47] N. B. Yang, L. A. Garza, C. E. Foote, S. Kang, and J. H. Meyerle, "High prevalence of stump dermatoses 38 years or more after amputation," *Archives Of Dermatology*, vol. 148, no. 11, pp. 1283-1286, 2012.
 - [48] A. Westergren, S. Karlsson, P. Andersson, O. Ohlsson, and I. R. Hallberg, "Eating difficulties, need for assisted eating, nutritional status and pressure ulcers in patients admitted for stroke rehabilitation," *Journal Of Clinical Nursing*, vol. 10, no. 2, pp. 257-269, 2001.
 - [49] M. Guihan, S. L. Garber, C. H. Bombardier, B. Goldstein, S. A. Holmes, and L. Cao, "Predictors of pressure ulcer recurrence in veterans with spinal cord injury," *Journal of Spinal Cord Medicine*, vol. 31, no. 5, pp. 551-559, 2008.
 - [50] I. Olsson, M. Dahl, S. Mattsson, M. Wendelius, E. Aström, and L. Westbom, "Medical problems in adolescents with myelomeningocele (MMC): an inventory of the Swedish MMC population born during 1986-1989," *Acta Paediatrica (Oslo, Norway: 1992)*, vol. 96, no. 3, pp. 446-449, 2007.
 - [51] U. Källman and M. Lindgren, "Predictive Validity of 4 Risk Assessment Scales for Prediction of Pressure Ulcer Development in a Hospital Setting," *Advances in Skin & Wound Care*, vol. 27, no. 2, pp. 70-76, 2014.
 - [52] H. Meulenbelt, P. Dijkstra, M. Jonkman, and J. Geertzen, "Skin problems in lower limb amputees: A systematic review," *Disability & Rehabilitation*, Article vol. 28, no. 10, pp. 603-608, 2006.
 - [53] M. M. Lusardi, M. Jorge, and C. C. Nielsen, *Orthotics and prosthetics in rehabilitation*, 3. ed.. ed. (Orthotics and prosthetics in rehabilitation). St. Louis, Mo.: St. Louis, Mo. : Elsevier Saunders, 2013.
 - [54] *ISO 8548 Prosthetics and Orthotics - Limb deficiencies - Part 5: Description of the clinical condition of the person who has had an amputation*, 2003.
 - [55] *ISO 8551 Prosthetics and orthotics — Functional deficiencies — Description of the person to be treated with an orthosis, clinical objectives of treatment, and functional requirements of the orthosis*, 2003.
 - [56] P. Wriggers, *Nonlinear finite element methods*. Berlin ; London: Berlin ; London : Springer, 2008.
 - [57] G. A. Holzapfel, *Nonlinear solid mechanics : a continuum approach for engineering*. Chichester: Chichester : John Wiley, 2000.
 - [58] P. Hansbo, *Non-linear Finite Element Analysis, Advanced topics*. Jönköping, Sweden, 2016.
 - [59] W. D. Callister, *Materials science and engineering: an introduction*, 3rd ed. New York: John Wiley & sons, Inc., 1994.

- [60] T. A. Philpot, *Mechanics of materials: An intergrated learning system*. Hoboken, NJ: John Wiley & sons, Inc, 2008.
- [61] S. L. Evans, "On the implementation of a wrinkling, hyperelastic membrane model for skin and other materials," *Computer Methods in Biomechanics & Biomedical Engineering*, Article vol. 12, no. 3, pp. 319-332, 2009.
- [62] F. Frauziols *et al.*, "In vivo Identification of the Passive Mechanical Properties of Deep Soft Tissues in the Human Leg," *Strain*, vol. 52, no. 5, pp. 400-411, Oct 2016.
- [63] C. Then *et al.*, "A method for a mechanical characterisation of human gluteal tissue," *Technology And Health Care: Official Journal Of The European Society For Engineering And Medicine*, vol. 15, no. 6, pp. 385-398, 2007.
- [64] E. Linder-Ganz, N. Shabshin, Y. Itzhak, and A. Gefen, "Assessment of mechanical conditions in sub-dermal tissues during sitting: a combined experimental-MRI and finite element approach," *Journal Of Biomechanics*, vol. 40, no. 7, pp. 1443-1454, 2007.
- [65] E. Linder-Ganz, N. Shabshin, Y. Itzhak, Z. Yizhar, I. Siev-Ner, and A. Gefen, "Strains and stresses in sub-dermal tissues of the buttocks are greater in paraplegics than in healthy during sitting," (in English), *Journal of Biomechanics*, Article vol. 41, no. 3, pp. 567-580, 2008.
- [66] Y. Zheng and A. F. Mak, "Effective elastic properties for lower limb soft tissues from manual indentation experiment," *IEEE TRANSACTIONS ON REHABILITATION ENGINEERING*, vol. 7, no. 3, pp. 257-267, 1999.
- [67] A. Delalleau, G. Josse, J. M. Lagarde, H. Zahouani, and J. M. Bergheau, "Characterization of the mechanical properties of skin by inverse analysis combined with the indentation test," *Journal of Biomechanics*, vol. 39, no. 9, pp. 1603-1610, 2006.
- [68] C. Pailler-Mattei, S. Bec, and H. Zahouani, "In vivo measurements of the elastic mechanical properties of human skin by indentation tests," *Medical Engineering & Physics*, vol. 30, no. 5, pp. 599-606, Jun 2008.
- [69] B. Silver-Thorn, "In vivo indentation of lower extremity limb soft tissues," *IEEE Transactions on Rehabilitation Engineering*, vol. 7, no. 3, pp. 268-277, 1999.
- [70] E. Tonuk and M. B. Silver-Thorn, "Nonlinear viscoelastic material property estimation of lower extremity residual limb tissues," *Journal of Biomechanical Engineering-Transactions of the Asme*, vol. 126, no. 2, pp. 289-300, Apr 2004.
- [71] E. Tonuk and M. B. Silver-Thorn, "Nonlinear elastic material property estimation of lower extremity residual limb tissues," *Ieee Transactions on Neural Systems and Rehabilitation Engineering*, vol. 11, no. 1, pp. 43-53, Mar 2003.

- [72] E. Linder-Ganz, "Strains and stresses in sub-dermal tissues of the buttocks are greater in paraplegics than in healthy during sitting," *Journal of Biomechanics*, vol. 41, no. 3, pp. 567-580, 2008.
- [73] H. V. Tran, F. Charleux, M. Rachik, A. Ehrlacher, and M. C. H. B. Tho, "In vivo characterization of the mechanical properties of human skin derived from MRI and indentation techniques," *Computer Methods in Biomechanics & Biomedical Engineering*, Article vol. 10, no. 6, pp. 401-407, 2007.
- [74] J. S. Affagard, S. F. Bensamoun, and P. Feissel, "Development of an Inverse Approach for the Characterization of In Vivo Mechanical Properties of the Lower Limb Muscles," *Journal of Biomechanical Engineering-Transactions of the Asme*, vol. 136, no. 11, Nov 2014, Art. no. 111012.
- [75] J. S. Affagard, P. Feissel, and S. F. Bensamoun, "Identification of hyperelastic properties of passive thigh muscle under compression with an inverse method from a displacement field measurement," *Journal of Biomechanics*, Article vol. 48, no. 15, pp. 4081-4086, Nov 2015.
- [76] R. M. A. Al-Dirini, M. P. Reed, and D. Thewlis, "Deformation of the gluteal soft tissues during sitting," *Clinical Biomechanics*, vol. 30, no. 7, pp. 662-668, Aug 2015.
- [77] C. B. Clemen, G. E. K. Benderoth, A. Schmidt, F. Hubner, T. J. Vogl, and G. Silber, "Human skeletal muscle behavior in vivo: Finite element implementation, experiment, and passive mechanical characterization," (in English), *Journal of the Mechanical Behavior of Biomedical Materials*, Article vol. 65, pp. 679-687, Jan 2017.
- [78] Y.-K. Jan, C.-W. Lung, E. Cuaderes, D. Rong, and K. Boyce, "Effect of viscoelastic properties of plantar soft tissues on plantar pressures at the first metatarsal head in diabetics with peripheral neuropathy," *Physiological Measurement*, vol. 34, no. 1, pp. 53-66, 2013.
- [79] E. Linder-Ganz, G. Yarnitzky, Z. Yizhar, I. Siev-Ner, and A. Gefen, "Real-time finite element monitoring of sub-dermal tissue stresses in individuals with spinal cord injury: toward prevention of pressure ulcers," *Annals Of Biomedical Engineering*, vol. 37, no. 2, pp. 387-400, 2009.
- [80] C. Then *et al.*, "Analysis of mechanical interaction between human gluteal soft tissue and body supports," *Technology And Health Care: Official Journal Of The European Society For Engineering And Medicine*, vol. 16, no. 1, pp. 61-76, 2008.
- [81] C. Then, J. Menger, T. J. Vogl, F. Hübner, and G. Silber, "Mechanical gluteal soft tissue material parameter validation under complex tissue loading," *Technology And Health Care: Official Journal Of The European Society For Engineering And Medicine*, vol. 17, no. 5-6, pp. 393-401, 2009.

- [82] T. J. Vogl *et al.*, "Mechanical Soft Tissue Property Validation in Tissue Engineering Using Magnetic Resonance Imaging: Experimental Research," *Academic Radiology*, vol. 17, no. 12, pp. 1486-1491, Dec 2010.
- [83] C. Then, T. J. Vogl, and G. Silber, "Method for characterizing viscoelasticity of human gluteal tissue," *Journal of Biomechanics*, vol. 45, no. 7, pp. 1252-1258, Apr 2012.
- [84] W. Vannah and D. Childress, "Indentor tests and finite element modeling of bulk muscular tissue in vivo," *Journal of Rehabilitation Research and Development*, vol. 33, no. 3, pp. 239-252, 1996.
- [85] C. Y. L. Chao, Y. P. Zheng, Y. P. Huang, and G. L. Y. Cheing, "Biomechanical properties of the forefoot plantar soft tissue as measured by an optical coherence tomography-based air-jet indentation system and tissue ultrasound palpation system," *Clinical Biomechanics*, vol. 25, no. 6, pp. 594-600, Jul 2010.
- [86] A. Gefen, "The in vivo elastic properties of the plantar fascia during the contact phase of walking," (in English), *Foot & Ankle International*, Article vol. 24, no. 3, pp. 238-244, Mar 2003.
- [87] A. Gefen, M. Megido-Ravid, M. Azariah, Y. Itzhak, and M. Arcan, "Integration of plantar soft tissue stiffness measurements in routine MRI of the diabetic foot," *Clinical Biomechanics*, vol. 16, no. 10, pp. 921-925, Dec 2001.
- [88] M. Petre, A. Erdemir, and P. R. Cavanagh, "An MRI-compatible foot-loading device for assessment of internal tissue deformation," *Journal of Biomechanics*, vol. 41, no. 2, pp. 470-474, 2008.
- [89] G. Yarnitzky, Z. Yizhar, and A. Gefen, "Real-time subject-specific monitoring. of internal deformations and stresses in the soft tissues of the foot: A new approach in gait analysis," *Journal of Biomechanics*, vol. 39, no. 14, pp. 2673-2689, 2006.
- [90] C. G. Fontanella *et al.*, "Investigation on the load-displacement curves of a human healthy heel pad: In vivo compression data compared to numerical results," *Medical Engineering & Physics*, Article vol. 34, no. 9, pp. 1253-1259, Nov 2012.
- [91] S. Matteoli *et al.*, "Investigations on the viscoelastic behaviour of a human healthy heel pad: In vivo compression tests and numerical analysis," *Proceedings of the Institution of Mechanical Engineers Part H-Journal of Engineering in Medicine*, Article vol. 227, no. H3, pp. 334-342, 2013.
- [92] R. Suzuki, K. Ito, T. Lee, and N. Ogihara, "Parameter identification of hyperelastic material properties of the heel pad based on an analytical contact mechanics model of a spherical indentation," *Journal of the Mechanical Behavior of Biomedical Materials*, vol. 65, pp. 753-760, 2017/01/01/ 2017.

- [93] S. C. Wearing, J. E. Smeathers, B. Yates, S. R. Urry, and P. Dubois, "Bulk compressive properties of the heel fat pad during walking: A pilot investigation in plantar heel pain," *Clinical Biomechanics*, vol. 24, no. 4, pp. 397-402, 2009.
- [94] Y. P. Zheng and A. F. T. Mak, "Extraction of quasi-linear viscoelastic parameters for lower limb soft tissues from manual indentation experiment," *Journal of Biomechanical Engineering-Transactions of the Asme*, vol. 121, no. 3, pp. 330-339, Jun 1999.
- [95] A. F. T. Mak, G. H. W. Liu, and S. Y. Lee, "BIOMECHANICAL ASSESSMENT OF BELOW-KNEE RESIDUAL LIMB TISSUE," *Journal of Rehabilitation Research and Development*, vol. 31, no. 3, pp. 188-198, 1994.
- [96] K. M. Moerman, A. M. J. Sprengers, A. J. Nederveen, and C. K. Simms, "A novel MRI compatible soft tissue indenter and fibre Bragg grating force sensor," *Medical Engineering & Physics*, vol. 35, no. 4, pp. 486-499, Apr 2013.
- [97] M. H. Lu, W. Yu, Q. H. Huang, Y. P. Huang, and Y. P. Zheng, "A Hand-Held Indentation System for the Assessment of Mechanical Properties of Soft Tissues In Vivo," *Ieee Transactions on Instrumentation and Measurement*, vol. 58, no. 9, pp. 3079-3085, Sep 2009.
- [98] G. Boyer, J. Molimard, M. Ben Tkaya, H. Zahouani, M. Pericoi, and S. Avril, "Assessment of the in-plane biomechanical properties of human skin using a finite element model updating approach combined with an optical full-field measurement on a new tensile device," *Journal of the Mechanical Behavior of Biomedical Materials*, vol. 27, no. 0, pp. 273-282, 11// 2013.
- [99] K. M. Moerman, C. A. Holt, S. L. Evans, and C. K. Simms, "Digital image correlation and finite element modelling as a method to determine mechanical properties of human soft tissue in vivo," *Journal of Biomechanics*, vol. 42, no. 8, pp. 1150-1153, May 2009.
- [100] S. Portnoy, N. Shabshin, I. Siev-Ner, A. Kristal, and A. Gefen, "MRI Integrated with Computational Methods for Determining Internal Soft Tissue Loads as Related to Chronic Wounds," in *Bioengineering Research of Chronic Wounds: A Multidisciplinary Study Approach*, vol. 1, A. Gefen, Ed. (Studies in Mechanobiology Tissue Engineering and Biomaterials, 2009, pp. 169-180.
- [101] S. Portnoy, I. Siev-Ner, N. Shabshin, A. Kristal, Z. Yizhar, and A. Gefen, "Patient-specific analyses of deep tissue loads post transtibial amputation in residual limbs of multiple prosthetic users," *Journal Of Biomechanics*, vol. 42, no. 16, pp. 2686-2693, 2009.

- [102] S. Portnoy *et al.*, "Internal mechanical conditions in the soft tissues of a residual limb of a trans-tibial amputee," *Journal Of Biomechanics*, vol. 41, no. 9, pp. 1897-1909, 2008.
- [103] S. C. Bushong, *Magnetic resonance imaging : physical and biological principles*, 4. ed. / Stewart Carlyle Bushong, Geoffrey Clarke. ed. St. Louis: St. Louis : Elsevier, 2015.
- [104] N. S. Ottesen and H. Petersson, *Introduction to the finite element method*. Harlow, England: Pearson Prentice Hall, 1992.
- [105] A. e. Gefen, *Patient-Specific Modeling in Tomorrow's Medicine*. Springer Berlin Heidelberg, 2012.
- [106] P. S. Ginestra, E. Ceretti, and A. Fiorentino, "Potential of modeling and simulations of bioengineered devices: Endoprostheses, prostheses and orthoses," *Proceedings of the Institution of Mechanical Engineers Part H-Journal of Engineering in Medicine*, vol. 230, no. 7, pp. 607-638, Jul 2016.
- [107] W. C. C. Lee, "Computational and experimental analysis of the use of lower-limb prostheses, concerning comfort, structural design and gait performance," Ph.D., Hong Kong Polytechnic University (People's Republic of China), 2006.
- [108] S. Portnoy and A. Gefen, "Patient-specific modeling of subjects with a lower limb amputation," in *Patient-specific modeling in tomorrow's medicine*, vol. 9, A. Gefen, Ed. 1 ed. (Studies in mechanobiology, tissue engineering and biomaterials, Heidelberg: Springer, 2012, pp. 441-459.
- [109] A. S. Dickinson, J. W. Steer, and P. R. Worsley, "Finite element analysis of the amputated lower limb: A systematic review and recommendations," (in English), *Medical Engineering & Physics*, vol. 43, pp. 1-18, May 2017.
- [110] J. C. Cagle *et al.*, "A finite element model to assess transtibial prosthetic sockets with elastomeric liners," *Medical & Biological Engineering & Computing*, vol. 56, no. 7, pp. 1227-1240, Jul 2018.
- [111] F. Desbiens-Blais, J. Clin, S. Parent, H. Labelle, and C. E. Aubin, "New brace design combining CAD/CAM and biomechanical simulation for the treatment of adolescent idiopathic scoliosis," *Clinical Biomechanics*, vol. 27, no. 10, pp. 999-1005, Dec 2012.
- [112] J. P. Little and C. J. Adam, "Geometric sensitivity of patient-specific finite element models of the spine to variability in user-selected anatomical landmarks," (in English), *Computer Methods in Biomechanics and Biomedical Engineering*, vol. 18, no. 6, pp. 676-688, Apr 2015.
- [113] W. Wang, G. R. Baran, R. R. Betz, A. F. Samdani, J. M. Pahys, and P. J. Cahill, "The Use of Finite Element Models to Assist Understanding and Treatment For Scoliosis: A Review Paper," (in eng), *Spine Deform*, vol. 2, no. 1, pp. 10-27, Jan 2014.

- [114] A. F. T. Mak, M. Zhang, and D. A. Boone, "State-of-the-art research in lower-limb prosthetic biomechanics-socket interface: a review," *Journal of Rehabilitation Research & Development*, vol. 38, no. 2, pp. 161-173, 2001.
- [115] A. Gefen, N. Gefen, E. Linder-Ganz, and S. S. Margulies, "In vivo muscle stiffening under bone compression promotes deep pressure sores," *Journal Of Biomechanical Engineering*, vol. 127, no. 3, pp. 512-524, 2005.
- [116] J. W. Fernandez, M. Z. U. Haque, P. J. Hunter, and K. Mithraratne, "Mechanics of the foot Part 1: A continuum framework for evaluating soft tissue stiffening in the pathologic foot," (in English), *International Journal for Numerical Methods in Biomedical Engineering*, Article vol. 28, no. 10, pp. 1056-1070, Oct 2012.
- [117] Y. Wang, S. Downie, N. Wood, D. Firmin, and X. Y. Xu, "Finite element analysis of the deformation of deep veins in the lower limb under external compression," *Medical Engineering & Physics*, vol. 35, no. 4, pp. 515-523, Apr 2013.
- [118] M. Zhang, A. F. T. Mak, and V. C. Roberts, "Finite element modelling of a residual lower-limb in a prosthetic socket: a survey of the development in the first decade," *Medical Engineering & Physics*, vol. 20, no. 5, pp. 360-373, 7// 1998.
- [119] S. Portnoy *et al.*, "Real-time patient-specific finite element analysis of internal stresses in the soft tissues of a residual limb: A new tool for prosthetic fitting," *Annals of Biomedical Engineering*, vol. 35, no. 1, pp. 120-135, Jan 2007.
- [120] S. Avril, L. Bouten, L. Dubuis, S. Drapier, and J. F. Pouget, "Mixed Experimental and Numerical Approach for Characterizing the Biomechanical Response of the Human Leg Under Elastic Compression," *Journal of Biomechanical Engineering-Transactions of the Asme*, vol. 132, no. 3, Mar 2010, Art. no. 031006.
- [121] B. Derby and R. Akhtar, *Mechanical Properties of Aging Soft Tissues*. Springer, 2015.
- [122] M. Petre, A. Erdemir, V. P. Panoskaltsis, T. A. Spirka, and P. R. Cavanagh, "Optimization of Nonlinear Hyperelastic Coefficients for Foot Tissues Using a Magnetic Resonance Imaging Deformation Experiment," *Journal of Biomechanical Engineering-Transactions of the Asme*, vol. 135, no. 6, Jun 2013, Art. no. 061001.
- [123] L. Dubuis, S. Avril, J. Debayle, and P. Badel, "Identification of the material parameters of soft tissues in the compressed leg," *Computer Methods in Biomechanics and Biomedical Engineering*, vol. 15, no. 1, pp. 3-11, 2012.
- [124] P. Y. Rohan, P. Badel, B. Lun, D. Rastel, and S. Avril, "Prediction of the Biomechanical Effects of Compression Therapy on Deep Veins

- Using Finite Element Modelling," *Annals of Biomedical Engineering*, Article vol. 43, no. 2, pp. 314-324, Feb 2015.
- [125] J. E. Sanders and C. H. Daly, "Normal and shear stresses on a residual limb in a prosthetic socket during ambulation - Comparison of finite-element results with experimental measurements," *Journal of Rehabilitation Research and Development*, vol. 30, no. 2, pp. 191-204, 1993.
 - [126] M. Zhang and C. Roberts, "Comparison of computational analysis with clinical measurement of stresses on below-knee residual limb in a prosthetic socket," *Medical Engineering & Physics*, vol. 22, no. 9, pp. 607-612, Nov 2000.
 - [127] D. Lacroix and J. F. R. Patino, "Finite Element Analysis of Donning Procedure of a Prosthetic Transfemoral Socket," *Annals of Biomedical Engineering*, vol. 39, no. 12, pp. 2972-2983, Dec 2011.
 - [128] Y. N. Chen, J. Wang, C. W. Lung, T. D. Yang, B. A. Crane, and Y. K. Jan, "Effect of Tilt and Recline on Ischial and Coccygeal Interface Pressures in People with Spinal Cord Injury," (in English), *American Journal of Physical Medicine & Rehabilitation*, vol. 93, no. 12, pp. 1019-1030, Dec 2014.
 - [129] S. Loerakker, D. L. Bader, F. P. T. Baaijens, and C. W. J. Oomens, "Which factors influence the ability of a computational model to predict the in vivo deformation behaviour of skeletal muscle?," *Computer Methods in Biomechanics & Biomedical Engineering*, Article vol. 16, no. 3, pp. 338-345, 2013.
 - [130] M. Viceconti, S. Olsen, L. P. Nolte, and K. Burton, "Extracting clinically relevant data from finite element simulations," *Clinical Biomechanics*, vol. 20, no. 5, pp. 451-454, Jun 2005.
 - [131] M. Bellgran and K. Safsten, *Production Development: Design and Operation of Production Systems* (Production Development: Design and Operation of Production Systems). Godalming: Springer-Verlag London Ltd, 2010, pp. 1-340.
 - [132] K. T. Ulrich and S. D. Eppinger, *Product design and development*, 5. ed.. ed. Boston, Mass.: McGraw-Hill/Irwin, 2012.
 - [133] K. Williamson, *Research methods for students, academics and professionals : information management and systems*, 2. ed.. ed. Wagga Wagga, N.S.W.: Centre for Information Studies, Charles Sturt University, 2002.
 - [134] S. Kallin, A. Rashid, K. Salomonsson, and P. Hansbo, "Comparison of mechanical conditions in a lower leg model with 5 or 6 tissue types while exposed to prosthetic sockets applying finite element analysis [Preprint]," ed. arXiv.org: 1907.13340: arXiv.org, 2019.

- [135] J. Fergason and D. G. Smith, "Socket considerations for the patient with a transtibial amputation," *Clinical Orthopaedics and Related Research*, Article no. 361, pp. 76-84, Apr 1999.
- [136] "Abaqus/CAE Users Guide V. 6.14-3," in *Abaqus Documentation*, 6.14-3 ed: Dassault Systèmes.
- [137] T. Payne, S. Mitchell, R. Bibb, and M. Waters, "The evaluation of new multi-material human soft tissue simulants for sports impact surrogates," (in English), *Journal of the Mechanical Behavior of Biomedical Materials*, vol. 41, pp. 336-356, Jan 2015.
- [138] P. G. Pavan, P. Pachera, C. Stecco, and A. N. Natali, "Biomechanical behavior of human crural fascia in anterior and posterior regions of the lower limb," *Medical & Biological Engineering & Computing*, vol. 53, no. 10, pp. 951-959, Oct 2015.
- [139] B. K. Hoffmeister, S. R. Smith, S. M. Handley, and J. Y. Rho, "Anisotropy of Young's modulus of human tibial cortical bone," *Medical & Biological Engineering & Computing*, vol. 38, no. 3, pp. 333-338, May 2000.
- [140] M. J. Gerschutz, M. L. Haynes, D. M. Nixon, and J. M. Colvin, "Tensile strength and impact resistance properties of materials used in prosthetic check sockets, copolymer sockets, and definitive laminated sockets," *Journal of Rehabilitation Research and Development*, vol. 48, no. 8, pp. 987-1004, 2011.
- [141] O. A. Shergold, N. A. Fleck, and D. Radford, "The uniaxial stress versus strain response of pig skin and silicone rubber at low and high strain rates," *International Journal of Impact Engineering*, vol. 32, no. 9, pp. 1384-1402, Sep 2006.
- [142] K. Comley and N. Fleck, "The compressive response of porcine adipose tissue from low to high strain rate," *International Journal of Impact Engineering*, vol. 46, pp. 1-10, 2012/08/01/ 2012.
- [143] M. Lilja, "Prosthetic fitting. Stump-socket interaction in transtibial amputees," PhD, Faculty of health sciences, Linköping University, Sweden, Linköping University, Linköping, Sweden, 1998.
- [144] B. Asa, M. W. C. Payne, T. D. Wilson, C. E. Dunning, and T. A. Burkhart, "In vitro biomechanical evaluation of fibular movement in below knee amputations," *Clinical Biomechanics*, vol. 29, no. 5, pp. 551-555, May 2014.
- [145] S. Derler and L. C. Gerhardt, "Tribology of Skin: Review and Analysis of Experimental Results for the Friction Coefficient of Human Skin," *Tribology Letters*, vol. 45, no. 1, pp. 1-27, Jan 2012.
- [146] J. Black *et al.*, "National Pressure Ulcer Advisory Panel's updated pressure ulcer staging system," *Advances In Skin & Wound Care*, vol. 20, no. 5, pp. 269-274, 2007.

- [147] J. McLeod Roberts, "Vascular assessment," in *Assessment of the lower limb*, L. M. Merriman and W. Turner, Eds. 2nd ed. Edinburgh: Churchill Livingstone, 2002.
- [148] K. Hagberg, R. Brånemark, and O. Hägg, "Questionnaire for Persons with a Transfemoral Amputation (Q-TFA): initial validity and reliability of a new outcome measure," *Journal Of Rehabilitation Research And Development*, vol. 41, no. 5, pp. 695-706, 2004.
- [149] J. S. Ulbrecht, T. Hurley, D. T. Mauger, and P. R. Cavanagh, "Prevention of recurrent foot ulcers with plantar pressure-based in-shoe orthoses: the CareFUL prevention multicenter randomized controlled trial," *Diabetes Care*, vol. 37, no. 7, pp. 1982-1989, 2014.
- [150] R. Vilchis-Aranguren, D. Gayol-Mérida, J. Quinzaños-Fresnedo, R. Pérez-Zavala, and C. Galíndez-Novoa, "A prospective, longitudinal, descriptive study of the effect of a customized wheelchair cushion on clinical variables, satisfaction, and functionality among patients with spinal cord injury," *Ostomy/Wound Management*, vol. 61, no. 2, pp. 26-36, 2015.
- [151] G. Jarl, "The Orthotics and Prosthetics Users' Survey - Translation and validity evidence for the Swedish version," PhD in Medicine Doctoral dissertation, School of Health and Medical Sciences, Örebro University, Örebro, Sweden, Örebro, Örebro Studies in Medicine 104, 2014.
- [152] G. Jarl, M. Holmefur, and L. M. N. Hermansson, "Test-retest reliability of the Swedish version of the Orthotics and Prosthetics Users' Survey," *Prosthetics And Orthotics International*, vol. 38, no. 1, pp. 21-26, 2014.
- [153] G. M. Jarl, A. W. Heinemann, and L. M. Norling Hermansson, "Validity evidence for a modified version of the Orthotics and Prosthetics Users' Survey," *Disability And Rehabilitation. Assistive Technology*, vol. 7, no. 6, pp. 469-478, 2012.
- [154] G. M. Jarl and L. M. N. Hermansson, "Translation and linguistic validation of the Swedish version of Orthotics and Prosthetics Users' Survey," *Prosthetics And Orthotics International*, vol. 33, no. 4, pp. 329-338, 2009.
- [155] L. Orwelius *et al.*, "The Swedish RAND-36 Health Survey - reliability and responsiveness assessed in patient populations using Svensson's method for paired ordinal data," *Journal Of Patient-Reported Outcomes*, vol. 2, no. 1, pp. 4-4, 2017.
- [156] E. Carlsson, "The importance of psychological and physical stressors on diabetes-related immunity in a young population – an interdisciplinary approach," 072 Doctoral thesis, comprehensive summary, Dissertation Series. School of Health and Welfare, Jönköping University, School of Health and Welfare, Jönköping, 2016.

- [157] T. L. Beauchamp and J. F. Childress, *Principles of biomedical ethics*, 7. ed.. ed. New York: New York : Oxford University Press, 2013.
- [158] *WMA Declaration of Helsinki - Ethical Principles for Medical Research Involving Human Subjects*, W. M. Association, 2013.
- [159] M. T. Avila, R. R. Conley, and W. T. Carpenter, "A comparison of symptom provocation procedures in psychiatry and other areas of medicine: implications for their ethical use in research," *Biological Psychiatry*, vol. 50, no. 7, pp. 479-486, 2001.
- [160] K. L. Andrews *et al.*, "Lower limb amputations due to vascular disease: A multidisciplinary approach to surgery and rehabilitation," in "ISPO Report," International Society for Prosthetics and Orthotics2017.
- [161] L. M. Merriman and W. Turner, L. M. Merriman and W. Turner, Eds. *Assessment of the lower limb*, 2nd ed. Churchill Livingstone, 2002.
- [162] C. Boks and T. C. McAloone, "Transitions in sustainable product design research," *International Journal of Product Development*, vol. 9, no. 4, pp. 429-449, 2009.
- [163] L. Bouten, "Identification of mechanical properties of the leg's constitutive tissues for the mechanical study of the support," Ecole Nationale Supérieure des Mines de Saint-Etienne, 2009.
- [164] A. Palevski, I. Glaich, S. Portnoy, E. Linder-Ganz, and A. Gefen, "Stress relaxation of porcine gluteus muscle subjected to sudden transverse deformation as related to pressure sore modeling," *Journal of Biomechanical Engineering-Transactions of the Asme*, vol. 128, no. 5, pp. 782-787, Oct 2006.
- [165] T. Brosh and M. Arcan, "Modeling the body/chair interaction – an integrative experimental–numerical approach," *Clinical Biomechanics*, vol. 15, no. 3, pp. 217-219, 2000/03/01/ 2000.

List of Figures

Figure #	Page	Source
Figure 1 Tissues at the mid-height of a human transtibial transverse cross section	6	Author S. Kallin, based on Netter [17]
Figure 2 A. Skin layers of human skin	7	Wikimedia commons, Madhero88, https://commons.wikimedia.org/wiki/File:Skin_layers.png
Figure 2 B. Muscle tissue structure	7	Wikimedia Commons, National Institutes of Health, https://commons.wikimedia.org/wiki/File:Skeletal_muscle.png
Figure 3 Multistructural model with defined levels, applied to the lower leg structures,	8	Author S. Kallin
Figure 4 New Pressure Ulcer Conceptual framework, Coleman <i>et al</i> 2014	11	Coleman <i>et al</i> [3] figure 3 from p.2232
Figure 5 Deformation of a line element in a 2D body, displacement, rotation and elongation	18	Author S. Kallin
Figure 6 Transformation node-to-node, Isoparametric mapping	26	Author S. Kallin
Figure 7 The product realisation process: part of the innovation process and product lifecycle	29	Figure 1.3. p.6. in Säfsten and Johansson, 2005 [131]
Figure 8 Product development process related to soft tissue material properties	30	Adopted and modified from exhibit 2-2, p.14 in [132]
Figure 9 Application of the PI framework by Coleman <i>et al</i> [3] to this research.	33	Adapted by author S.Kallin from Coleman <i>et al</i> [3] figure 3 p.2232
Figure 10 Overview research approach.	35	Author S. Kallin
Figure 11 The FE model geometry for the trans-tibial cross-section of a human adult	37	Author S. Kallin from FE model by A Rashid
Figure 12 The cross-section geometries of socket models and limb overlap.	38	Author S. Kallin
Figure 13 Calibration of material data sets.	42	Author S. Kallin
Figure 14 Schematic process of research	45	Author S. Kallin
Figure 15 TIM Tissue Indenter Measurement device for indentation and force-displacement data	47	Author S. Kallin

Figure #	Page	Source
Figure 16 Body support, leg fixation and TIM with frame fixture.	49	Author S. Kallin
Figure 17 The TIM frame connected anteriorly to the plaster shell, loaded condition.	53	Author S. Kallin
Figure 18 MR images of non-loaded (A) and loaded (B) conditions at the slice of indenter apex.	55	Author S. Kallin
Figure 19 Mapping from parent to global domain.	57	Author S. Kallin
Figure 20 Effective Stress S (vonMises) in [Pa], displayed distribution per material set and socket design.	62	Author S. Kallin
Figure 21 Shear Strain distribution per material set and socket design.	63	Author S. Kallin
Figure 22 Relative change of maxima, per tissue type, for Combined set compared to Separate set.	64	Author S. Kallin
Figure 23 Relative change of stresses per sites of maxima and tissue types.	65	Author S. Kallin
Figure 24 Relative change of strains per sites of maxima.	66	Author S. Kallin
Figure 25 Contact pressure distribution at skin-socket interface with three socket designs and two material sets	67	Author S. Kallin
Figure 26 Blood pressure data.	70	Author S. Kallin
Figure 27 Examples of identified tissues in MR image of no-loaded condition at the level of indentation.	71	Author S. Kallin
Figure 28 Corresponding MR images with identified tissue reference points	72	Author S. Kallin
Figure 29 Stretch ratio in y, per tissue layer	73	Author S. Kallin
Figure 30 The local bilinear test-element's defined nodes	74	Author S. Kallin
Figure 31 Digital model from MR images	76	Author S. Kallin
Figure 32 Example evaluation maximum effective stress found at nodes in elements with small-angled corners.	80	Author S. Kallin
Figure 33 Example MR data of the loaded condition in three planes.	84	Author S. Kallin
Figure 34 Schematic overview of contributions	94	Author S. Kallin
Figure 35 Algorithm of Clinical process incorporating suggested steps addressing soft tissue parameters based on current research.	97	Author S. Kallin

Appendices

I. Material parameters from indentation studies on human leg

Table 10 Indentation studies and material parameters

Reference, comment	Tissue	Material model, measures	Parameters
Vannah & Childress, 1996 [84] Experimental, indentation, FEA 2 females, 5 males	Posterior calf, compound of tissues Relaxed vs mild exertion	Nonlinear Force-displacement; hysteresis nonlinear curve, with Parabolic fit 2nd order polynomial regression, fitting to onloading curve FEA simulation to obtain C parameters, using James-Green-Simpson and assuming $I_3 = 1$, $\lambda_1 = \lambda$, $\lambda_2 = \lambda_3 = \frac{1}{\sqrt{\lambda}}$	Hysteresis; constant across rest times 5-60 s, Force peak 7N, Displacement mean 21.2mm on relaxed calf, 18.25 mm at mild exertion. Stress relaxation <10%, Stiffness (slope of force-displacement, df/du): 0.519 N/mm relaxed, 0.769 N/mm at mild exertion. c_{10} : 2.6 kPa, $c_{01} = \frac{c_{10}}{4}$: 0.64 kPa, c_{11} : 5.7 kPa
Silver-Thorn 1999, [69], Experiment, indentation. 5 trans-tibial amputees, 5 non-amputees	Calf, compound of tissues, posterior	Nonlinear, standard viscoelastic model. 3 rd order polynomial, regression to data. Force, displacement, time Cyclic loading, rate-controlled, different loading rates. $f(t)$ force relaxation response, $d(t)$ creep response, d displacement $E = \mu_0$ relaxed elastic modulus μ_1, η_1	$\tau_\varepsilon = \eta_1/\mu_1$ time constant at constant strain, Relaxation: 29-82% amputees, 87-96% nonamputees Equilibrate (τ_ε) in approx. 60s. Maximum tolerated d : 4.2 – 11.8 mm amputees, 6.6 - 10.5 mm nonamputees
Tönük & Silver-Thorn, 2003, [71] FE Simulation based on indentation experiment of 7 amputees from [69]	Calf, compound of tissues, 9-11 sites/limb	Simulation model of the site and indenter, Tissue thickness from image data Nonlinear, elastic, incompressible, Homogenous, isotropic Simulated cyclic loading, obtain tissue stiffness James-Green-Simpson strain energy model, reduced $C_{10} = C_{01} = C_1$ small strains $C_{11} = C_{20} = C_2$ approximated tissue stiffness at higher strains $C_{30} = C_3$ approximated tissue stiffness at higher strains Manual iterative optimization, minimize error for reaction force.	C_1 : 0.01-700 kPa C_2 : 0.01-2350 kPa C_3 : 0.01 kPa – 250 MPa

Continue next page

Reference, comment	Tissue	Material model, measures	Parameters
Avril <i>et al</i> 2010 [120] Experiment, compression sock FE simulation 1 female	Calf	Large deformations, nonlinear.	C_{10}^f : 4.5 kPa, (2-7 kPa)
	Fat/Skin	Homogenous, Compressible, hyperelastic.	K_v^f : 106 kPa (71.3-140 kPa)
	Calf	Neo-Hookean strain energy function	C_{10}^m : 11.2 kPa (9.4-12.9 kPa)
	Muscles	$C_{10}^f, C_{10}^m, K_v^f, K_m^f$ Optimization by Nelder-Mead and minimizing difference	K_m^f : 69.5 kPa (61-78 kPa)
Frauziols <i>et al</i> 2016 [62] Experiment, indentation, Ultrasound, FE simulation 1 female, 3 male Displacement 30mm	Calf, Superficial soft tissues	Neo-Hookean, Hyper-elastic J^{el} elastic volume ratio, \bar{I}_1 1 st invariant of the isochoric deformation Force, Displacement	C_{10}^H : 2 kPa (from [163]) D_1 : 22.5 MPa ⁻¹ (from [163])
	Calf, Deep soft tissues below crural fascia	A. Neo-Hookean Hyper-elastic B. 2 nd order-reduced polynomial, hyper-elastic (from Abaqus User Manual v.6.9)	C_{10}^H : 0.5-2.11 kPa D_1 : 28 MPa ⁻¹ (from [163]) C_{10}^{Deep} : 0.19-0.82 kPa, C_{20}^{Deep} : 0.24-2.61 kPa D_1 28 MPa ⁻¹ (from [163]), D_2 28 MPa ⁻¹ (from [163])
	Calf, Fascia cruris	Neo-Hookean, Hyper-elastic	C_{10}^H : 100 kPa from [86] D_1 : 22.5 MPa ⁻¹ (from [163])
	Calf	Nonlinear, elastic, hyperelastic by 2 nd order Ogden, nearly incompressible.	Bulk modulus $\kappa = 100 \times C$ C : 5.20 kPa m : 4.78 γ : 3.47 MPa, τ : 0.34 s
	Internal soft tissues as one, except skin/fat layer.	$C_{10} = C_{20} = C$, $m_1 = m_2 = m$	
Sengeh <i>et al.</i> 2016 [11] Experiment, indentation, MRI for non-loaded geometry. FE simulation. 1 subject, trans-tibial amputee	Calf	shear γ , τ	Bulk modulus $\kappa = 100 \times C$
	Skin/fat	Bulk modulus κ	C : 5.22 kPa
		Viscoelastic portion by quasi-linear viscoelastic theory (QLV)	m : 4.79
		Force-time-displacement, 18 sites. Optimization of parameters for one site, applied to 14 other in FE	γ : 3.57 MPa, τ : 0.32 s

Continue next page

Reference, comment	Tissue	Material model, measures	Parameters
Then <i>et al</i> , 2007 [63], Experiment, indentation, MRI. FE simulation 1 subject	Muscle	Elastic, nonlinear, hyperelastic, isotropic	μ_1 : 0.103×10^{-2} MPa μ_2 : 0.145×10^{-6} MPa
	Posterior-lateral gluteal region	Cauchy stress tensor, S , Ogden for slightly incompressible materials combined.	α_1 : 1.32 α_2 : -183.60
		$\bar{\lambda}_i = J^{(-1/3)} \lambda_i \ i=(1,2,3)$	D_1 : 19.50 MPa^{-1} D_2 : 166.32 MPa^{-1}
		$\mu_0, \alpha_0, D_1, K_0, \nu$	(values obtained from table 1 in [63] and rounded off)
	Skin-Fat layer	Incremental displacement, loading- unloading	μ_1 : 0.118×10^{-2} MPa μ_2 : 0.644×10^{-7} MPa
	Posterior-lateral gluteal region	Thickness of each layer at each increment, Displacement of each layer.	α_1 : -0.11 α_2 : -0.32
		Optimization of material parameters per tissue type	D_1 : 16.91 MPa^{-1} D_2 : 4.77 MPa^{-1}
			(values obtained from table 1 in [63] and rounded off)
Linder-Ganz <i>et al</i> , 2007 [64] Experiment, flat indentation, sitting, open-MRI, FE simulation 6 healthy (3 female, 3 male)	Muscle, Gluteus	Nonlinear, incompressible, Neo-Hookean by Ogden 1 st order and excluding the last term	$\mu_0 = 8.5 \text{ kPa}$ from porcine [164]
		Viscoelastic by Prony series expansion but without transient response	$\sigma_c = 32 \pm 9 \text{ kPa}$ $\varepsilon_c = 74 \pm 7 \%$
	Fat-skin	Tissues thickness at non-weight bearing, weight bearing	$\mu_0 = 31.9 \text{ kPa}$ from [165]
		Thickness change $\Delta d = d_1 - d_2$, Mean $\Delta d = 13 \pm 2 \text{ mm}$	$\sigma_c = 18 \pm 4 \text{ kPa}$ $\varepsilon_c = 46 \pm 7 \%$
		External interface pressures at weight bearing	
		Peak pressure: $17 \pm 4 \text{ kPa}$	
		FEA:	
		Cauchy maximum principal compressive stress σ_c	
		Cauchy maximum principal compressive strain ε_c	

Continue next page

Reference, comment	Tissue	Material model, measures	Parameters
Linder-Ganz <i>et al</i> , 2008 [72] Experiment, flat indentation, sitting, lying, open-MRI, FEA 6 healthy (from [64]) (3 females) 6 paraplegics (2 females)	Muscle, Gluteus	Same material models as in [64] Same measures for thickness and interface pressures Lying, sitting. FEA: Maximum principal compressive stress and strain, σ_c, ϵ_c Maximum principal tensile stress and strain, σ_t, ϵ_t Maximum shear stress and strain, σ_s, ϵ_s	Healthy subjects $\Delta d = 21 \pm 3$ mm Paraplegics: $\Delta d = 11 \pm 10$ mm Sitting H: $\epsilon_c 74 \pm 7\%$, $\epsilon_t 75 \pm 7\%$, $\epsilon_s 91 \pm 17\%$ Sitting P: $\epsilon_c 88 \pm 6\%$, $\epsilon_t 235 \pm 48\%$, $\epsilon_s 128 \pm 23\%$
	Fat-skin		Healthy subjects $\Delta d = 13 \pm 4$ mm Paraplegics: $\Delta d = 14 \pm 9$ mm Sitting H: $\epsilon_c 46 \pm 7\%$, $\epsilon_t 31 \pm 5\%$, $\epsilon_s 42 \pm 11\%$ Sitting P: $\epsilon_c 57 \pm 16\%$, $\epsilon_t 88 \pm 36\%$, $\epsilon_s 61 \pm 19\%$
Al-Dirini <i>et al</i> 2015 [76], Experiment, flat indentation, MRI. 6 subjects.	Muscle, gluteus maximus (GM)	Deformation $D_x = T_2 - T_1$. T: thickness, 1: undeformed, 2: deformed $\text{Strain}_{\text{average}} = (T_1 - T_2) / T_1$	D_x median (range): (i) 18.8 mm (29.9-30.2), (pf) 16.6 mm (-9.7-12.0), (df) 24.3 mm (15.4-29.8) $\text{Strain}_{\text{average}}$ median (range): (i) 38.1% (14.6%), (pf) 26.6% (32.85)
	Fat-skin	Sites: below ischium (i), proximal femur (pf), distal femur (df),	D_x median (range): (i) 0.4 mm (-2.1-3.9), (pf) 2.7mm (-8.3-8.7), (df) - $\text{Strain}_{\text{average}}$ median (range): (i) 11.8% (31.2%), (pf) 25.2% (53.4%)
	Inter muscular fat (IMF)		D_x median (range): (pf) 8.9 mm (-8.7-53.7), (i) -, (df) - $\text{Strain}_{\text{average}}$ median (range): (pf) 32.4% (58.4%)

Continue next page

Reference, comment	Tissue	Material model, measures	Parameters
Al-Dirini <i>et al</i> 2016 [12] FE simulation, 1 male from [76]	Thigh	Hyper elastic, isotropic,	μ_m : 1907.4 Pa
	Muscles, 28	Ogden, 1 st order.	α_m : 4.6
	separately	Elastic deformation determinant J	D_m : 19.4987 MPa ⁻¹ (from table 5.3 p.196 in [9])
	modelled	Nearly incompressible, D from [9] based on μ_0 and ν .	Maximum Strain _{compressive} 41%
		Long term shear moduli μ	Maximum Strain _{shear} 110%
	Fat, subcutaneous	Estimations of Strain _{compressive} , Strain _{shear}	μ_f : 1166.7 Pa
		Optimization of parameters	α_f : 16.2
			D_f : 16.912 MPa ⁻¹ (from table 5.3 p.196 in [9])
			Maximum Strain _{compressive} 20%
			Maximum Strain _{shear} 58%
	Inter muscular fat (IMF)		μ_{imf} : 1166.7 Pa
			α_{imf} : 16.2
			D_{imf} : -
			Maximum Strain _{compressive} 21%
			Maximum Strain _{shear} 62%

II. Study II Clinical assessment protocol



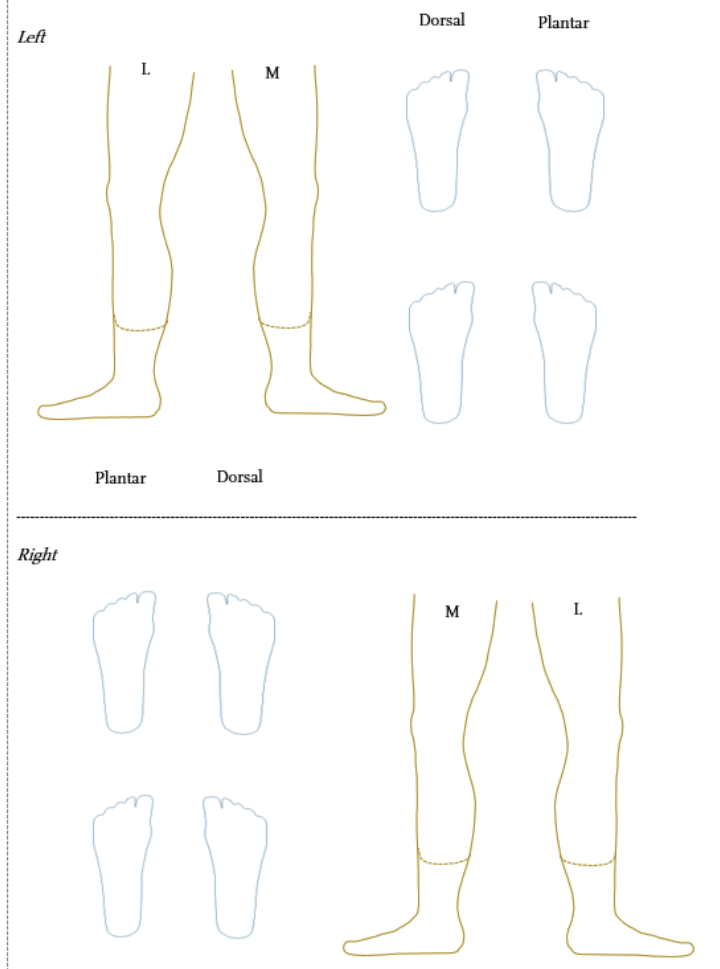
Forskningsprotokoll
Klinisk undersökning

Ortopedteknisk undersökning av deltagares mjukdelar i underben,
begränsad undersökning för forskningsprotokoll. (vidareutvecklad från ISO 8548-2[1] och [2, 3]) Delar av anamnes finns i
frågeformuläret bil.5 till Fokprövningsansökan, Dnr: 2015/397-31.

Datum:		a. Vikt:		b. Längd:		Kodnr:	
1.Diagnos:						Har inte någon diagnos <input type="checkbox"/>	
2.Amputationsorsak:							
3.Nuvarande ortopedtekniskt hjälpmedel: Inkl. interface material.						Foto av hjälpmedel	Sida: Vänster <input type="checkbox"/> Höger <input type="checkbox"/>
4. Foto av underben & fot, bilateralt. Statiskt stående + avlastat.		Frontal: Anterior Posterior	Sagittal: Medial Lateral	Dorsal:		Plantar:	
MÅTT:							
5. a) Distans ledspringa-TIM position [mm] b) Cirkulärmått [mm] Vid TIM-position c) Diameter vid TIM-position: A-P / M-L [mm]		Vänster ben/fot		Höger ben/fot			
		a) _____ b) _____ c) A-P: _____ M-L: _____		a) _____ b) _____ c) A-P: _____ M-L: _____			
6. Stumplängd (sl): Tibias längd ledspringa – distal ände. [mm] Normaliserad till % av andra sidans tibiallängd, beräknas vid data-analys. Normal tibiallängd: ledspringa – mediala malleol distala tip. Optimal sl: 1/3-sl<2/3 av andra sidans tibiallängd. Kom sl: <1/3. Läng sl >2/3							
SKELETT		Vänster		Höger			
7. Benprominenser; notera om anatomiska prominenser avviker från normalutseende, eller andra sidans. Ua/Vilka avviker? Kan markeras i figur 1.							

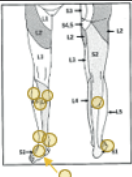
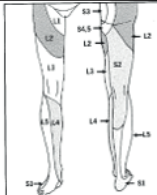
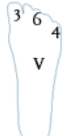
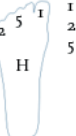
MUSKELSTYRKA underbenens större muskelgrupper. Manuellt test, Mo-M5 (Medical Research Council / Oxford scale) [4]				ROM Ua (utan anmärkning) Om onormalt ange ungefär grader, goniometer	
Knä flexion	8			12	
Knä extension	9			13	
Plantarflexion	10			14	
Dorsalflexion	11			15	
MOTION, TRÄNING		Typ		Hur ofta	

Figure 1. Mark place and distribution, with numbers related to questions.



MJKDELAR (jämför relativ normal BMI)					
<p>16. Palpativ Konsistens (beskrivn egenskaper) hos respektive strukturer/ vävnader (muskler i avslappnat (A) resp. kontraherat (K) tillstånd)</p> <p>Beskrivande ord:</p> <p>Tjocklek (T): Tunn (Ttu / Normal (TN)) / Tjock (Tti)</p> <p>Fast (F): Kompakt (FK) Muskulös (FMu) / Ödem (FÖ) / Stumt (FSt)</p> <p>Lös (L): Atrofisk (LAT) / Fettrik (LFr) / Paralytisk (LP).</p> <p>Elastisk, (töjning återgår) (E): Lågt motstånd (EL) / Tydligt motstånd (ET) / Stort motstånd (EST)</p> <p>Plastisk (töjning består) (P): Liten töjning (PL), Moderat töjning (PM), Stor töjning (PS)</p>					
	Tjocklek (T):	Fast (F):	Lös (L):	Elastisk (E):	Plastisk (P):
a) hud					
b) underhudsfett,					
c) muskler i A					
d) muskler i K					
e) senor, ligament					
f) trampdynor framfot					
g) hälkudde					
h) annat (ange).					
i) Standard Flabby: Indurated: se förklaringar längst bak.	Vä: Normal/ Flabby/ Indurated			Hö: Normal/ Flabby/ Indurated	
17. Mängd; Mer (+) / "Normal" (N) / Mindre (-) (subjektiv, jämför m normal BMI)	Vä			Hö	
18. Stump-form: Cylindrisk (C), Konisk (K), Bullig/utbuktande (B) Def: C: Omkres knä-ände +/- 1cm, K: knä-ände, B: knä-ände	Vä			Hö	
Klinisk Inspektion HUD (inkl. cirkulation)					
Faktor; Beskrivning: ringa in lämplig. (cirkulation [s])	Vänster ben/fot		Höger ben/fot		
	Beskrivning	Plats	Beskrivning	Plats	
19. Hudfärg (cirkulation); rodnad/normal/ rodnad/normal/blåaktig/ vit	rodnad/normal/ blåaktig/vit		rodnad/normal/ blåaktig/vit		
20. Kapilläråterfyllnad (cirkulation); Nedsatt, >2sek / Normal / Ökad	Nedsatt, >2sek / Normal / Ökad		Nedsatt, >2sek / Normal / Ökad		
21. Puls (cirkulation); Palpabel, ej palpabel. (1/0) a) a. dorsalis pedis (pmpi prox. dors), b) anterior tibial (dors, TCbörd) c) a. tibialis posterior (post medial malleolen.)	a) 1/0 b) 1/0 c) 1/0		a) 1/0 b) 1/0 c) 1/0		

Forts Inspektion HUD.	Beskrivning	Plats	Beskrivning	Plats
22. Temperatur [°C] (<i>cirkulation</i>); Mättn laser. Prox ant, post tib, Dist ant, post tib, TIM-placering, MTP ₃ dorsal, plantar.	_____	Prox Ant tib Prox post tib, Dist Ant tib Dist post tib, TIM-plac, MTP ₃ dors. MTP ₃ plant.	_____	Prox Ant tib Prox post tib, Dist Ant tib Dist post tib, TIM-plac, MTP ₃ dors. MTP ₃ plant.
23. Fuktighet; fuktig/normal/torr	fuktig/normal/ torr		fuktig/normal/ torr	
24. Behåring Ökad/Normal/Reducerad (+/o/-)	+ o -		+ o -	
25. Förhårdnader Callus Finns/saknas (1/o)	1 o		1 o	
26. Sår a) se listade nedan enl beskrivn i bil. 5, sektion F; nr 1–10, 12–14. Dokumentera geometrisk storlek i figur 1. *: exklusionskriterie PEOPLE 01				
1. Rodnad i huden som varit i var mer än 1 minut efter att hjälpmedlet tagits bort				
2. Skavsår utan bläsa				
3. Skrubbsår, skrubbmärke				
4. Bläsa				
5. Prickar, röda små utslag				
6. Inflammerad hårsäck				
7. Sår genom huden, yttligt *				
8. Sår genom huden med synlig muskelhävnad *				
10. Vättskande öppet sår (var, sårvätska) *				
12. Eksam *				
13. Infektion *				
14. Blåmärke *				
26.b. PU kategori				
27. Hudsprickor, Självsprickor i hud 1/o. Markeras i figur 1.				
28. Ärr a) läkt / oläkt* b) adherent / mobilt	a) läkt / oläkt* b) adherent / mobilt		a) läkt / oläkt* b) adherent / mobilt	
29. Ödem				

Känsl: [4, 5]	Vänster	Höger
<p>30. Ytlig känsel; Monofilament; 10g, beröring r: känner, o: känner inte (patologiskt). a) DP_r, MTP_r, MTP₅, b) Dermatom [4]: Prox Ant, M+L: L₅, L₄, Post: S₂/S₁ TIM-nivå. Fot: S₁ lat + plant, L₅ dorsalt+med, L₄ dist. medalt.</p>	<p>a) DP_r, MTP_r, MTP₅ b)</p> 	<p>a) DP_r, MTP_r, MTP₅ b)</p> 
<p>31. Ipswich touch test fot [6, 7] <i>Förenkla Neuropat-test.</i> Neuropati: känner inte ≥ 2 av de 6 o/i på 1-6. o: känner inte</p>	<p>3 6 4 4 6 V</p> 	<p>1 1 2 2 5 5 H</p> 
<p>32. Djup känsel; a) Vibration (med stängaffel) fib: huvud lat malleol tib: med. Malleol b) Ledpositionsuppfattning Normal: $< +/ - 10^\circ$, Nedsatt: $> 15^\circ$</p>	<p>a) fib: huvud lat malleol tib: med. Malleol b) Normal Nedsatt</p>	<p>a) fib: huvud lat malleol tib: med. Malleol b) Normal Nedsatt</p>
<p>33. Skyddskänsl/ smärtkänsl Särskilja varmt resp trubbigt samt varmt resp kallt. (o/i)</p>	<p>Vasst Trubbigt Varmt Kallt</p>	<p>Vasst Trubbigt Varmt Kallt</p>
<p>SMÄRTA</p>		
<p>34. Förekomst: Nej: N. Ja: nr 35-46</p>	<p>Ja Nej</p>	<p>Ja Nej</p>
<p>35. Karaktäristika Beskrivning enligt BPI-SF [8-10] och Vardhandboken [11]. Molande (M), Huggande (H), Tryckande (T), Brännande (B), Itande (I), Stuckande (S), Övrigt (O).</p>		
<p>36. Utbredning Markeras med symboler (25) i figur 1. Noteras även Djup (D) eller ylig (Y).</p>		
<p>37. Hur allvarlig/intensitet Numerisk: 0-10 (ingen - värsta tänkbara)</p>		
<p>38. Duration/ hur länge Tillfällig: sek/ min/ Långvarig: tim/ dag/ vecka</p>		
<p>39. Frekvens, periodicitet Ettstaka tillfällen, Återkommande, Regelbundet/oregelbundet n/Sek. /min /tim /dag /vecka</p>		
<p>40. När, vilka situationer Fritext</p>		

41. Spontan smärta		
42. Ömhet		
43. Smärtsamt neurom		
44. Fantomsmärta		
45. Smärta efter träning/aktivitet		
46. Annat		

FRIKTION HUD/TIM		
47. Digital dynamometer Medelvärde av 5 test/vikt: 500 [g]		

Kommentarer:

|

UTRUSTNING:

Kamera, Måttband, [mm], Skjuvmät, [mm], Termometer, laser, Monofilament, ryg, Sårspädd för neurologi, Reflexhammare, kall/varmt, vass/trubbigt, evi reflexer, Dynamometer, Friktionsbox, Vikter,

Flabby: adjective A nonmedical term referring to a body region with a paucity in muscle tone or tissue resilience and an excess of adipose tissue. Flabby is typically used as a euphemism for overweight and/or having a lack of exercise.

Indurated: Hardened, usually used with reference to soft tissues becoming extremely firm but not as hard as bone. Indurated; indurated oedema woody fibrosis of soft tissues, secondary to long-standing pathology

Oedema type Cause

Unilateral Within the limb, Local, e.g. as the result of local trauma, inflammation or infection, Regional, e.g. as the result of proximal limb trauma, inflammation, infection or venous compromise

Bilateral Systemic disease (e.g. heart disease, renal dysfunction, abdominal mass, hypertension, lung dysfunction)

Pitting Systemic disease (e.g. heart disease; hypertension; venous compromise)

Indurated/non-pitting Long-standing oedema (e.g. marked venous compromise; subsequent to deep-vein thrombosis)

Illustrated Dictionary of Podiatry and Foot Science by Jean Mooney, 2009

Kallor.

1. Standardization, I.O.F., *ISO 8548-2 Prosthetics and orthotics - Limb deficiencies - Part 2: Method of describing lower limb amputation stumps* 1993, International Organisation for Standardization: Genève, Switzerland.
2. *Merriman's assessment of the lower limb*, 3. ed., ed. Assessment of the lower limb, ed. B. Yates and L.M. Merriman. 2008, Edinburgh. New York: Elsevier.
3. Merriman, L.M. and W. Turner, *Assessment of the lower limb*, 2nd ed. 2002: Churchill Livingstone.
4. McRae, R., *Clinical orthopaedic examination*, 6. ed., ed. 2010, Edinburgh, New York: Churchill Livingstone/Elsevier.
5. Fors, P., *Diabeteseshandboken.se*. Diabeteseshandboken.se [web page] 2015 [cited 2015-12-15 2016-04-13]; Available from: <http://www.diabeteseshandboken.se/inneh%C3%A5ll/12-1963%3BGuetr-s%3C%3A5r-13755%3B89%3Bans>
6. Rayman, G., et al., *The Ipswich Touch Test: a simple and novel method to identify inpatients with diabetes at risk of foot ulceration*. Diabetes Care, 2011, 34(7): p. 157-8.
7. Sharma, S., et al., *The Ipswich Touch Test: a simple and novel method to screen patients with diabetes at home for increased risk of foot ulceration*. Diabet Med, 2014, 31(9): p. 1100-3.
8. Zelman, D.C., et al., *Validation of a Modified Version of the Brief Pain Inventory for Painful Diabetic Peripheral Neuropathy*. Journal of Pain and Symptom Management, 2005, 29(4): p. 401-410.
9. Mendoza, T., et al., *Reliability and validity of a modified Brief Pain Inventory short form in patients with osteoarthritis*. European Journal of Pain, 2006, 10(4): p. 353-361.
10. Erdemoglu, A.K. and R. Koc., *Brief Pain Inventory score identifying and discriminating neuropathic and nociceptive pain*. Acta Neurologica Scandinavica, 2013.
11. Brantberg, Å.L., *Smärtskanningsinstrument. Vårdhandboken*. [digital] 2008, 2016 2016-08-23; Available from: <http://www.vardhandboken.se/Texter/Smartskaning-av-akut-och-postoperativ-smarta/Smartskaningsinstrument/>.

III. Study II Questionnaire



Frågeformulär

Kodnummer: _____ Datum: _____

1. Kön: Kvinna ☐ Man ☐ 2. Ålder: _____ 3. Kroppslängd: _____ cm 4. Kroppsvikt: _____ kg

Om du undrar över något om frågorna, prata med kontaktpersonen, se information sist i formuläret.

DEL I

A. Hälsa och funktion i vardagen

	Utmärkt	Mycket god	God	Någorlunda	Dålig
1. I allmänhet, skulle du säga din hälsa är:	<input type="checkbox"/>	<input type="checkbox"/>	<input type="checkbox"/>	<input type="checkbox"/>	<input type="checkbox"/>
	Mycket bättre	Något bättre	Ungefär densamma	Något sämre	Mycket sämre
2. Jämfört med för ett år sedan, hur skulle du bedöma din hälsa nu?	<input type="checkbox"/>	<input type="checkbox"/>	<input type="checkbox"/>	<input type="checkbox"/>	<input type="checkbox"/>

Följande frågor handlar om aktiviteter du kan tänkas ägna dig åt en vanlig dag.

Begränsar din nuvarande hälsa dig i dessa aktiviteter? Om ja, hur mycket?

	Ja, mycket begränsad	Ja, lite begränsad	Nej, inte alls begränsad
3. Fysiskt ansträngande aktiviteter, t.ex. löpning, lyfta tunga föremål, delta i ansträngande idrotter	<input type="checkbox"/>	<input type="checkbox"/>	<input type="checkbox"/>
4. Måttligt ansträngande aktiviteter, t.ex. flytta ett bord, dammsuga, promenera eller cykla	<input type="checkbox"/>	<input type="checkbox"/>	<input type="checkbox"/>
5. Lyfta eller bära matkassar	<input type="checkbox"/>	<input type="checkbox"/>	<input type="checkbox"/>
6. Gå upp för flera trappor	<input type="checkbox"/>	<input type="checkbox"/>	<input type="checkbox"/>
7. Gå upp för en trappa	<input type="checkbox"/>	<input type="checkbox"/>	<input type="checkbox"/>
8. Böja dig eller gå ner på knä	<input type="checkbox"/>	<input type="checkbox"/>	<input type="checkbox"/>
9. Gå mer än ett par kilometer	<input type="checkbox"/>	<input type="checkbox"/>	<input type="checkbox"/>
10. Gå flera kvarter (flera hundra meter)	<input type="checkbox"/>	<input type="checkbox"/>	<input type="checkbox"/>
11. Gå ett kvarter (hundra meter)	<input type="checkbox"/>	<input type="checkbox"/>	<input type="checkbox"/>
12. Bada/duscha eller klä på dig	<input type="checkbox"/>	<input type="checkbox"/>	<input type="checkbox"/>

Under de senaste 4 veckorna, har du haft något av följande problem med ditt arbete eller andra vanliga dagliga aktiviteter på grund av din fysiska hälsa?

	Ja	Nej
13. Dragit ner på tiden du ägnat åt arbete eller andra aktiviteter	<input type="checkbox"/>	<input type="checkbox"/>
14. Fått mindre gjort än du skulle vilja	<input type="checkbox"/>	<input type="checkbox"/>
15. Begränsats i vissa arbetsuppgifter eller andra aktiviteter	<input type="checkbox"/>	<input type="checkbox"/>
16. Haft svårt att utföra arbete eller andra aktiviteter (t.ex. det krävdes mer ansträngning)	<input type="checkbox"/>	<input type="checkbox"/>

Under de senaste 4 veckorna, har du haft något av följande problem med ditt arbete eller andra vanliga dagliga aktiviteter på grund av känslomässiga problem (t.ex. att du känt dig nere eller orolig)?

	Ja	Nej
17. Dragit ner på tiden du ägnat åt arbete eller andra aktiviteter	<input type="checkbox"/>	<input type="checkbox"/>
18. Fått mindre gjort än du skulle vilja	<input type="checkbox"/>	<input type="checkbox"/>
19. Utfört arbete eller andra aktiviteter mindre noggrant än vanligt	<input type="checkbox"/>	<input type="checkbox"/>

	Inte alls	Lite grand	Måttligt	Ganska mycket	Extremt mycket	
20. Under de senaste 4 veckorna, i vilken omfattning har din fysiska hälsa eller känslomässiga problem stört dina vanliga sociala aktiviteter med familj, släkt, vänner, grannar eller föreningar etc. ?	<input type="checkbox"/>	<input type="checkbox"/>	<input type="checkbox"/>	<input type="checkbox"/>	<input type="checkbox"/>	
	Ingen	Mycket lätt	Lätt	Måttlig	Svår	Mycket svår
21. Hur mycket fysisk smärta har du haft under de senaste 4 veckorna?	<input type="checkbox"/>	<input type="checkbox"/>	<input type="checkbox"/>	<input type="checkbox"/>	<input type="checkbox"/>	<input type="checkbox"/>
	Inte alls	Lite grand	Måttligt	Ganska mycket	Extremt mycket	
22. Under de senaste 4 veckorna, hur mycket har smärta stört ditt vanliga arbete (gäller både arbete utanför hemmet och hushållsarbete)?	<input type="checkbox"/>	<input type="checkbox"/>	<input type="checkbox"/>	<input type="checkbox"/>	<input type="checkbox"/>	<input type="checkbox"/>
Följande frågor handlar om hur du känner dig och hur det varit under de senaste 4 veckorna. Ange det svar som stämmer bäst med hur du känt dig.						
Hur mycket av tiden under de senaste 4 veckorna...	Hela tiden	Största delen av tiden	En stor del av tiden	En viss del av tiden	En liten del av tiden	Inget av tiden
23. Har du känt dig pigg?	<input type="checkbox"/>	<input type="checkbox"/>	<input type="checkbox"/>	<input type="checkbox"/>	<input type="checkbox"/>	<input type="checkbox"/>
24. Har du känt dig mycket nervös?	<input type="checkbox"/>	<input type="checkbox"/>	<input type="checkbox"/>	<input type="checkbox"/>	<input type="checkbox"/>	<input type="checkbox"/>
25. Har du känt dig så nere att ingenting kunnat muntra upp dig?	<input type="checkbox"/>	<input type="checkbox"/>	<input type="checkbox"/>	<input type="checkbox"/>	<input type="checkbox"/>	<input type="checkbox"/>
26. Har du känt dig lugn och harmonisk?	<input type="checkbox"/>	<input type="checkbox"/>	<input type="checkbox"/>	<input type="checkbox"/>	<input type="checkbox"/>	<input type="checkbox"/>
27. Har du känt dig energisk?	<input type="checkbox"/>	<input type="checkbox"/>	<input type="checkbox"/>	<input type="checkbox"/>	<input type="checkbox"/>	<input type="checkbox"/>
28. Har du känt dig dystert och ledsen?	<input type="checkbox"/>	<input type="checkbox"/>	<input type="checkbox"/>	<input type="checkbox"/>	<input type="checkbox"/>	<input type="checkbox"/>
29. Har du känt dig utsliten?	<input type="checkbox"/>	<input type="checkbox"/>	<input type="checkbox"/>	<input type="checkbox"/>	<input type="checkbox"/>	<input type="checkbox"/>
30. Har du känt dig lycklig?	<input type="checkbox"/>	<input type="checkbox"/>	<input type="checkbox"/>	<input type="checkbox"/>	<input type="checkbox"/>	<input type="checkbox"/>
31. Har du känt dig trött?	<input type="checkbox"/>	<input type="checkbox"/>	<input type="checkbox"/>	<input type="checkbox"/>	<input type="checkbox"/>	<input type="checkbox"/>
	Hela tiden	Största delen av tiden	En viss del av tiden	En liten del av tiden	Inget av tiden	
32. Under de senaste 4 veckorna, hur mycket av tiden har din fysiska hälsa eller känslomässiga problem stört dina sociala aktiviteter (som att träffa vänner, släktingar etc.)?	<input type="checkbox"/>	<input type="checkbox"/>	<input type="checkbox"/>	<input type="checkbox"/>	<input type="checkbox"/>	<input type="checkbox"/>
Hur väl stämmer följande in på dig?	Stämmer helt	Stämmer ganska bra	Vet inte	Stämmer ganska dåligt	Stämmer inte alls	
33. Jag verkar ha något lättare att bli sjuk än andra människor	<input type="checkbox"/>	<input type="checkbox"/>	<input type="checkbox"/>	<input type="checkbox"/>	<input type="checkbox"/>	<input type="checkbox"/>
34. Jag är lika frisk som andra jag känner	<input type="checkbox"/>	<input type="checkbox"/>	<input type="checkbox"/>	<input type="checkbox"/>	<input type="checkbox"/>	<input type="checkbox"/>
35. Jag tror min hälsa kommer försämrats	<input type="checkbox"/>	<input type="checkbox"/>	<input type="checkbox"/>	<input type="checkbox"/>	<input type="checkbox"/>	<input type="checkbox"/>
36. Min hälsa är utmärkt.	<input type="checkbox"/>	<input type="checkbox"/>	<input type="checkbox"/>	<input type="checkbox"/>	<input type="checkbox"/>	<input type="checkbox"/>

B. Frågor om sjukdomar, infektioner och några andra hälsotillstånd

Har du haft någon av följande sjukdomar eller infektioner under det senaste året? Om ja, ungefär hur många gånger?	Nej	Ja	1-5 ggr	6-10 ggr	Fler ggr	Kan ej besvara antal ggr
1. Vanlig förkylning	<input type="checkbox"/>	<input type="checkbox"/>	<input type="checkbox"/>	<input type="checkbox"/>	<input type="checkbox"/>	<input type="checkbox"/>
2. Halsfluss	<input type="checkbox"/>	<input type="checkbox"/>	<input type="checkbox"/>	<input type="checkbox"/>	<input type="checkbox"/>	<input type="checkbox"/>
3. Maginfluensa	<input type="checkbox"/>	<input type="checkbox"/>	<input type="checkbox"/>	<input type="checkbox"/>	<input type="checkbox"/>	<input type="checkbox"/>
4. Vanlig influensa	<input type="checkbox"/>	<input type="checkbox"/>	<input type="checkbox"/>	<input type="checkbox"/>	<input type="checkbox"/>	<input type="checkbox"/>
5. Oroninflammation	<input type="checkbox"/>	<input type="checkbox"/>	<input type="checkbox"/>	<input type="checkbox"/>	<input type="checkbox"/>	<input type="checkbox"/>
6. Lunginflammation	<input type="checkbox"/>	<input type="checkbox"/>	<input type="checkbox"/>	<input type="checkbox"/>	<input type="checkbox"/>	<input type="checkbox"/>
7. Hjärnhinneinflammation	<input type="checkbox"/>	<input type="checkbox"/>	<input type="checkbox"/>	<input type="checkbox"/>	<input type="checkbox"/>	<input type="checkbox"/>
8. Infektion som krävt antibiotika (penicillin)	<input type="checkbox"/>	<input type="checkbox"/>	<input type="checkbox"/>	<input type="checkbox"/>	<input type="checkbox"/>	<input type="checkbox"/>
9. Borelia (fästingburen infektion)	<input type="checkbox"/>	<input type="checkbox"/>	<input type="checkbox"/>	<input type="checkbox"/>	<input type="checkbox"/>	<input type="checkbox"/>
10. Annan speciell infektion, i så fall vad?	<input type="checkbox"/>	<input type="checkbox"/>	<input type="checkbox"/>	<input type="checkbox"/>	<input type="checkbox"/>	<input type="checkbox"/>
11. Annan speciell infektion, i så fall vad?	<input type="checkbox"/>	<input type="checkbox"/>	<input type="checkbox"/>	<input type="checkbox"/>	<input type="checkbox"/>	<input type="checkbox"/>

Har du eller någon i din nära släkt någon/eller flera av följande sjukdomar? (Svarsalternativ: Nej, Ja, Vet ej/Osäker)	Du själv			Föräldrar			Sysstrar/ Bröder			Mor-/Far-föräldrar		
	Nej	Ja	Hur länge? (Antal år)	Nej	Ja	Vet ej/ osäker	Nej	Ja	Vet ej/ osäker	Nej	Ja	Vet ej/ osäker
12. Hjärtsjukdom	<input type="checkbox"/>	<input type="checkbox"/>	___	<input type="checkbox"/>	<input type="checkbox"/>	<input type="checkbox"/>	<input type="checkbox"/>	<input type="checkbox"/>	<input type="checkbox"/>	<input type="checkbox"/>	<input type="checkbox"/>	<input type="checkbox"/>
13. Kärtsjukdom	<input type="checkbox"/>	<input type="checkbox"/>	___	<input type="checkbox"/>	<input type="checkbox"/>	<input type="checkbox"/>	<input type="checkbox"/>	<input type="checkbox"/>	<input type="checkbox"/>	<input type="checkbox"/>	<input type="checkbox"/>	<input type="checkbox"/>
14. Barmdiabetes (diabetes typ 1) som kräver insulinbehandling	<input type="checkbox"/>	<input type="checkbox"/>	___	<input type="checkbox"/>	<input type="checkbox"/>	<input type="checkbox"/>	<input type="checkbox"/>	<input type="checkbox"/>	<input type="checkbox"/>	<input type="checkbox"/>	<input type="checkbox"/>	<input type="checkbox"/>
15. Äldersdiabetes (diabetes typ 2) som inte kräver insulinbehandling	<input type="checkbox"/>	<input type="checkbox"/>	___	<input type="checkbox"/>	<input type="checkbox"/>	<input type="checkbox"/>	<input type="checkbox"/>	<input type="checkbox"/>	<input type="checkbox"/>	<input type="checkbox"/>	<input type="checkbox"/>	<input type="checkbox"/>
16. Äldersdiabetes (diabetes typ 2) som kräver insulinbehandling	<input type="checkbox"/>	<input type="checkbox"/>	___	<input type="checkbox"/>	<input type="checkbox"/>	<input type="checkbox"/>	<input type="checkbox"/>	<input type="checkbox"/>	<input type="checkbox"/>	<input type="checkbox"/>	<input type="checkbox"/>	<input type="checkbox"/>
17. Allergi (hösnuva, eksem, pälsdjur etc)	<input type="checkbox"/>	<input type="checkbox"/>	___	<input type="checkbox"/>	<input type="checkbox"/>	<input type="checkbox"/>	<input type="checkbox"/>	<input type="checkbox"/>	<input type="checkbox"/>	<input type="checkbox"/>	<input type="checkbox"/>	<input type="checkbox"/>
18. Astma som kräver kortisonbehandling	<input type="checkbox"/>	<input type="checkbox"/>	___	<input type="checkbox"/>	<input type="checkbox"/>	<input type="checkbox"/>	<input type="checkbox"/>	<input type="checkbox"/>	<input type="checkbox"/>	<input type="checkbox"/>	<input type="checkbox"/>	<input type="checkbox"/>
19. Ledgångsreumatism (RA, Bechterews sjukdom)	<input type="checkbox"/>	<input type="checkbox"/>	___	<input type="checkbox"/>	<input type="checkbox"/>	<input type="checkbox"/>	<input type="checkbox"/>	<input type="checkbox"/>	<input type="checkbox"/>	<input type="checkbox"/>	<input type="checkbox"/>	<input type="checkbox"/>
20. Psoriasis	<input type="checkbox"/>	<input type="checkbox"/>	___	<input type="checkbox"/>	<input type="checkbox"/>	<input type="checkbox"/>	<input type="checkbox"/>	<input type="checkbox"/>	<input type="checkbox"/>	<input type="checkbox"/>	<input type="checkbox"/>	<input type="checkbox"/>
21. Glutenintolerans	<input type="checkbox"/>	<input type="checkbox"/>	___	<input type="checkbox"/>	<input type="checkbox"/>	<input type="checkbox"/>	<input type="checkbox"/>	<input type="checkbox"/>	<input type="checkbox"/>	<input type="checkbox"/>	<input type="checkbox"/>	<input type="checkbox"/>
22. Struma	<input type="checkbox"/>	<input type="checkbox"/>	___	<input type="checkbox"/>	<input type="checkbox"/>	<input type="checkbox"/>	<input type="checkbox"/>	<input type="checkbox"/>	<input type="checkbox"/>	<input type="checkbox"/>	<input type="checkbox"/>	<input type="checkbox"/>
23. Inflammatorisk tarmsjukdom (Chrons sjukdom, Ulcerös colit)	<input type="checkbox"/>	<input type="checkbox"/>	___	<input type="checkbox"/>	<input type="checkbox"/>	<input type="checkbox"/>	<input type="checkbox"/>	<input type="checkbox"/>	<input type="checkbox"/>	<input type="checkbox"/>	<input type="checkbox"/>	<input type="checkbox"/>
24. Annan sjukdom som inte nämnts ovan? Vad? (Skriv här):	<input type="checkbox"/>	<input type="checkbox"/>	___	<input type="checkbox"/>	<input type="checkbox"/>	<input type="checkbox"/>	<input type="checkbox"/>	<input type="checkbox"/>	<input type="checkbox"/>	<input type="checkbox"/>	<input type="checkbox"/>	<input type="checkbox"/>
.....	<input type="checkbox"/>	<input type="checkbox"/>	___	<input type="checkbox"/>	<input type="checkbox"/>	<input type="checkbox"/>	<input type="checkbox"/>	<input type="checkbox"/>	<input type="checkbox"/>	<input type="checkbox"/>	<input type="checkbox"/>	<input type="checkbox"/>
.....	<input type="checkbox"/>	<input type="checkbox"/>	___	<input type="checkbox"/>	<input type="checkbox"/>	<input type="checkbox"/>	<input type="checkbox"/>	<input type="checkbox"/>	<input type="checkbox"/>	<input type="checkbox"/>	<input type="checkbox"/>	<input type="checkbox"/>

C. Andra omständigheter

	Nej	Lite	Måttligt	Mycket	Vet ej
1. Har du lätt för att få blåmärken?	<input type="checkbox"/>	<input type="checkbox"/>	<input type="checkbox"/>	<input type="checkbox"/>	<input type="checkbox"/>
2. Har du känslig hud på annat sätt än beskrivet i tidigare frågor? (t.ex. lätt för att få skoskav, hudirritation av märkningar i kläder, utslag)	<input type="checkbox"/>	<input type="checkbox"/>	<input type="checkbox"/>	<input type="checkbox"/>	<input type="checkbox"/>

Beskriv hur det ytrar sig:

.....

3. Har du förändrad känsel i underben eller fötter?	<input type="checkbox"/>	<input type="checkbox"/>	<input type="checkbox"/>	<input type="checkbox"/>	<input type="checkbox"/>
4. Upplevs som nedsatt känsel?	<input type="checkbox"/>	<input type="checkbox"/>	<input type="checkbox"/>	<input type="checkbox"/>	<input type="checkbox"/>
5. Upplevs som ökad känsel?	<input type="checkbox"/>	<input type="checkbox"/>	<input type="checkbox"/>	<input type="checkbox"/>	<input type="checkbox"/>
6. Upplevs som domningar?	<input type="checkbox"/>	<input type="checkbox"/>	<input type="checkbox"/>	<input type="checkbox"/>	<input type="checkbox"/>
7. Upplevs som pinnningar?	<input type="checkbox"/>	<input type="checkbox"/>	<input type="checkbox"/>	<input type="checkbox"/>	<input type="checkbox"/>
8. Upplevs som kyla?	<input type="checkbox"/>	<input type="checkbox"/>	<input type="checkbox"/>	<input type="checkbox"/>	<input type="checkbox"/>
9. Upplevs som kuddkänsla?	<input type="checkbox"/>	<input type="checkbox"/>	<input type="checkbox"/>	<input type="checkbox"/>	<input type="checkbox"/>
10. Om annat, beskriv med egna ord:	<input type="checkbox"/>	<input type="checkbox"/>	<input type="checkbox"/>	<input type="checkbox"/>	<input type="checkbox"/>

.....

11. Använder du några mediciner dagligen?	Nej	Ja
	<input type="checkbox"/>	<input type="checkbox"/>

12. Om Ja i fråga 11, vilka mediciner? Ange namn och om möjligt vilken mängd och styrka (t.ex. Bufren 800mg, 1 tabl/dag)

.....

.....

	Nej, har inte rökt/smusat alls	Nej, har slutat, inte rökt/smusat senaste året.	Ja, 1-4 ggr/ månad	Ja, varje dag
13. Röker du?	<input type="checkbox"/>	<input type="checkbox"/>	<input type="checkbox"/>	<input type="checkbox"/>
14. Smusar du?	<input type="checkbox"/>	<input type="checkbox"/>	<input type="checkbox"/>	<input type="checkbox"/>

DEL II.

D. Hjälpmedel:

1. Använder du något gånghjälpmedel eller ortopedtekniskt hjälpmedel? Nej ☐ Ja ☐
Om du svarat Nej, gå direkt till DEL III.

Har du något/några av följande hjälpmedel?	JA. Vilken/vilka sidor?		Hur länge har du haft just detta hjälpmedel? (om både höger och vänster skriv H eller V till höger om valt tidsalternativ)			
	Vänster ben	Höger ben	Mindre än 1 månad	1-6 mån.	7-12 mån.	Mer än 12 mån.
Ortopedtekniskt hjälpmedel:						
2. Underbensprotes	<input type="checkbox"/>	<input type="checkbox"/>	<input type="checkbox"/>	<input type="checkbox"/>	<input type="checkbox"/>	<input type="checkbox"/>
3. Inlägg (fotortos)	<input type="checkbox"/>	<input type="checkbox"/>	<input type="checkbox"/>	<input type="checkbox"/>	<input type="checkbox"/>	<input type="checkbox"/>
4. Specialanpassade skor	<input type="checkbox"/>	<input type="checkbox"/>	<input type="checkbox"/>	<input type="checkbox"/>	<input type="checkbox"/>	<input type="checkbox"/>
5. Ankel-fot-ortos (underben och fot)	<input type="checkbox"/>	<input type="checkbox"/>	<input type="checkbox"/>	<input type="checkbox"/>	<input type="checkbox"/>	<input type="checkbox"/>
6. Annat.	Nej <input type="checkbox"/>	Ja <input type="checkbox"/>	Vad:			
7. När fick du din första protes eller ortos?	Vilket år och månad:					
8. Om du är amputerad, när blev du det på nuvarande amputationsnivå?	Vilket år och månad:					

Gånghjälpmedel:	Inomhus	Utomhus	Hur länge har du haft just detta hjälpmedel?			
			Mindre än 1 månad	1-6 mån.	7-12 mån.	Mer än 12 mån.
9. En käpp/krycka	<input type="checkbox"/>	<input type="checkbox"/>	<input type="checkbox"/>	<input type="checkbox"/>	<input type="checkbox"/>	<input type="checkbox"/>
10. Två käppar/kryckor	<input type="checkbox"/>	<input type="checkbox"/>	<input type="checkbox"/>	<input type="checkbox"/>	<input type="checkbox"/>	<input type="checkbox"/>
11. Rullator	<input type="checkbox"/>	<input type="checkbox"/>	<input type="checkbox"/>	<input type="checkbox"/>	<input type="checkbox"/>	<input type="checkbox"/>
Annat förflyttningshjälpmedel:						
12. Rullstol	<input type="checkbox"/>	<input type="checkbox"/>				
13. Elrullstol	<input type="checkbox"/>	<input type="checkbox"/>				
14. Annat (t.ex. stöd av person):	<input type="checkbox"/>	<input type="checkbox"/>	Vad:			

Användning ortopedtekniskt hjälpmedel:

Hur många dagar per vecka har du, normalt sett, på dig ditt hjälpmedel?

	1 dag	2 dagar	3 dagar	4 dagar	5 dagar	6 dagar	7 dagar
15. Underbensprotes	<input type="checkbox"/>	<input type="checkbox"/>	<input type="checkbox"/>	<input type="checkbox"/>	<input type="checkbox"/>	<input type="checkbox"/>	<input type="checkbox"/>
16. Inlägg (fotortos)	<input type="checkbox"/>	<input type="checkbox"/>	<input type="checkbox"/>	<input type="checkbox"/>	<input type="checkbox"/>	<input type="checkbox"/>	<input type="checkbox"/>
17. Specialanpassade skor	<input type="checkbox"/>	<input type="checkbox"/>	<input type="checkbox"/>	<input type="checkbox"/>	<input type="checkbox"/>	<input type="checkbox"/>	<input type="checkbox"/>
18. Ankel-fot-ortos (underben och fot)	<input type="checkbox"/>	<input type="checkbox"/>	<input type="checkbox"/>	<input type="checkbox"/>	<input type="checkbox"/>	<input type="checkbox"/>	<input type="checkbox"/>

Hur många timmar per dag har du normalt sett ditt hjälpmedel på dig?

	0-3 timmar	4-6 timmar	7-9 timmar	10-12 timmar	13-15 timmar	Mer än 15 timmar
19. Underbensprotes	<input type="checkbox"/>	<input type="checkbox"/>	<input type="checkbox"/>	<input type="checkbox"/>	<input type="checkbox"/>	<input type="checkbox"/>
20. Inlägg (fotortos)	<input type="checkbox"/>	<input type="checkbox"/>	<input type="checkbox"/>	<input type="checkbox"/>	<input type="checkbox"/>	<input type="checkbox"/>
21. Specialanpassade skor	<input type="checkbox"/>	<input type="checkbox"/>	<input type="checkbox"/>	<input type="checkbox"/>	<input type="checkbox"/>	<input type="checkbox"/>
22. Ankel-fot-ortos (underben och fot)	<input type="checkbox"/>	<input type="checkbox"/>	<input type="checkbox"/>	<input type="checkbox"/>	<input type="checkbox"/>	<input type="checkbox"/>

E. Benen och fötternas funktionsstatus

Använd skalan till höger för att ange hur du utför följande aktiviteter:

1. Mycket lätt
2. Ganska lätt
3. Ganska svårt
4. Mycket svårt
5. Kan ej

EA = Ej aktuellt (gör det aldrig oavsett om du kan eller ej)

1 2 3 4 5 EA

Använder du vanligen ditt ortopedtekniska hjälpmedel när du utför denna aktivitet?

Använder Använder inte

1. Kliva i och ur badkar eller dusch	<input type="checkbox"/>	<input type="checkbox"/>	<input type="checkbox"/>	<input type="checkbox"/>	<input type="checkbox"/>	<input type="checkbox"/>	<input type="checkbox"/>	<input type="checkbox"/>
2. Klä på underkroppen	<input type="checkbox"/>	<input type="checkbox"/>	<input type="checkbox"/>	<input type="checkbox"/>	<input type="checkbox"/>	<input type="checkbox"/>	<input type="checkbox"/>	<input type="checkbox"/>
3. Sätta sig på och resa sig upp från toaletten	<input type="checkbox"/>	<input type="checkbox"/>	<input type="checkbox"/>	<input type="checkbox"/>	<input type="checkbox"/>	<input type="checkbox"/>	<input type="checkbox"/>	<input type="checkbox"/>
4. Komma upp från golvet	<input type="checkbox"/>	<input type="checkbox"/>	<input type="checkbox"/>	<input type="checkbox"/>	<input type="checkbox"/>	<input type="checkbox"/>	<input type="checkbox"/>	<input type="checkbox"/>
5. Hålla balansen i stående (med stöd)	<input type="checkbox"/>	<input type="checkbox"/>	<input type="checkbox"/>	<input type="checkbox"/>	<input type="checkbox"/>	<input type="checkbox"/>	<input type="checkbox"/>	<input type="checkbox"/>
6. Stå upp i en halvtimme (med stöd)	<input type="checkbox"/>	<input type="checkbox"/>	<input type="checkbox"/>	<input type="checkbox"/>	<input type="checkbox"/>	<input type="checkbox"/>	<input type="checkbox"/>	<input type="checkbox"/>
7. Stående plocka upp ett föremål från golvet	<input type="checkbox"/>	<input type="checkbox"/>	<input type="checkbox"/>	<input type="checkbox"/>	<input type="checkbox"/>	<input type="checkbox"/>	<input type="checkbox"/>	<input type="checkbox"/>
8. Resa sig upp från en stol	<input type="checkbox"/>	<input type="checkbox"/>	<input type="checkbox"/>	<input type="checkbox"/>	<input type="checkbox"/>	<input type="checkbox"/>	<input type="checkbox"/>	<input type="checkbox"/>
9. Stiga i och ur en bil	<input type="checkbox"/>	<input type="checkbox"/>	<input type="checkbox"/>	<input type="checkbox"/>	<input type="checkbox"/>	<input type="checkbox"/>	<input type="checkbox"/>	<input type="checkbox"/>
10. Gå inomhus	<input type="checkbox"/>	<input type="checkbox"/>	<input type="checkbox"/>	<input type="checkbox"/>	<input type="checkbox"/>	<input type="checkbox"/>	<input type="checkbox"/>	<input type="checkbox"/>
11. Gå utomhus på ojämn mark	<input type="checkbox"/>	<input type="checkbox"/>	<input type="checkbox"/>	<input type="checkbox"/>	<input type="checkbox"/>	<input type="checkbox"/>	<input type="checkbox"/>	<input type="checkbox"/>
12. Gå utomhus i dåligt väder (t.ex. regn, snö, bläst, halka)	<input type="checkbox"/>	<input type="checkbox"/>	<input type="checkbox"/>	<input type="checkbox"/>	<input type="checkbox"/>	<input type="checkbox"/>	<input type="checkbox"/>	<input type="checkbox"/>
13. Promenera i upp till två timmar	<input type="checkbox"/>	<input type="checkbox"/>	<input type="checkbox"/>	<input type="checkbox"/>	<input type="checkbox"/>	<input type="checkbox"/>	<input type="checkbox"/>	<input type="checkbox"/>
14. Gå uppför brant ramp	<input type="checkbox"/>	<input type="checkbox"/>	<input type="checkbox"/>	<input type="checkbox"/>	<input type="checkbox"/>	<input type="checkbox"/>	<input type="checkbox"/>	<input type="checkbox"/>
15. Stiga på och av rulltrappa	<input type="checkbox"/>	<input type="checkbox"/>	<input type="checkbox"/>	<input type="checkbox"/>	<input type="checkbox"/>	<input type="checkbox"/>	<input type="checkbox"/>	<input type="checkbox"/>
16. Gå uppför en trappa med ledstång	<input type="checkbox"/>	<input type="checkbox"/>	<input type="checkbox"/>	<input type="checkbox"/>	<input type="checkbox"/>	<input type="checkbox"/>	<input type="checkbox"/>	<input type="checkbox"/>
17. Gå uppför en trappa utan ledstång	<input type="checkbox"/>	<input type="checkbox"/>	<input type="checkbox"/>	<input type="checkbox"/>	<input type="checkbox"/>	<input type="checkbox"/>	<input type="checkbox"/>	<input type="checkbox"/>
18. Springa 100-200 meter	<input type="checkbox"/>	<input type="checkbox"/>	<input type="checkbox"/>	<input type="checkbox"/>	<input type="checkbox"/>	<input type="checkbox"/>	<input type="checkbox"/>	<input type="checkbox"/>
19. Gående bära en tallrik med mat	<input type="checkbox"/>	<input type="checkbox"/>	<input type="checkbox"/>	<input type="checkbox"/>	<input type="checkbox"/>	<input type="checkbox"/>	<input type="checkbox"/>	<input type="checkbox"/>
20. Ta på och av ortopedtekniskt hjälpmedel	<input type="checkbox"/>	<input type="checkbox"/>	<input type="checkbox"/>	<input type="checkbox"/>	<input type="checkbox"/>	<input type="checkbox"/>	<input type="checkbox"/>	<input type="checkbox"/>
21. Stå upp i en timme (t.ex. i kö eller som åskådare)	<input type="checkbox"/>	<input type="checkbox"/>	<input type="checkbox"/>	<input type="checkbox"/>	<input type="checkbox"/>	<input type="checkbox"/>	<input type="checkbox"/>	<input type="checkbox"/>
22. Gå i affärer en halv dag	<input type="checkbox"/>	<input type="checkbox"/>	<input type="checkbox"/>	<input type="checkbox"/>	<input type="checkbox"/>	<input type="checkbox"/>	<input type="checkbox"/>	<input type="checkbox"/>
23. Stå och gå en halv arbetsdag (4-5 timmar)	<input type="checkbox"/>	<input type="checkbox"/>	<input type="checkbox"/>	<input type="checkbox"/>	<input type="checkbox"/>	<input type="checkbox"/>	<input type="checkbox"/>	<input type="checkbox"/>
24. Stå och gå en hel arbetsdag (8-9 timmar)	<input type="checkbox"/>	<input type="checkbox"/>	<input type="checkbox"/>	<input type="checkbox"/>	<input type="checkbox"/>	<input type="checkbox"/>	<input type="checkbox"/>	<input type="checkbox"/>
25. Gå nerför trappa utan ledstång	<input type="checkbox"/>	<input type="checkbox"/>	<input type="checkbox"/>	<input type="checkbox"/>	<input type="checkbox"/>	<input type="checkbox"/>	<input type="checkbox"/>	<input type="checkbox"/>
26. Gå nerför trappa med ledstång	<input type="checkbox"/>	<input type="checkbox"/>	<input type="checkbox"/>	<input type="checkbox"/>	<input type="checkbox"/>	<input type="checkbox"/>	<input type="checkbox"/>	<input type="checkbox"/>

F. Besvär och smärta pga ortopedtekniskt hjälpmedel

Ange med skalorna till höger du har haft respektive typ av besvär	Senaste 4 veckorna					Senaste året Obs! inte medräknat senaste 4 veckorna				
	Antal gånger 0, 1, 2-3, Fler gånger X: Vet ej/ kan ej svara					Antal gånger 0, 1, 2-3, Fler gånger X: Vet ej/ kan ej svara				
Hur många gånger under den angivna perioden har du haft följande besvär på grund av hjälpmedlet, eller i området som hjälpmedlet täcker:	0	1	2-3	Fler	X	0	1	2-3	Fler	X
1. Rodnad i huden som varit kvar mer än 1 minut efter att hjälpmedlet tagits bort	<input type="checkbox"/>	<input type="checkbox"/>	<input type="checkbox"/>	<input type="checkbox"/>	<input type="checkbox"/>	<input type="checkbox"/>	<input type="checkbox"/>	<input type="checkbox"/>	<input type="checkbox"/>	<input type="checkbox"/>
2. Skavsår utan blåsa	<input type="checkbox"/>	<input type="checkbox"/>	<input type="checkbox"/>	<input type="checkbox"/>	<input type="checkbox"/>	<input type="checkbox"/>	<input type="checkbox"/>	<input type="checkbox"/>	<input type="checkbox"/>	<input type="checkbox"/>
3. Skrubbsår, skrubbmärke	<input type="checkbox"/>	<input type="checkbox"/>	<input type="checkbox"/>	<input type="checkbox"/>	<input type="checkbox"/>	<input type="checkbox"/>	<input type="checkbox"/>	<input type="checkbox"/>	<input type="checkbox"/>	<input type="checkbox"/>
4. Blåsa	<input type="checkbox"/>	<input type="checkbox"/>	<input type="checkbox"/>	<input type="checkbox"/>	<input type="checkbox"/>	<input type="checkbox"/>	<input type="checkbox"/>	<input type="checkbox"/>	<input type="checkbox"/>	<input type="checkbox"/>
5. Prickar, röda små utslag	<input type="checkbox"/>	<input type="checkbox"/>	<input type="checkbox"/>	<input type="checkbox"/>	<input type="checkbox"/>	<input type="checkbox"/>	<input type="checkbox"/>	<input type="checkbox"/>	<input type="checkbox"/>	<input type="checkbox"/>
6. Inflammerad hårsäck	<input type="checkbox"/>	<input type="checkbox"/>	<input type="checkbox"/>	<input type="checkbox"/>	<input type="checkbox"/>	<input type="checkbox"/>	<input type="checkbox"/>	<input type="checkbox"/>	<input type="checkbox"/>	<input type="checkbox"/>
7. Sår genom huden, yttligt	<input type="checkbox"/>	<input type="checkbox"/>	<input type="checkbox"/>	<input type="checkbox"/>	<input type="checkbox"/>	<input type="checkbox"/>	<input type="checkbox"/>	<input type="checkbox"/>	<input type="checkbox"/>	<input type="checkbox"/>
8. Sår genom huden med synlig muskelvävnad	<input type="checkbox"/>	<input type="checkbox"/>	<input type="checkbox"/>	<input type="checkbox"/>	<input type="checkbox"/>	<input type="checkbox"/>	<input type="checkbox"/>	<input type="checkbox"/>	<input type="checkbox"/>	<input type="checkbox"/>
9. Sår genom huden ända in till ben	<input type="checkbox"/>	<input type="checkbox"/>	<input type="checkbox"/>	<input type="checkbox"/>	<input type="checkbox"/>	<input type="checkbox"/>	<input type="checkbox"/>	<input type="checkbox"/>	<input type="checkbox"/>	<input type="checkbox"/>
10. Vätskande öppet sår (var, såravskada)	<input type="checkbox"/>	<input type="checkbox"/>	<input type="checkbox"/>	<input type="checkbox"/>	<input type="checkbox"/>	<input type="checkbox"/>	<input type="checkbox"/>	<input type="checkbox"/>	<input type="checkbox"/>	<input type="checkbox"/>
11. Förhårdnad	<input type="checkbox"/>	<input type="checkbox"/>	<input type="checkbox"/>	<input type="checkbox"/>	<input type="checkbox"/>	<input type="checkbox"/>	<input type="checkbox"/>	<input type="checkbox"/>	<input type="checkbox"/>	<input type="checkbox"/>
12. Eksem	<input type="checkbox"/>	<input type="checkbox"/>	<input type="checkbox"/>	<input type="checkbox"/>	<input type="checkbox"/>	<input type="checkbox"/>	<input type="checkbox"/>	<input type="checkbox"/>	<input type="checkbox"/>	<input type="checkbox"/>
13. Infektion	<input type="checkbox"/>	<input type="checkbox"/>	<input type="checkbox"/>	<input type="checkbox"/>	<input type="checkbox"/>	<input type="checkbox"/>	<input type="checkbox"/>	<input type="checkbox"/>	<input type="checkbox"/>	<input type="checkbox"/>
14. Blåmärke	<input type="checkbox"/>	<input type="checkbox"/>	<input type="checkbox"/>	<input type="checkbox"/>	<input type="checkbox"/>	<input type="checkbox"/>	<input type="checkbox"/>	<input type="checkbox"/>	<input type="checkbox"/>	<input type="checkbox"/>
15. Kliande hud	<input type="checkbox"/>	<input type="checkbox"/>	<input type="checkbox"/>	<input type="checkbox"/>	<input type="checkbox"/>	<input type="checkbox"/>	<input type="checkbox"/>	<input type="checkbox"/>	<input type="checkbox"/>	<input type="checkbox"/>
16. Varm hud/vävnad	<input type="checkbox"/>	<input type="checkbox"/>	<input type="checkbox"/>	<input type="checkbox"/>	<input type="checkbox"/>	<input type="checkbox"/>	<input type="checkbox"/>	<input type="checkbox"/>	<input type="checkbox"/>	<input type="checkbox"/>
17. Vit hud	<input type="checkbox"/>	<input type="checkbox"/>	<input type="checkbox"/>	<input type="checkbox"/>	<input type="checkbox"/>	<input type="checkbox"/>	<input type="checkbox"/>	<input type="checkbox"/>	<input type="checkbox"/>	<input type="checkbox"/>
18. Blåaktig hud	<input type="checkbox"/>	<input type="checkbox"/>	<input type="checkbox"/>	<input type="checkbox"/>	<input type="checkbox"/>	<input type="checkbox"/>	<input type="checkbox"/>	<input type="checkbox"/>	<input type="checkbox"/>	<input type="checkbox"/>
19. Svullnad	<input type="checkbox"/>	<input type="checkbox"/>	<input type="checkbox"/>	<input type="checkbox"/>	<input type="checkbox"/>	<input type="checkbox"/>	<input type="checkbox"/>	<input type="checkbox"/>	<input type="checkbox"/>	<input type="checkbox"/>
20. Ökad svettning	<input type="checkbox"/>	<input type="checkbox"/>	<input type="checkbox"/>	<input type="checkbox"/>	<input type="checkbox"/>	<input type="checkbox"/>	<input type="checkbox"/>	<input type="checkbox"/>	<input type="checkbox"/>	<input type="checkbox"/>
21. Öm i huden	<input type="checkbox"/>	<input type="checkbox"/>	<input type="checkbox"/>	<input type="checkbox"/>	<input type="checkbox"/>	<input type="checkbox"/>	<input type="checkbox"/>	<input type="checkbox"/>	<input type="checkbox"/>	<input type="checkbox"/>
22. Smärta i huden	<input type="checkbox"/>	<input type="checkbox"/>	<input type="checkbox"/>	<input type="checkbox"/>	<input type="checkbox"/>	<input type="checkbox"/>	<input type="checkbox"/>	<input type="checkbox"/>	<input type="checkbox"/>	<input type="checkbox"/>
23. Öm inne i vävnaderna	<input type="checkbox"/>	<input type="checkbox"/>	<input type="checkbox"/>	<input type="checkbox"/>	<input type="checkbox"/>	<input type="checkbox"/>	<input type="checkbox"/>	<input type="checkbox"/>	<input type="checkbox"/>	<input type="checkbox"/>
24. Smärta inne i vävnaderna	<input type="checkbox"/>	<input type="checkbox"/>	<input type="checkbox"/>	<input type="checkbox"/>	<input type="checkbox"/>	<input type="checkbox"/>	<input type="checkbox"/>	<input type="checkbox"/>	<input type="checkbox"/>	<input type="checkbox"/>
25. Fantomsmärta (smärta i en del av benet/foten som inte finns kvar efter amputation)	<input type="checkbox"/>	<input type="checkbox"/>	<input type="checkbox"/>	<input type="checkbox"/>	<input type="checkbox"/>	<input type="checkbox"/>	<input type="checkbox"/>	<input type="checkbox"/>	<input type="checkbox"/>	<input type="checkbox"/>
Andra besvär? Ange vilka nedan och markera på motsvarande sätt till höger:										
26.	<input type="checkbox"/>	<input type="checkbox"/>	<input type="checkbox"/>	<input type="checkbox"/>	<input type="checkbox"/>	<input type="checkbox"/>	<input type="checkbox"/>	<input type="checkbox"/>	<input type="checkbox"/>	<input type="checkbox"/>
27.	<input type="checkbox"/>	<input type="checkbox"/>	<input type="checkbox"/>	<input type="checkbox"/>	<input type="checkbox"/>	<input type="checkbox"/>	<input type="checkbox"/>	<input type="checkbox"/>	<input type="checkbox"/>	<input type="checkbox"/>
28. Vilka var de vanligaste orsakerna till de besvär du haft? Beskriv med egna ord för de besvär du markerat och skrivit om ovan. (ex: nr 5: reaktion mot material, nr 19: varmt klimat)										

DEL III.

G. Frågor efter intryckningstest

Gradera eventuella besvär:	Inga besvär/ Nej	Mycket lätta	Lätta	Måttliga	Svåra	Mycket svåra
Upplövde du besvär i vävnaderna						
1. när intryckning pågick?	<input type="checkbox"/>	<input type="checkbox"/>	<input type="checkbox"/>	<input type="checkbox"/>	<input type="checkbox"/>	<input type="checkbox"/>
2. direkt efter intryckningstest?	<input type="checkbox"/>	<input type="checkbox"/>	<input type="checkbox"/>	<input type="checkbox"/>	<input type="checkbox"/>	<input type="checkbox"/>
3. två timmar efter intryckningstest?	<input type="checkbox"/>	<input type="checkbox"/>	<input type="checkbox"/>	<input type="checkbox"/>	<input type="checkbox"/>	<input type="checkbox"/>
4. ett dygn efter intryckningstest?	<input type="checkbox"/>	<input type="checkbox"/>	<input type="checkbox"/>	<input type="checkbox"/>	<input type="checkbox"/>	<input type="checkbox"/>
5. två dygn efter intryckningstest?	<input type="checkbox"/>	<input type="checkbox"/>	<input type="checkbox"/>	<input type="checkbox"/>	<input type="checkbox"/>	<input type="checkbox"/>
6. Hade du kvarvarande besvär mer än två dygn efter intryckningstest?	<input type="checkbox"/>	<input type="checkbox"/>	<input type="checkbox"/>	<input type="checkbox"/>	<input type="checkbox"/>	<input type="checkbox"/>
7. Beskriv eventuella besvär som uppkommit i samband med intryckningstest: <i>Använd egna ord eller med beskrivningar i denna sektion och/eller sektion F.</i> <i>Ex. Rödhet direkt efter intryckningstest, Öm inne i vävnaderna (23) i 2 tim efter.</i>						
8. Kommentarer om studien och/eller ytterligare information du vill ge: <i>Skriv här</i>						

Kontaktperson:

Sara Kallin, Leg. Ortopedingenjör, doktorand
 Tekniska högskolan, Högskolan i Jönköping tel. 036-10 12 74 sara.kallin@ju.se

Forskningsansvarig:

Maria Faresjö, professor i biomedicinsk laboratorievetenskap
 Hälsohögskolan, Högskolan i Jönköping tel. 036-10 12 96 maria.faresjo@ju.se

IV. Study II Data collection sequence

Table 11 Protocol for procedures Day 1

Action steps		Agent
1	Check if exclusion criteria had arisen.	CPO
2	Clinical assessment	CPO
3	Friction measurements at Skin-Indenter interface. 5 measurements on untreated skin, at site for indentation.	CPO
4	Blood pressure, blood sample*. Baseline	Nurse
5	Body position determined, and body support equipment adjusted accordingly on an examining table.	CPO
6	Making of the individual specific plaster shell with TIM fixating plate, on the chosen leg and subject in the determined body position.	CPO
7	Plaster shell removed, subject raised and left position to relax for a minimum of 10 minutes	CPO
8	Body support equipment placed on the MR-transporter Subject returned into position, with the plaster shell and TIM fixation frame applied. (Figure 16).	CPO
9	Blood pressure	Nurse
10	MR scan, non-loaded. T1 axial, sagittal, STIR axial	MR techn
11	Outside MR room, base-plate distal end moved sideways, and TIM mounted to the frame. TIM Indenter applied, loading data collected. At tolerated load, displacement held constant 120 s to reach a steady state of deformation [69, 70], indenter position locked.	CPO
12	TIM dismounted, base-plated returned in position	CPO
13	MR scan, loaded. T1 axial, sagittal, STIR axial	MR techn
14	Transporter moved outside MR room Blood pressure in loaded condition	CPO Nurse
15	Outside MR room repeated mounting of TIM, Load sensor positioned in contact with locked indenter, Indenter un-locked and retracted, unloading data collected. TIM dismounted, fixation frame and plaster shell removed. Inspection skin.	CPO
16	Blood pressure, blood sample*, 5 min after unloading	Nurse
17	Blood pressure, 15 min after unloading	Nurse
18	Clinical assessment, continued	CPO
19	Blood pressure, blood sample*, 60 min after unloading	Nurse
20	Questionnaire	Subject
21	Blood pressure, blood sample*, 120 min after unloading	Nurse
22	Clinical assessment, follow-up.	CPO

*Note: CPO certified prosthetist-orthotist, MR techn: radiology technician. *blood samples collected for another study*

V. Study I Additional data

Table 12 Stress maxima, magnitudes per tissue and model condition

Stress Maxima [kPa]		Conditions: Socket type, Material Set					
Tissue	Stress	TC		TSB		HS	
		Sep.	Comb.	Sep.	Comb.	Sep.	Comb.
Skin	Eff.	51.2	77.4	53.0	59.7	155.0	178.0
	Shear	28.6	40.1	-23.2	26.8	-73.0	-68.5
Fat	Eff.	27.5	32.2	12.8	15.2	35.0	12.5
	Shear	-10.8	16.16	-2.68	3.6	-40.0	6.9
Muscle	Eff.	2.6	14.53	1.87	5.1	5.8	4.5
	Shear	-1.09	-7.62	-1.04	-2.76	-2.95	-2.27
Fascia	Eff.	450.0	32.6	270.0	18.2	1120	25.0
	Shear	-190.0	-6.55	-140.0	-3.5	500.0	-5.0
Vessel	Eff.	0.91	1.23	2.18	3.2	1.57	2.7
	Shear	0.398	-0.6	0.69	1.26	-0.28	-0.9

Note : Numbers in bold: range for that tissue, regardless condition. Negative sign means opposite direction. TC: Total Contact, TSB: total Surface Bearing, HS: Hydrostatic Socket. Sep.: Separate material set, Comb.: Combined material set. Eff.: Effective stress, (von Mises). Shear: Shear stress.

Table 13 Strain Maxima Magnitudes per condition

Strain Maxima [%]		Conditions: Socket type, Material Set					
Tissue	Strain	TC		TSB		HS	
		Sep.	Comb.	Sep.	Comb.	Sep.	Comb.
Skin	AMP	-6.00	-8.4	6.3	6.91	-13.4	-13.2
	Shear	11.90	15.77	-9.6	-10.95	24.1	-23.2
Fat	AMP	-26.20	-42.97	-21.1	-25.92	-40.1	-40.2
	Shear	35.80	49.85	-29.5	-29.77	-43.5	44.3
Muscle	AMP	-31.60	-16.87	-24.5	-9.44	-49.5	-10.8
	Shear	-46.00	-31.72	-45.6	-18.04	-84.1	-16.0
Fascia	AMP	-7.10	-22.92	-5.7	-17.94	-11.5	-29.0
	Shear	-11.10	-29.34	-10.0	-20.74	18.5	27.0
Vessel	AMP	-10.70	-17.71	-21.9	-31.49	-19.6	-37
	Shear	11.80	-18.1	19.2	35.66	-8.0	-28.2

Note Range limits per outcome and tissue type marked in bold (regardless condition), based on absolute value. AMP: Absolute Maximum Principal. Negative values mean the strain is in opposite direction to those with positive values

Table 14 Contact pressure Maximum Magnitude

Contact pressures [kPa]		Condition Socket type		
Material set		TC	TSB	HS
Separate		29.1	14.6	52.2
Combined		68.3	23.1	71.6

Note TC: Total Contact, TSB: Total Surface Bearing, HS: Hydrostatic Socket

School of Engineering Dissertation Series

1. Olofsson, Jakob. (2012). Microstructure-based Mechanical Behaviour in Structural Analyses of Cast Components. Licentiate Thesis.
School of Engineering Dissertation Series No 1. ISBN 978-91-87289-01-9
2. Bäckstrand, Jenny. (2012). A Method for Customer-driven Purchasing Aligning Supplier interaction and Customer-driven manufacturing. Doctoral Thesis.
School of Engineering Dissertation Series No 2. ISBN 978-91-87289-02-6
3. Olofsson, Jakob. (2014). Simulation of Microstructure-based Mechanical Behaviour of Cast Components. Doctoral Thesis.
School of Engineering Dissertation Series No 3. ISBN 978-91-87289-04-0
4. Fourlakidis, Vasilios. (2014). Dendritic Morphology and Ultimate Tensile Strength in Lamellar Graphite Iron. Licentiate Thesis.
School of Engineering Dissertation Series No 4. ISBN 978-91-87289-05-7
5. Ghasemi, Rohollah. (2015). Tribological and Mechanical Behaviour of Lamellar and Compacted Graphite Irons in Engine Applications. Licentiate Thesis.
School of Engineering Dissertation Series No 5. ISBN 978-91-87289-06-4
6. Payandeh, Mostafa. (2015). Rheocasting of Aluminium Alloys: Slurry Formation, Microstructure, and Properties. Licentiate Thesis.
School of Engineering Dissertation Series No 6. ISBN 978-91-87289-07-1
7. Zamani, Mohammadreza. (2015). Al-Si Cast Alloys – Microstructure and mechanical properties at ambient and elevated temperature. Licentiate Thesis.
School of Engineering Dissertation Series No 7. ISBN 978-91-87289-08-8
8. Bjurenstedt, Anton. (2015). Imperfections in Recycled Aluminium-Silicon Cast Alloys. Licentiate Thesis.
School of Engineering Dissertation Series No 8. ISBN 978-91-87289-09-5
9. Kasvayee, Keivan Amiri. (2015). Microstructure and deformation behaviour of ductile iron under tensile loading. Licentiate Thesis.
School of Engineering Dissertation Series No 9. ISBN 978-91-87289-10-1
10. Dini, Hoda. (2015). As-cast AZ91D magnesium alloy properties. Effect of microstructure and temperature. Licentiate Thesis.
School of Engineering Dissertation Series No 10. ISBN 978-91-87289-11-8
11. Poorkiany, Morteza (2015). Support Maintenance of Design Automation Systems – A framework to Capture, Structure and Access Design Rationale. Licentiate Thesis.
School of Engineering Dissertation Series No 11. ISBN 978-91-87289-12-5

12. Cenanovic, Mirza (2015). Finite element methods on surfaces. Licentiate Thesis. School of Engineering Dissertation Series No 12. ISBN 978-91-87289-13-2
13. Amouzgar, Kaveh (2015). Metamodel based multi-objective optimization. Licentiate Thesis. School of Engineering Dissertation Series No 13. ISBN 978-91-87289-14-9
14. Wlazlak, Paraskeva (2016). Integration in global development projects: a study of new product development and production relocation projects. Licentiate Thesis. School of Engineering Dissertation Series No 14. ISBN 978-91-87289-15-6
15. Payandeh, Mostafa (2016). Rheocasting of Aluminium Alloys: Process and Components Characteristics. Doctoral Thesis. School of Engineering Dissertation Series No 15. ISBN 978-91-87289-16-3
16. Alayón, Claudia (2016). Exploring Sustainable Manufacturing Principles and Practices. Licentiate Thesis. School of Engineering Dissertation Series No 16. ISBN 978-91-87289-17-0
17. Ghasemi, Rohollah (2016). Influence of Microstructure on Mechanical and Tribological Properties of Lamellar and Compacted Irons in Engine Applications. Doctoral Thesis. School of Engineering Dissertation Series No 17. ISBN 978-91-87289-18-7
18. Tiedemann, Fredrik (2017). Strategic Lead-Times and their Implications on Financial Performance. Licentiate Thesis. School of Engineering Dissertation Series No 18. ISBN 978-91-87289-19-4
19. Zhu, Baiwei (2017). On the Influence of Si on Anodising and Mechanical Properties of Cast Aluminium Alloys. Licentiate Thesis. School of Engineering Dissertation Series No 19. ISBN 978-91-87289-20-0
20. André, Samuel (2017). Supporting the Utilization of a Platform Approach in the Engineer-to-Order Supplier Industry. Licentiate Thesis. School of Engineering Dissertation Series No 20. ISBN 978-91-87289-21-7
21. Zamani, Mohammadreza (2017). Al-Si Cast Alloys – Microstructure and Mechanical Properties at Ambient and Elevated Temperatures. Doctoral Thesis. School of Engineering Dissertation Series No 21. ISBN 978-91-87289-22-4
22. Cenanovic, Mirza (2017). Finite element methods for surface problems. Doctoral Thesis. School of Engineering Dissertations Series No. 22. ISBN 978-91-87289-23-1
23. Hernando, Juan Carlos (2017). Morphological Characterization of Primary Austenite in Cast Iron. Licentiate Thesis. School of Engineering Dissertation Series No. 23. ISBN 978-91-87289-24-8

24. Domeij, Björn (2017). On the Solidification of Compacted and Spheroidal Graphite Iron. Licentiate Thesis.
School of Engineering Dissertation Series No. 24. ISBN 978-91-87289-25-5
25. Salim, Roaa (2017). Exploring aspects of automation decisions – A study in the Swedish wood products industry. Licentiate Thesis.
School of Engineering Dissertation Series No. 25. ISBN 978-91-87289-26-2
26. de Goey, Heleen (2017). Exploring design-driven innovation: A study on value creation by SMEs in the Swedish wood products industry. Licentiate Thesis.
School of Engineering Dissertation Series No. 26. ISBN 978-91-87289-27-9
27. Kasvayee, Keivan Amiri (2017). On deformation behavior and cracking of ductile iron; effect of microstructure. Doctoral Thesis.
School of Engineering Dissertation Series No. 27. ISBN 978-91-87289-28-6
28. Bjurenstedt, Anton (2017). On the influence of imperfections on microstructure and properties of recycled Al-Si casting alloys. Doctoral Thesis.
School of Engineering Dissertation Series No. 28. ISBN 978-91-87289-29-3
29. Sifakas, Dimitrios (2017). The influence of deoxidation practice on the as-cast grain size of austenitic manganese steels. Licentiate Thesis.
School of Engineering Dissertation Series No. 29. ISBN 978-91-87289-30-9
30. Dini, Hoda (2017). As-Cast AZ91D Magnesium Alloy Properties – Effect of Microstructure and Temperature. Doctoral Thesis.
School of Engineering Dissertation Series No. 30. ISBN 978-91-87289-31-6
31. Poorkiany, Morteza (2017). Design Rationale Management as Part of Engineering Design and Design Automation. Doctoral Thesis.
School of Engineering Dissertation Series No. 31. ISBN 978-91-87289-32-3
32. Hellström, Kristina (2017). Density variations during solidification of lamellar graphite iron. Licentiate Thesis.
School of Engineering Dissertation Series No. 32. ISBN 978-91-87289-33-0
33. Riestra, Martin (2017). High Performing Cast Aluminium Silicon Alloys. Licentiate Thesis.
School of Engineering Dissertation Series No. 33. ISBN 978-91-87289-34-7
34. Sansone, Cinzia (2018). Critical operations capabilities in a high cost environment. Licentiate Thesis.
School of Engineering Dissertation Series No. 34. ISBN 978-91-87289-35-4
35. Popovic, Djordje (2018). Off-site manufacturing systems development in timber house building. Towards mass customization-oriented manufacturing. Licentiate Thesis.
School of Engineering Dissertation Series No. 35. ISBN 978-91-87289-36-1

36. Santos, Jorge (2018). Al-7Si-Mg Semi-Solid Castings – Microstructure and Mechanical Properties. Licentiate Thesis.
School of Engineering Dissertation Series No. 36. ISBN 978-91-87289-37-8
37. Heikkinen, Tim (2018). Multidisciplinary Design Automation: Working with Product Model Extensions. Licentiate Thesis.
School of Engineering Dissertation Series No 37. ISBN 978-91-87289-38-5
38. Fournalakidis, Vasilios (2019). Dendritic Morphology and Ultimate Tensile Strength of Pearlitic Lamellar Graphite Iron. Doctoral Thesis.
School of Engineering. Dissertation Series No 38. ISBN 978-91-87289-40-8
39. Pinate, Santiago (2019). Study of Particle-Current-Electrocrystallization Interactions in Electroplating of Ni/SiC Coatings. Licentiate Thesis.
School of Engineering. Dissertation Series No 39. ISBN 978-91-87289-41-5
40. Hernando Sanz, Juan Carlos (2019). The Role of Primary Austenite Morphology in Cast Iron. Doctoral Thesis.
School of Engineering. Dissertation Series No 40. ISBN 978-91-87289-42-2
41. Zhu, Baiwei (2019). Casting and Anodising of Al Alloys - Alloy Design, Manufacturing Process and Material Properties. Doctoral Thesis.
School of Engineering. Dissertation Series No 41. ISBN 978-91-87289-43-9
42. Hedvall, Lisa (2019). Reducing and Absorbing Variations in a Manufacturing Context. Licentiate Thesis.
School of Engineering. Dissertation Series No. 42. ISBN 978-91-87289-45-3
43. Siafakas, Dimitrios (2019). On Particles and Slags in Steel Casting. Doctoral Thesis.
School of Engineering. Dissertation Series No. 43. ISBN 978-91-87289-46-0
44. Samvin, David (2019). Finite Element Methods for Interface Problems. Licentiate Thesis.
School of Engineering. Dissertation Series No. 44. ISBN 978-91-87289-47-7
45. Jansson Johan (2019). Process-Induced Local Material Variations in Finite Element Simulations of Cast and Fibre Reinforced Injection Moulded Components. Licentiate Thesis.
School of Engineering. Dissertation Series No. 45. ISBN 978-91-87289-48-4
46. Domeij, Björn (2019). Compacted Graphite Iron: On Solidification Phenomena Related to Shrinkage Defects. Doctoral Thesis.
School of Engineering. Dissertation Series No. 46. ISBN 978-91-87289-49-1
47. Wlazlak, Paraskeva (2019). Management of the Industrialisation Process in Distributed Geographical and Organisational Context. Doctoral Thesis.
School of Engineering. Dissertation Series No. 47. ISBN 978-91-87289-50-7

48. André, Samuel (2019). The Design Platform Approach – Enabling Platform-Based Development in the Engineer-to-Order Industry. Doctoral Thesis. School of Engineering. Dissertation Series No. 48. ISBN 978-91-87289-51-4
49. Kallin, Sara (2019). Deformation of human soft tissues – Experimental and numerical aspects. Licentiate Thesis. School of Engineering. Dissertation Series No. 49. ISBN 978-91-87289-52-1

